Organic Semiconducting Oligomers for Use in Thin Film Transistors

Amanda R. Murphy and Jean M. J. Fréchet*

Department of Chemistry, University of California, Berkeley, California 94720-1460, and Division of Materials Sciences, Lawrence Berkeley National Laboratory, Berkeley, California 94720

Received June 15, 2006

Contents

* To whom correspondence should be addressed. Mailing address: 727 Latimer Hall, UC Berkeley, Berkeley, CA 94720. Telephone: (510) 643-3077. Fax: (510) 643-3079. E-mail: frechet@berkeley.edu.

1. Introduction

Over the past decade, the number of research groups exploring the field of organic electronics has exploded due to the potential use of organic semiconducting materials as a low-cost alternative to silicon. Applications for organic semiconductors include organic thin film transistors (OTFTs),[1−4] light-emitting diodes (OLEDs),[5,6] photovoltaic cells,[7,8] sensors,[9,10] and radio frequency identification (RF-ID) tags[11−13] for integration into low-cost, large-area electronics.[14] The main advantages of using organic materials lie in cost and processibility. Organic materials that are suitably modified are compatible with solution processing techniques, thereby eliminating the need for expensive lithography and vacuum deposition steps necessary for silicon-based materials. Low-temperature solution processing also expands the repertoire of tolerant substrates and processing options, allowing flexible plastics or fabrics to be used in conjunction with methods such as spin coating,[15,16] stamping,[17,18] or inkjet printing.[19,20]

To realize truly all-organic electronic devices, the development of a number of new materials is needed including conducting polymer electrodes, organic semiconductors, insulating dielectric materials, and plastic substrates. While there is much ongoing research into each of these components, this review will focus on the development of organic semiconductors, specifically small molecule or oligomeric materials. For brevity, polymeric materials will not be included here, but they should not be disregarded for this application as many promising semiconducting polymers are currently being developed.[21−24] Synthetic approaches to produce organic semiconductors with a wide variety of

10.1021/cr0501386 CCC: $65.00
Published on Web 04/11/2007

Amanda R. Murphy was born in Curitiba, Brazil, in 1978 and moved to Washington State shortly thereafter. She received a Bachelor of Science in Engineering Technology and a Bachelor of Arts in Chemistry at Western Washington University in Bellingham, WA, in 2001. In 2006, she obtained her Ph.D. degree from the University of California, Berkeley, working in the laboratory of Professor Fréchet in the Department of Chemistry. Her doctoral research focused on the design and synthesis of solution-processible organic semiconductors. She is now a postdoctoral researcher in Prof. Kaplan's laboratory at Tufts University in the Biomedical Engineering department.

Jean M. J. Fréchet obtained his first degree at the Institut de Chimie et Physique Industrielles (now CPE) in Lyon, France, and Ph.D. degrees from the College of Environmental Sciences and Forestry (SUNY-CESF) and Syracuse University. Following academic appointments at the University of Ottawa (1973–1986) and Cornell University (1987–1996), he joined the Department of Chemistry at the University of California, Berkeley. He has received American Chemical Society awards both in Polymer Chemistry and in Applied Polymer Science. The recipient of the 2007 Arthur C. Cope Award, Fréchet was earlier elected a Fellow of the American Academy of Arts and Sciences, a member of the National Academy of Science, and a member of the National Academy of Engineering. His research at the interface of organic, polymer, and biological chemistry is in the broad area of nanoscience and nanotechnology and is directed toward functional macromolecules and their design, synthesis, and applications.

functional groups and physical properties and the resulting structure−property relationships will be discussed. Materials will be divided into three broad classes determined by the method in which they were processed—vacuum-deposited, single-crystalline, or solution-processed—then further classified as either p-type (hole-conducting) or n-type (electron-conducting).

1.1. Charge Transport in Organic Semiconductors

The theory of charge transport in organic semiconductors has been reviewed extensively,[1,3,25,26] and many transport models have been proposed based on the well-documented behavior of inorganic semiconductors.[27−31] However, the exact mechanisms of charge injection and transport are still heavily debated.[32] The general mechanisms that are pertinent to the design of new semiconducting materials are outlined here, but for more detailed discussions, one may refer to the papers cited in this section.

In classical inorganic semiconductors such as silicon, atoms are held together with strong covalent or ionic bonds forming a highly crystalline three-dimensional solid. Therefore, strong interactions of the overlapping atomic orbitals cause charge transport to occur in highly delocalized bands that are mainly limited by defects, lattice vibrations, or phonon scattering in the solid. In contrast, organic semiconductors are composed of individual molecules that are only weakly bound together through van der Waals, hydrogen-bonding, and $\pi-\pi$ interactions and typically produce disordered, polycrystalline films. Charge delocalization can only occur along the conjugated backbone of a single molecule or between the π-orbitals of adjacent molecules. Therefore, charge transport in organic materials is thought to rely on charge hopping from these localized states and can be thought of as an electron transfer between a charged oligomer and an adjacent neutral oligomer. However, some organic oligomers have been found to form very ordered crystals, and within these materials, it may be possible that weak bands can form.

There are various methods for testing the electrical properties of organic materials including time-of-flight (TOF),[33,34] space charge limited current (SCLC),[35] the Hall effect,[36,37] and field-effect transistor (FET) (also referred to as thin film transistor, TFT) measurements. In TOF and SCLC devices, charge transport is typically measured perpendicular to the substrate, so these devices are not ideal for measuring mobility in organic semiconductors that typically have the highest π-orbital overlap parallel to the substrate. Therefore, FET devices, which measure mobility parallel to the substrate, give more relevant estimations of charge mobility. However, organic semiconductors usually form polycrystalline films, and the sample preparation can drastically affect the electrical properties.[38,39] Therefore, in order to measure intrinsic electrical properties, very pure single-crystalline samples must be obtained, which will be discussed further in section 4.[40,41]

1.2. Thin Film Transistors

There are many applications for organic semiconductors such as photovoltaic cells and OLEDs. However, this review will focus on the use of organic semiconductors as the active layer in transistors. Transistors essentially act as an on/off switch and are a vital part of the integrated circuits that operate RF-ID tags and sensors and are used to drive individual pixels in active matrix displays.

1.2.1. Organic Thin Film Transistor Device Fabrication

Illustrations of typical thin film transistors are shown in Figure 1. The device consists of a gate electrode, a dielectric insulating layer, and an organic semiconducting material sandwiched between a source and drain electrode. In the most commonly used devices, heavily doped silicon is used as both the substrate and the gate electrode. Oxidation of the silicon surface forms an insulating SiO_2 layer, usually with thicknesses of ∼100−300 nm. While these silicon devices are used for standard comparisons, the use of plastic

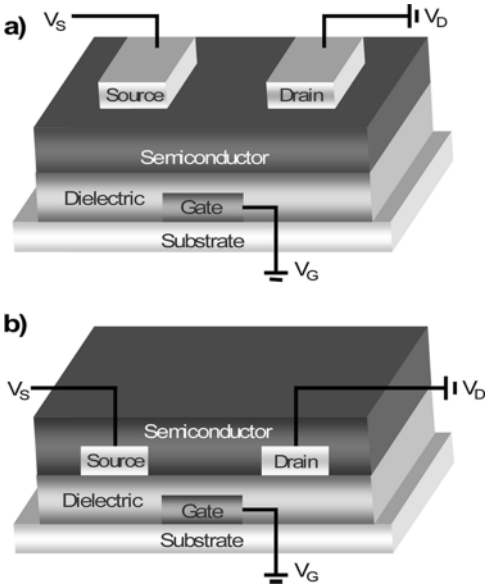

Figure 1. Illustration of (a) top contact and (b) bottom contact OTFT devices.

substrates,[13,15,19,42] polymeric insulators,[2,43] and conductive inks as the source and drain electrodes[44,45] are also being developed for flexible electronics applications.

Devices can be constructed in either top or bottom contact geometry, each with their own advantages. In top contact geometry (Figure 1a), the organic film is deposited on a uniform dielectric surface, and then the source and drain electrodes are deposited on top by metal evaporation through a shadow mask. In this device geometry, contact resistance is usually minimal due to intimate contact between the semiconductor and the electrodes, and the charge mobilities tend to be higher. However, due to shadowing effects, this type of device has a limit to how small the channel dimensions can be (usually >5 μm channels), and this process is not readily amenable to large-scale manufacturing. In bottom contact devices (Figure 1b), the source and drain electrodes are lithographically prepatterned on the substrate and the organic layer is deposited last. Bottom contact devices typically exhibit less than half the effective drive current of top contact devices due to contact resistance and the difficulty in preparing highly ordered films on an irregular surface.[24,46,47] However, bottom contact devices are more easily integrated into low-cost manufacturing processes, and smaller device feature sizes can be obtained through photolithographic techniques.

1.2.2. Device Operation and Electrical Measurements

The organic semiconductors used in these devices are not intentionally doped, so there should be a near-zero current between the source and drain when there is no voltage applied to the gate electrode. When a negative or positive bias is applied to the gate, a large electric field is produced at the semiconductor−dielectric interface. This field causes a shift in the HOMO and LUMO energy levels in the organic semiconductor. Depending on the work function of the electrodes relative to the HOMO/LUMO levels, electrons will either flow out of the HOMO into the electrodes (leaving behind holes) or flow from the electrodes into the LUMO, forming a conducting channel between the source and drain. Current can then be driven through the device by applying a voltage between the source and drain. In most cases, however, a conductive channel is not immediately formed due to energy level mismatches with the electrodes and the presence of traps that must be overcome before charges become mobile.

The quality of the interface between the dielectric and the semiconductor is a crucial parameter, because it has been shown that the majority of charge carriers are generated in the first one to two monolayers of semiconductor nearest to the dielectric surface.[48,49] Charge transfer between molecules is also strongly dependent on the trap concentrations at the dielectric−semiconductor interface and at the grain boundaries in the film.[28,29,50] Therefore, tight packing of adjacent molecules is desired to maximize the π-orbital overlap between neighboring molecules, thus increasing charge delocalization and minimizing trapping at defect sites.[51] This can be achieved by increasing the crystallinity of the bulk materials by designing very planar aromatic molecules with little or no other steric bulk. It is also essential that the materials be pure, because impurities can introduce charge carriers or traps within the material leading to erroneous results.

The most critical properties of an organic semiconductor are the charge mobility and I_{on}/I_{off} ratio. The charge mobility is the average drift velocity per unit electric field and can be calculated in the saturation regime using eq 1, where W

$$I_{DS} = (WC_i/(2L))\mu(V_g - V_0)^2 \quad (1)$$

$=$ channel width, $L =$ channel length, $C_i =$ capacitance of the insulator, $\mu =$ field-effect mobility, $V_g =$ gate voltage, and $V_0 =$ threshold voltage.[29,31]

This equation assumes that the mobility of the material is constant. However, mobility in organic semiconductors has been found to be dependent on the gate voltage, which suggests that a larger gate voltage leads to a higher density of charge at the dielectric−semiconductor interface, resulting in an increased charge mobility.[52] The temperature dependence on charge mobility in organic semiconductors has been experimentally measured, and it has been determined that mobility is thermally activated at temperatures >25 K but is thermally independent <25 K.[29,53] Many models have been suggested to explain this behavior including the multiple trap and thermal release (MTR) model and the polycrystalline model where individual grains are assumed to be trap-free and all the traps are concentrated at the grain boundaries.[29]

In thin film transistors, the I_{on}/I_{off} ratio can be defined as the ratio of current flow between the source and drain when there is no gate bias and the current flow at maximum gate bias. However, this value is highly dependent on the voltages used, the device geometry, and the dielectric material. Therefore, this value provides a qualitative measure of semiconductor performance, but identical parameters must be used to quantify the results when comparing different materials. The I_{on}/I_{off} ratio is also a useful measure of purity, because a high off current can be indicative of high extrinsic doping levels in the semiconductor. To be useful in optoelectronic devices such as active matrix displays that require sharp turn-on and fast switching, charge mobilities of >0.1 $cm^2/(V\cdot s)$ and an I_{on}/I_{off} ratio $>10^6$ are needed.[54]

1.2.3. Charge Injection

In an ideal system, when conjugated organic molecules crystallize into an ordered lattice, the individual HOMO and LUMO energy levels would blend to form bands analogous

to the conduction and valence bands in inorganic materials. While most organic semiconductors do not form ideal lattices, charge injection can still be made by matching the work function of the injecting electrode to either the valence band (HOMO) for hole injection, or the conduction band (LUMO) for electron injection. Organic semiconductors are commonly classified as either p-type (hole-conducting) or n-type (electron-conducting) depending on which type of charge carrier is more efficiently transported through the material. In theory, all organic semiconductors should be able to conduct both holes and electrons, but the differences in internal reorganization energies or work function of the electrodes relative to the HOMO and LUMO energies of the material in the transistor can favor one type of charge transport.[55] Nevertheless, there are far fewer accounts of n-type than p-type organic semiconductors[3,25] primarily due to the inherent instability of organic anions in the presence of air and water[3,56] and problems with oxygen trapping within these materials.[57,58] P-type organic semiconductors typically have HOMO levels between −4.9 and −5.5 eV, resulting in ohmic contact with high work-function metals such as gold (5.1 eV) and platinum (5.6 eV).[59] Contact resistance is typically smaller than the bulk resistance of the semiconductor, but in some cases, contact resistance and barrier height can be significant, reducing on currents appreciably.[35] N-type materials typically have LUMO levels between −3 and −4 eV and should have better contact with low work-function metals such as calcium and lithium, but these metals are highly reactive and degrade rapidly with air exposure. It has been found that gold typically forms good top contacts with organic n-type materials, even though it has a much higher work function.[25]

1.3. Solid-State Structure of Organic Semiconductors

As discussed in section 1.1, charge propagation in organic semiconductors preferentially occurs along the π-stacking axis through the overlapping π-orbitals of adjacent molecules. Therefore, the degree of molecular organization largely affects the efficiency of charge transport through the film. Modification of the chemical structure as well as optimization of the deposition conditions can drastically affect the molecular orientation, crystal structure, and grain size. Therefore, it is important to deduce not only single-crystalline structures but also the molecular structure of thin films.

1.3.1. Single-Crystalline Structure

The majority of unsubstituted conjugated organic oligomers crystallize into a herringbone structure, as illustrated in Figure 2.[60] In this packing motif, molecules minimize π-orbital repulsion by adopting an edge-to-face arrangement forming a two-dimensional layer.[38,55,59] However, the addition of side chains to the conjugated core can drastically affect the packing structure. For example, when oligothiophenes are end-substituted with linear alkyl chains, crystallization of the alkyl chains forces the conjugated units to adopt a more face-to-face arrangement, but they likely still to maintain some herringbone structure. This results in a lamellar-like structure, where insulating alkyl chains separate the conjugated units.[61] The change in crystal structure of α-6T upon end-substitution with hexyl chains is shown in Figure 3.

It has been theorized that forcing the oligomers to adopt a face-to-face arrangement would increase the π-orbital overlap and thus enhance the charge mobility by maximizing electronic coupling between adjacent molecules.[51,62] However, theoretical calculations by Hutchinson and co-workers predict that optimal π-orbital overlap will occur when molecules are tilted at angles of ∼40−60° to decrease electrostatic repulsion.[55] Several oligomers that have been shown to adopt a cofacial packing arrangement include fused-ring oligomers,[63,64] oligomers containing bulky substituents,[65] and oligomers incorporating both electron-rich and electron-deficient aryl rings.[66,67] The crystal structures of a few of

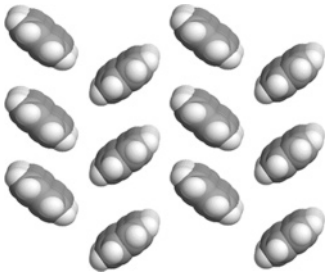

Figure 2. Illustration of a herringbone packing structure as viewed down the long axis of a molecule.

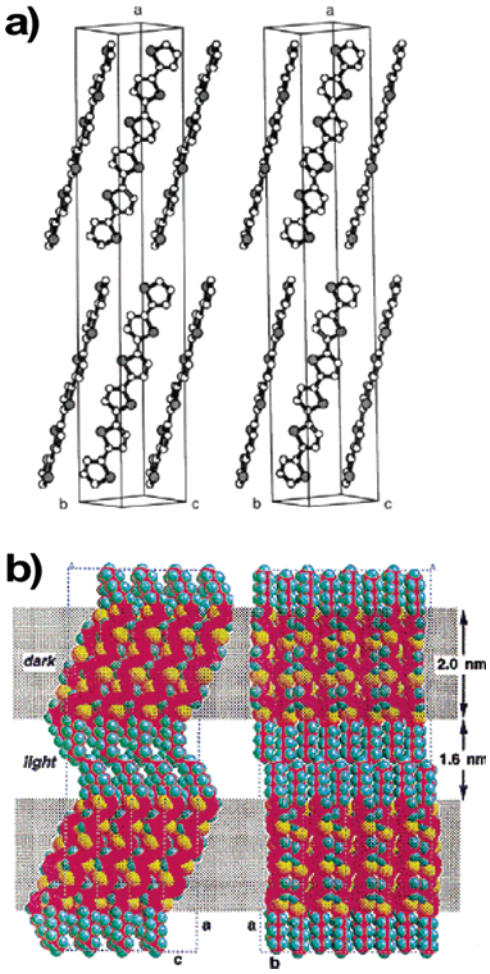

Figure 3. Change in crystal structure of α-6T upon end-substitution with hexyl chains: (a) Crystal structure of α-6T deposited from the vapor phase, displaying a typical herringbone packing motif[60] (Adapted with permission from ref 60. Copyright 1995 American Chemical Society); (b) the lamellar packing of α,ω-dihexyl-6T (Adapted with permission from ref 61. Copyright 1998 American Chemical Society). The dihexyl end groups effectively act as insulating barriers separating stacked assemblies of the 6T core segments from each other (dark refers to the α-6T cores; light refers to the alkyl chains).[61]

these types of oligomer are shown in Figure 4. The device data from these oligomers is quite promising as compared with analogs that adopt a herringbone structure, but further investigations are needed to demonstrate conclusively that face-to-face π-stacking results in higher charge mobility.

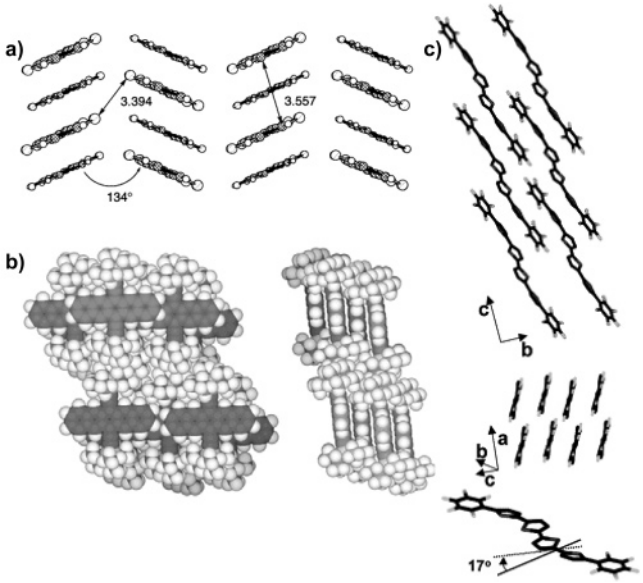

Figure 4. (a) Packing view of a bis(dithieno[3,2-b:2′,3′-d]-thiophene) single-crystal perpendicular to the *bc* plane[63] (Adapted with permission from ref 63. Copyright 1998 American Chemical Society), (b) solid-state ordering of bis(triisopropylsilylethynyl)-pentacene, (left) view of the *ac* layer (looking down the *b*-axis) and (right) view of the *bc* layer (looking down the *a*-axis)[65] (Adapted with permission from ref 65. Copyright 2001 American Chemical Society.), and (c) crystal structure of 5,5″-diperfluorophenyl-2,2′:5′,2″:5″,2‴-quaterthiophene showing packing characteristics and inter-ring torsional angles[66] (Adapted with permission from ref 66. Copyright 2006 American Chemical Society.)

1.3.2. Thin Film Structure and Characterization

While the X-ray crystal structures of single-crystalline organic semiconductors are useful for determining the packing structure in the bulk materials, they are not completely representative of how the molecules will behave when processed into a thin film. Deposition conditions and interactions with the surface play a critical role in determining the final molecular orientation, film continuity, and crystalline grain size within the film. For example, molecules can be oriented in specific directions by deposition onto anisotropic substrates,[50,68,69] grain size and structure can be affected surface chemistry[70−72] and temperature,[73−75] and substrates such as metal[76] or graphite[77] can strongly interact with π-orbitals causing the molecules to lie parallel to the substrate. Substrate effects are even more pronounced in solution-processed films.[78] Therefore, thorough investigation of the thin film molecular structure and morphology of organic semiconductors deposited in the same manner as OTFT devices is needed to arrive at a better understanding of structure−property relationships.

This section will highlight the common techniques used to probe the structure of thin films and give examples of typical data obtained for organic semiconductor films.

1.3.2.1. Microscopy. To study the film morphology and to determine the grain size within polycrystalline films, many microscopy techniques can be used. Scanning electron microscopy (SEM) and transmission electron microscopy (TEM) are used primarily to look at larger scale morphology and grain boundary size and can also be used to obtain diffraction patterns of crystalline films. Atomic force microscopy (AFM) and scanning tunneling microscopy (STM) can also be used to image film morphology. In addition, AFM can measure nanometer-scale vertical features such as step heights within the films. Examples of the film morphology observed using several microscopy techniques for a typical vacuum-deposited oligomer are shown in Figure 5. Features commonly seen in crystalline films include terraces with step heights corresponding to the height of the molecule, screw dislocations, and grains. Grain sizes vary but generally increase with deposition temperature to a point where cracks and discontinuities begin to occur.[73]

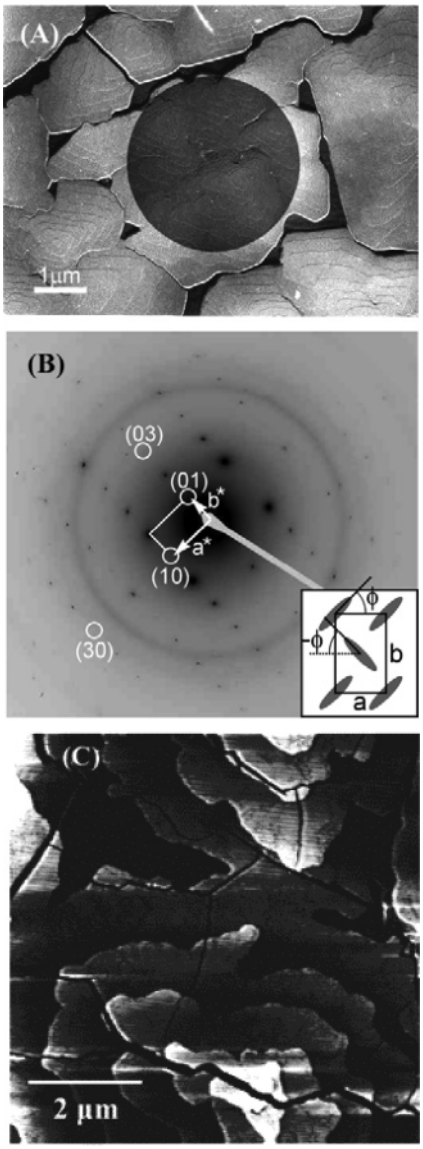

Figure 5. Characterization of thin films of 5,5′-bis-(7-cyclohexyl-9*H*-fluoren-2-yl)-2,2′-bithiophene using several microscopy techniques. These examples are representative of typical vacuum-deposited oligomer film morphology: (a) TEM image of a 400 Å thick film (T_{dep} = 120 °C) showing large, single-crystalline grains; (b) TEM diffraction pattern corresponding to a rectangular in-plane unit cell (lower-right inset) with two molecules per unit cell; from the apparent weak intensity of odd order (*h*0) and (0*k*) diffraction spots, a herringbone-like arrangement of the two molecules in the unit cell can be concluded; (c) AFM topography image of a 40 nm film deposited onto Si/SiO_2 at 130 °C.[79] Adapted with permission from ref 79. Copyright 2005 American Chemical Society.

1.3.2.2. X-ray Techniques. Further structural information such as the unit cell dimensions and preferential orientation relative to the substrate can be gathered from X-ray diffraction (XRD)[66,80−84] and grazing-incidence X-ray diffraction (GIXD) data.[85−88] In general, oligomeric semiconductors orient with their long axis nearly perpendicular to the substrate and form layered planes parallel to the substrate. Recently, near-edge X-ray absorption fine structure (NEXAFS) spectroscopy has also found utility in characterizing thin films of organic semiconductors. NEXAFS is depth-sensitive and can be used to measure chemical bond orientation as well as chemical identity.[89−92]

2. Vacuum-Deposited P-Type Oligomers

Strong π-interactions and the rigidity of conjugated organic semiconductors typically render the molecules insoluble in most common solvents. Therefore, the use of vacuum sublimation is required to process these materials into thin films. While this processing technique is expensive and time-consuming, it provides a high degree of control over variables such as time, sublimation temperature, temperature of the substrate during deposition, and base pressure. Optimization of these variables allows for deposition of films with precise thickness and molecular orientation.

2.1. Acenes

Pentacene (**1**, Chart 1) was among the first conjugated organic oligomers to be used as a p-type semiconductor and is still used as the standard for all newly developed organic semiconductors. Gundlach and co-workers were the first to report that pentacene OTFTs could achieve a field-effect mobility as large as 0.7 $cm^2/(V\cdot s)$ with I_{on}/I_{off} ratios $>10^8$.[93] Since the first report, numerous research groups have studied and optimized the performance of these devices.[3,4,39,94−97] Currently, Kelly and co-workers have obtained the highest hole mobility of any polycrystalline organic semiconductor in films of pentacene on a poly(α-methylstyrene) gate dielectric, giving measured mobilities >5.0 $cm^2/(V\cdot s)$ with I_{on}/I_{off} ratios of 10^6.[98] Efficient charge transport in pentacene has been attributed to high molecular order and the large grain sizes that can be obtained through optimization of the deposition conditions.[99]

Chart 1. Structures of Acene Derivatives

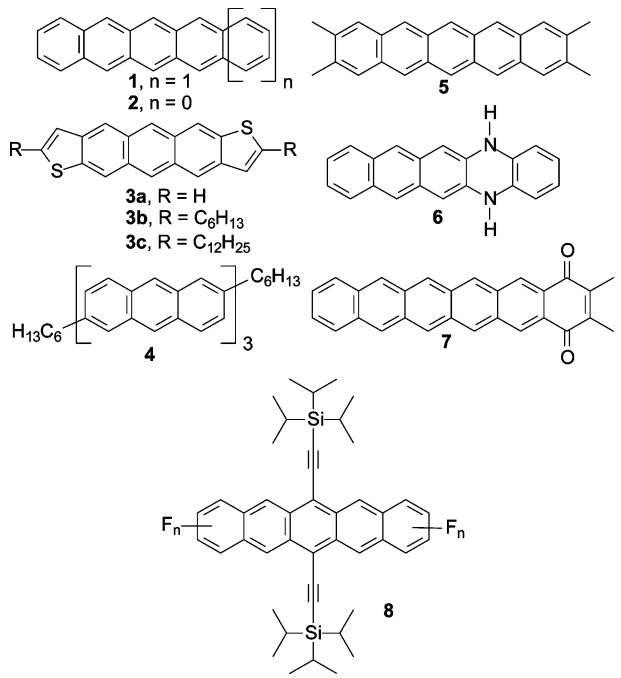

Gundlach and co-workers also investigated the electrical properties of tetracene (**2**, Chart 1) thin films. A hole mobility of 0.1 $cm^2/(V\cdot s)$ with an I_{on}/I_{off} ratio $>10^6$ was measured for films vacuum-sublimed onto Si/SiO_2 treated with octadecyltrichlorosilane (OTS).[82] Similar properties were also measured with films deposited at a high deposition rate onto unmodified SiO_2[70] and on SiO_2 modified with poly(α-methylstyrene).[100] Tetracene has also demonstrated utility in photodetectors[101] and light-emitting transistors (LETs).[102,103]

Laquindanum et al. have reported the use of unsubstituted and dialkylated anthradithiophenes in OTFTs.[104] The unsubstituted derivative **3a** (Chart 1) had mobilities ranging from 0.02 to 0.09 $cm^2/(V\cdot s)$ depending on the substrate deposition temperature. The dihexyl (**3b**) and didodecyl (**3c**) derivatives exhibited the highest mobilities between 0.11 and 0.15 $cm^2/(V\cdot s)$, while the mobility of the dioctadecyl derivative only reached 0.06 $cm^2/(V\cdot s)$. The increased mobility of **3b** and **3c** is attributed to the formation of an interconnected grain structure in the films and was also found to be dependent on the size of the device channel.[104]

Ito and co-workers have synthesized oligomers consisting of two or three anthracene units linked at the 2 and 6 positions.[105] Their motive for using this chemical structure is to mimic the extended π-orbital overlap of the longer acenes (such as pentacene) without having the same instability issues as the fused ring systems. The highest field-effect mobility obtained was 0.18 $cm^2/(V\cdot s)$ with I_{on}/I_{off} ratios of 10^4 for a dihexyl-substituted molecule with three linked anthracene units (**4**, Chart 1).[105] Interestingly, they found that adding hexyl end groups had a greater effect on the charge mobility than increasing the number of anthracene units from 2 to 3.

Meng and co-workers demonstrated that substitution of pentacene at the 2-, 3-, 9-, and 10-positions with a methyl group (**5**, Chart 1) did not significantly affect the field-effect mobility.[106] Mobilities as high as 0.26 $cm^2/(V\cdot s)$ with I_{on}/I_{off} ratios of 10^5 were measured when films were deposited on SiO_2 at 105 °C in top contact devices.

Miao and co-workers have synthesized and tested a family of dihydrodiazapentacene derivatives that have increased environmental and solution stability as compared with pentacene.[107] The solubility of these materials is enhanced in solvents such as DMF and DMSO due to the ability of the molecules to hydrogen bond with the solvent. The best performing derivative was the asymmetric molecule **6** (Chart 1), which had measured field-effect mobilities of 0.001−0.006 $cm^2/(V\cdot s)$ with I_{on}/I_{off} ratios of 10^3. These devices could be operated periodically in air without degradation for several days.

Miao et al. also reported on pentacene- and hexanequinones that self-assemble into antiparallel cofacial stacks with very small $\pi-\pi$ stacking distances of 3.25 Å.[108] The measured charge mobility for the derivative **7** (Chart 1) was 0.05 $cm^2/(V\cdot s)$ with I_{on}/I_{off} ratios of 10^4 when films were deposited on OTS-modified SiO_2, which is 200 times higher than mobilities obtained when depositing directly on SiO_2.

Swartz and co-workers investigated a series of electron-deficient pentacene derivatives (**8**, Chart 1). The addition of fluorine was found to increase the solubility and stability and lower the reduction potential. In a comparison using

identical processing conditions (thus unoptimized for each material), it was found that as the number of fluorine atoms increased from zero to eight, the charge mobility increased from 0.001 to 0.045 $cm^2/(V\cdot s)$, while the $\pi-\pi$ spacing decreased from 3.43 to 3.28 Å.[109]

2.2. Oligothiophenes

2.2.1. Unsubstituted Oligothiophenes

Polycrystalline films of unsubstituted linear oligothiophenes were among the first organic molecule films to be investigated for use in thin film transistors.[59,110,111] Oligomers with four (α-4T),[112] five (α-5T),[112] six (α-6T),[49] and eight (α-8T)[74,113] thiophene rings have been examined. X-ray diffraction studies of these oligomers prove that they all display similar solid-state ordering in the bulk and in thin films.[114,115] They all have planar conformations and herringbone-type packing motifs (see Figure 3a) and form polycrystalline films in which the molecules are orientated perpendicularly to the substrate. The charge mobility was found to be heavily dependent on purity of the oligomers[116−118] and the grain size,[28] where single-crystalline films were found to perform better than polycrystalline films.[60,119] Small increases in mobility were found with increasing oligomer length when compared side-by-side,[27,120] and odd−even effects have only been observed when the oligomers are deposited at low substrate temperatures.[121]

The α-4T (**9a**) and α-5T (**9b**) derivatives (Chart 2) have reported mobilities up to 0.006 [117] and 0.08 $cm^2/(V\cdot s)$,[122] respectively. The low mobility of the α-4T is primarily attributed to poor charge injection and not necessarily low charge mobility through the material, because the mobility could be doubled by using a layer of an electron-transport material to facilitate charge injection.[112] The α-6T (**9c**) derivative is reported to have a charge mobility around 0.03 $cm^2/(V\cdot s)$ when used in bottom contact Si/SiO_2 devices,[49] while single-crystalline films of the oligomer exhibit mobilities up to 0.075 $cm^2/(V\cdot s)$.[119] The highest reported mobility for α-8T (**9d**) is 0.33 $cm^2/(V\cdot s)$ and was obtained when the substrate was heated to 120 °C during deposition.[74] This mobility value is an order of magnitude higher than previously reported for α-8T[113,117] and is attributed to the formation of elongated, terraced grains.

Chart 2. Unsubstituted Oligothiophene Structures

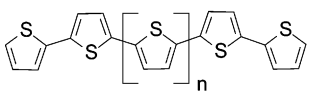

9a, n = 0
9b, n = 1
9c, n = 2
9d, n = 4

2.2.2. Substituted Oligothiophenes

Many synthetic methods have been developed to functionalize either the α- or β-positions of the thiophene ring, in order to increase the solubility or to influence the solid-state ordering of oligothiophenes.[59] Functionalization at the α-positions of the oligomer typically does not affect the planarity of the conjugated backbone but does little to help solubility unless branched substituents are used. End-substitution with alkyl chains has been found to be particularly useful, because it gives the molecules liquid-crystalline-like properties, which dramatically increases the ordering and enhances the charge mobility of the resulting evaporated films.[38,59] Functionalization of the β-positions in thiophene oligomers can significantly increase the solubility of the oligomers but tends to warp the conjugated plane and in most cases leads to low-mobility materials. The synthetic approaches and results of using vacuum-sublimed films of functionalized linear thiophenes are outlined below.

Methyl-terminated[123,124] and dihexyl-substituted oligomers with four (DHα-4T),[125,126] five (DHα-5T),[127] six (DHα-6T),[81] and eight (DHα-8T)[113] thiophene rings have been synthesized and characterized. Here again, the purity of these insoluble compounds was found to be of paramount importance to obtaining high performance transistors.[111,117,118]

The mobility of thermally evaporated polycrystalline films of DHα-4T (**10a**, Chart 3) has been measured to be 0.03 $cm^2/(V\cdot s)$ with an I_{on}/I_{off} ratio of 10^5,[125] while films exhibiting single-crystalline-like morphology have reported mobilities ranging from 0.05 to 0.23 $cm^2/(V\cdot s)$.[126] Addition of a hexyl chain at only one end of a 4T oligomer also led to an increase in mobility over α-4T from 0.001 to 0.01 $cm^2/(V\cdot s)$.[128] Films with single-crystalline morphologies could also be obtained by evaporation of DHα-5T (**10b**) on substrates held at 155 °C. These films had measured mobilities as high as 0.1 $cm^2/(V\cdot s)$.[127] The field-effect mobility of DHα-6T (**10c**) is typically reported to be between 0.02 and 0.07 $cm^2/(V\cdot s)$ depending on the deposition conditions and dielectric layer used.[81,129−131] The highest mobility values for DHα-6T were obtained by Dimitrakopoulos and co-workers using molecular beam deposition of the oligomer. Values up to 0.13 $cm^2/(V\cdot s)$ were measured when parylene was used as the insulating layer.[132] DHα-8T (**10d**) was found to have a hole mobility of 0.02 $cm^2/(V\cdot s)$, in the same range as the smaller

Chart 3. Substituted Oligothiophene Structures

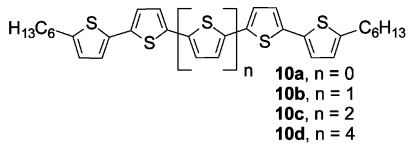

10a, n = 0
10b, n = 1
10c, n = 2
10d, n = 4

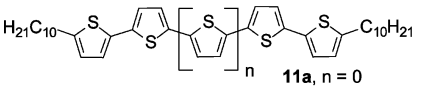

11a, n = 0
11b, n = 1
11c, n = 2

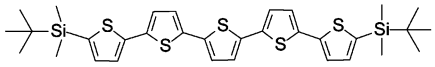

12

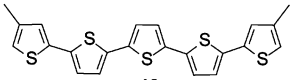

13

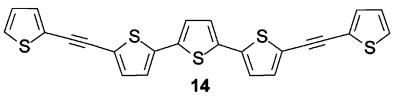

14

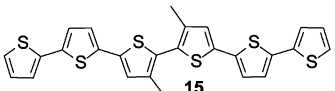

15

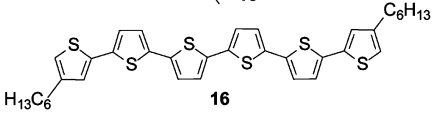

16

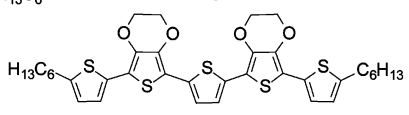

17

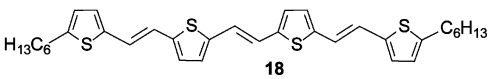

18

oligomers.[113] Comparing the mobility values for this series, one can conclude that increasing the conjugation length past four thiophene units does not affect mobility nearly as much as increasing molecular order within the films.

More recently, a series of α-α′-didecyloligothiophenes (DDαT*n*) containing four, five, and six thiophene rings have been synthesized and characterized by Halik et al.[133] An interesting discovery was that the smallest oligomer (DDαT4) (**11a**, Chart 3) had the greatest degree of ordering in the crystal phase, but lower mobilities (0.2 $cm^2/(V\cdot s)$) than the longer DDαT5 (**11b**) and DDαT6 (**11c**) derivatives (∼0.5 $cm^2/(V\cdot s)$) in OTFTs.[134,135] Devices were characterized in air, which may be the reason that a positive voltage was needed to actually turn the devices off. The mobilities reported here are much higher than that reported for the dihexyl derivatives,[81,113,125,132] and the authors claim that the use of cross-linked poly(hydroxystyrene) as the dielectric layer is responsible for the increase.[94,134]

Halik and co-workers have also demonstrated the sensitivity of alkyl-substituted oligothiophenes to device configuration.[136] Charge mobility in bottom contact devices was found to be independent of the oligomer length (4T−6T) and independent of the alkyl chain length (C_2-C_{10}). However, in top contact devices oligomers containing short alkyl end groups (less than six carbons) were found to have an order of magnitude higher mobility. The authors attribute this phenomenon to an intrinsic barrier to charge injection from top contact devices when large insulating alkyl chain groups are present.

The effect of end groups other than alkyl chains has also been studied. Barbarella and co-workers have synthesized a series of oligothiophenes (3, 4, 5, and 6T) that are end-capped with dimethyl-*t*-butylsilyl groups.[137] Vacuum-evaporated thin films of the quinquethiophene **12** (Chart 3) gave the highest charge mobilities of 3×10^{-4} $cm^2/(V\cdot s)$ with I_{on}/I_{off} ratios of 10^3. While the charge mobility of these oligomers is low, devices were found to be stable in air for months. Single-crystal analysis of the 3T and 4T derivatives revealed that these materials form a dimeric face-to-face π-stacked structure in the solid state, which has been theorized to give high charge mobility in organic semiconductors. However, the molecular structure in the thin films is likely much different than that in the solid state, leading to the low mobilities.

Barbarella and co-workers have also investigated the structure−property relationships between differentially substituted quinquethiophenes. Unsubstituted quinquethiophene (α-5T) (**9b**, Chart 2) was found to have the highest charge mobility when deposited at $T_{dep} = 90$ °C (0.08 $cm^2/(V\cdot s)$).[122] At this temperature, thin films exhibited large terraced grains with step heights corresponding to the length of the molecule. The two other molecules investigated had either methyl groups at the terminal β-positions (**13**, Chart 3) or acetylene spacers in the backbone (**14**, Chart 3) and were found to have mobilities that were 2 and 4 orders of magnitude lower than that of α-5T (**9b**), respectively.[122] The differences in mobility in these cases could not be attributed to film morphology because evaporated films of all the oligomers were crystalline and had comparable grain sizes. Further studies are needed to determine whether the lower mobilities are caused by poor π-orbital overlap of the molecules in the film, inefficient charge injection, or strong trapping states within the films.

The effect of substitution at the β-positions of sexithiophene oligomers has also been explored.[81,138] β-Substitution dramatically increases the solubility of thiophene oligomers, typically at the cost of losing planarity of the molecule. Previous studies using a β,β′-dihexylsexithiophene found that these materials had negligible charge mobility due to poor ordering of the molecules.[81] However, the dimethylated sexithiophene **15** (Chart 3) was found to have very close packing as determined by X-ray diffraction. Charge mobilities up to 0.02 $cm^2/(V\cdot s)$ were measured when the oligomer was deposited at 80 °C,[139] demonstrating that small substituents may be tolerated in the β-position of thiophene oligomers without a drastic decrease in mobility. Furthermore, Fachetti and co-workers later demonstrated that hexyl groups could be incorporated at the terminal β-positions of a sexithiophene oligomer (**16**, Chart 3) without inhibiting OTFT performance.[140] Hole mobilities up to 0.06 $cm^2/(V\cdot s)$ with I_{on}/I_{off} ratios up to 10^3 could be obtained with this material.

A series of co-oligomers of thiophene and 3,4-ethylenedioxythiophene (EDOT) ranging from four to seven rings have been synthesized by Turbiez and co-workers.[141] They found that alternating thiophene and EDOT rings leads to very rigid structures due to the S··O interactions between the sulfur in the thiophene ring and the adjacent EDOT oxygens. Only oligomer **17** (Chart 3) was tested in an OTFT device and was found to have a mobility of 6×10^{-4} $cm^2/(V\cdot s)$ when deposited at 80 °C. While this mobility is low, the authors stress that this was from an unoptimized device.

A series of oligothienylenevinylenes have been synthesized and characterized by Frère and co-workers containing varying numbers of directly linked double bonds and thiophene units.[142] Alternation of thiophene and a double bond was found to produce a faster decrease of the HOMO−LUMO gap than incorporation of additional thiophene rings, and addition of two consecutive double bonds stabilizes the dicationic state but does not lower the HOMO−LUMO gap further. In testing of these oligomers in OTFT devices, it was found that only the oligomers capable of reversible π-dimerization of radical cations had appreciable hole mobility.[143] The hexyl-substituted derivative **18** (Chart 3) was found to have a mobility of 0.055 $cm^2/(V\cdot s)$, which is more than an order of magnitude higher than the unsubstituted derivative.

2.2.3. Fused Oligothiophenes

As discussed in section 1.3, it has been theorized that forcing oligomers to adopt a face-to-face arrangement would increase the π-orbital overlap and thus enhance the charge mobility by maximizing electronic coupling between adjacent molecules.[51,62] Therefore, the following section discusses molecules containing fused ring systems intended to maximize the π-orbital overlap by reducing the freedom of rotation in the oligomer and possibly to induce face-to-face π-stacking motifs.

Laquindanum and co-workers were among the first to explore fused thiophenes, and they synthesized a dimeric fused ring thiophene derivative, bis(benzodithiophene) (**19**, Chart 4). They found that this material had mobilities up to 0.04 $cm^2/(V\cdot s)$ when vacuum-deposited at 100 °C.[144]

A more rigid benzodithiophene analog, namely, dibenzothienobenzothiophene (**20**, Chart 4), was investigated by Sirringhaus and co-workers.[145] The intramolecular cyclization reaction used to make these oligomers is not regioselective,

Chart 4. Fused Oligothiophene Structures

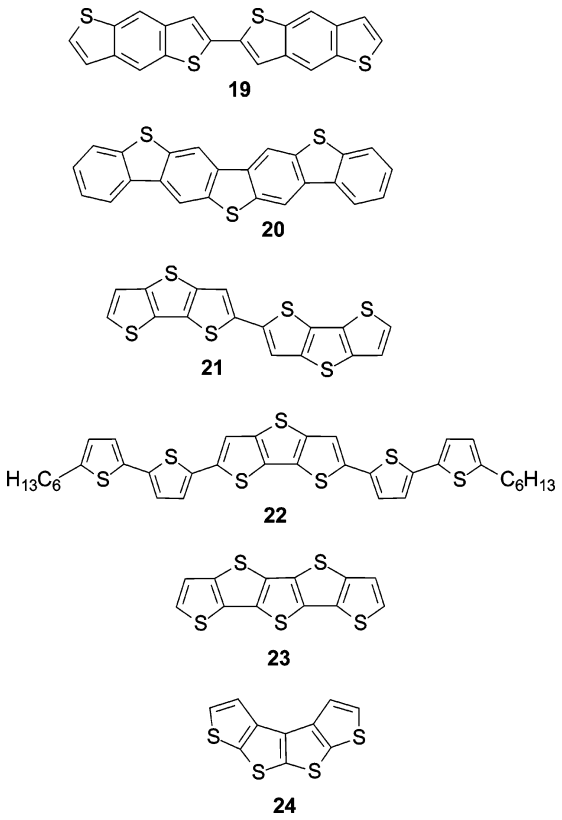

and the presence of regioisomers was found to degrade FET performance (0.03 $cm^2/(V\cdot s)$). However, utilization of a shutter during vacuum sublimation allowed different fractions of the material to be deposited on the devices, and fractions exhibiting high field-effect mobilities of 0.15 $cm^2/(V\cdot s)$ with I_{on}/I_{off} ratios $>10^6$ could be obtained.[145]

Sirringhaus and co-workers tested the fused thiophene derivative α,α′-bis(dithieno[3,2-*b*:2′,3′-*d*]thiophene) (**21**, Chart 4).[63,146] Crystal structures of this material reveal that this dimer does in fact pack in a face-to-face π-stacked structure (see Figure 4a). Hole mobilities up to 0.05 $cm^2/(V\cdot s)$ with an I_{on}/I_{off} ratio up to 10^8 were measured using this oligomer in both top and bottom contact FET devices.[63,146]

Iosip and co-workers have further utilized dithienothiophene in co-oligomers with thiophene (**22**, Chart 4).[147] Initial, unoptimized FET devices had hole mobilities of 0.02 $cm^2/(V\cdot s)$ with I_{on}/I_{off} ratios up to 10^6, which makes these co-oligomers very promising, and it will be interesting to see how optimized devices perform.

The dithienothiophene motif was extended out to seven linearly fused rings by Zhang and co-workers, and it was found that these oligomers also pack in a face-to-face π-stacking motif.[64,148] The electrical properties of the pentathienoacene (**23**, Chart 4) were measured in OTFT devices, and a mobility of 0.045 $cm^2/(V\cdot s)$ with I_{on}/I_{off} ratios up to 10^3 could be obtained when tested in the air.[149] The stability of this material is attributed to its large band gap of 3.29 eV.

Nenajdenko et al. have synthesized an annulated oligothiophene consisting of four fused thiophene rings (**24**, Chart 4).[150] X-ray crystallographic studies on single crystals of the material confirmed that the molecule is planar, which may give attractive electrical properties. However, the authors have not yet reported the thin film crystal structure or any mobility measurements.

2.3. Co-Oligomers

2.3.1. Thiophene–Thiazole Oligomers

A series of co-oligomers containing thiazole and thiophene rings were designed and synthesized by Li and co-workers.[127] Incorporation of electron-withdrawing thiazole rings reduced the HOMO levels of the molecules and increased the oxidative stability. The all-thiophene analogs showed severe p-doping when exposed to ambient conditions, but oligomers containing thiazole rings maintained a constant I_{on}/I_{off} ratio of 10^4 when devices were operated in air. The highest hole mobility was obtained with molecule **25** (Chart 5), giving a

Chart 5. Thiophene−Thiazole Oligomer Structures

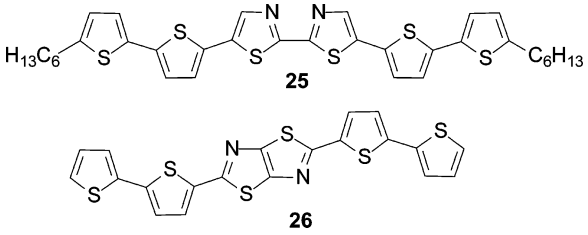

mobility of 0.01 $cm^2/(V\cdot s)$ when the substrate deposition temperature was 55 °C.[127] TEM images of the evaporated films show that the material forms discrete micrometer-sized crystals oriented in different directions, which may explain why these materials have the lower field-effect mobilities than the corresponding thiophene analogs.

A fused-ring derivative of thiazole, thiazolothiazole, has been used in co-oligomers with thiophene[151] and furan.[152] Thiazolothiazole rings are also electron-withdrawing, which should enhance the oxygen stability, and adding rigidity to the molecule should improve the planarity allowing for good π-orbital overlap. While the furan derivatives only exhibit hole mobilities in the range of $10^{-4}-10^{-3}$ $cm^2/(V\cdot s)$,[152] the thiophene derivative **26** (Chart 5) could achieve mobilities up to 0.02 $cm^2/(V\cdot s)$ when a substrate deposition temperature of 50 °C was used.[151]

2.3.2. Thiophene–Phenylene Oligomers

As an extension of previous work by Li et al.,[127] an effort to further deduce a correlation between HOMO levels and charge mobility was carried out with a larger series of co-oligomers of thiophene and either phenyl or thiazole rings.[153] Several oligomers containing different numbers of thiophene and phenyl rings with HOMO levels as different as 0.5 eV exhibited hole mobilities ranging from 0.01 to 0.03 $cm^2/(V\cdot s)$, and no correlation between mobility and HOMO energy was found. However, the authors did observe that lowering the HOMO energies, making the compounds harder to oxidize, led to lower off currents in devices. The authors conclude that the differences in mobility are mostly due to film morphology and the size of the grain boundaries[154] or problems with charge injection,[155] rather than the intrinsic charge transport ability of the material. The most notable oligomer in this series was a dihexyl-substituted bithiophene−phenylene−bithiophene (**27a**, Chart 6), with which mobilities of 0.02 $cm^2/(V\cdot s)$ could be obtained by both sublimation and solution processing.

Ponomarenko and co-workers used this same bithiophene−phenylene−bithiophene conjugated core and extended the alkyl chains from 6 to 10 carbons (**27b**). With this molecule they obtain mobilities of 0.3 $cm^2/(V\cdot s)$,[135] which is more than

Chart 6. Thiophene−Phenylene Oligomer Structures

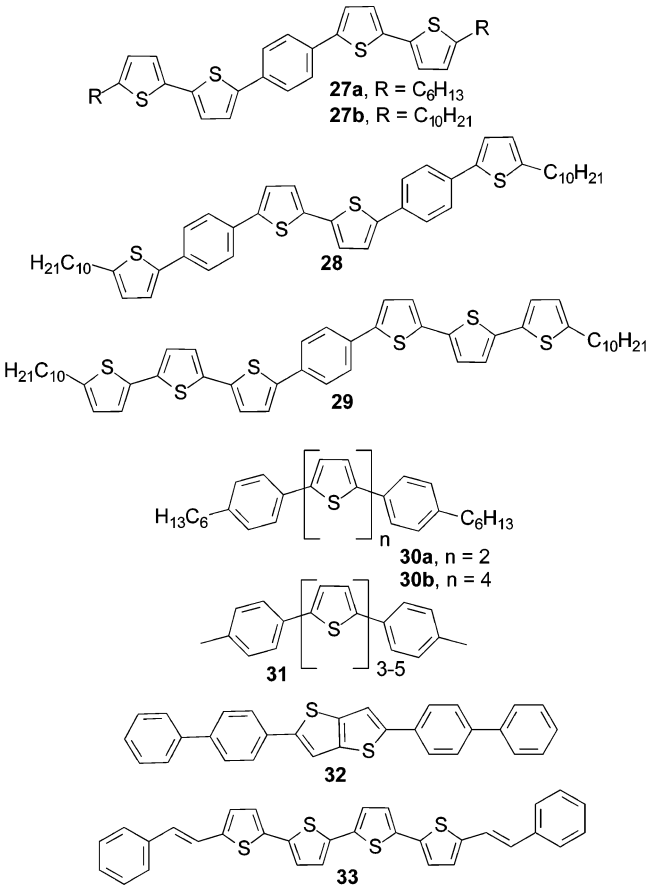

an order of magnitude higher than those that Hong et al. obtained with **27a**. The reason for this large increase in performance is not clear, but the authors attribute it to material purity and the use of cross-linked poly(hydroxystyrene) as the dielectric. Other phenylene−thiophene derivatives **28** and **29** (Chart 6) were also synthesized. It was found that **29** had similar properties to **27b**, whereas **28** had an order of magnitude lower mobility due to poor molecular ordering.[156] Electrochemical measurements of the oligomers containing a phenyl ring were shown to have better oxidative stability than the all-thiophene analogues, and FET devices could be operated in air.

Mushrush and co-workers completed another study on a series of phenylene−thiophene co-oligomers. While many of the oligomers studied displayed charge mobilities higher than 0.01 $cm^2/(V\cdot s)$, the bithiophene and quarterthiophene derivatives with hexyl−phenyl end groups (**30a,b**, Chart 6) had measured mobilities as high as 0.09 $cm^2/(V\cdot s)$ with I_{on}/I_{off} ratios up to 10^5.[157] These derivatives were also soluble enough to solution-process and are discussed in section 5.6. Each of the oligomers was found to orient with its long axis perpendicular to the surface, and the tilt angle of the molecule with respect to the substrate normal got smaller as the length of the longer oligomer increased. The authors also demonstrate the use of these materials in simple nonvolatile memory elements.

End substitution of thiophene oligomers with toluene has also been shown to be effective, regardless of the length of the thiophene core. Mohapatra and co-workers synthesized end-functionalized oligothiophenes with three, four, and five thiophene rings (**31**, Chart 6) and found that they all demonstrated field-effect mobilities around 0.03 $cm^2/(V\cdot s)$ and impressive I_{on}/I_{off} ratios approaching 10^9.[158] Interestingly, it was determined through X-ray diffraction and AFM studies that the odd-numbered oligomers assume a different crystal structure than the even-numbered oligomer, yet they all have similar electrical properties.

An oligomer containing a fused bithiophene core with biphenyl end groups (**32**, Chart 6) has been shown to perform well in FET devices. A field-effect mobility of 0.08−0.09 $cm^2/(V\cdot s)$ with an I_{on}/I_{off} ratio of 10^4 was measured when the oligomer was deposited at a $T_{dep} = 150$ °C.[159] The X-ray crystal structure reveals that the molecule has a planar structure, and devices were found to be stable in air for more than 1 month and upon exposure to UV irradiation for several hours.

An α-α′-distyryl-substituted quarterthiophene (**33**, Chart 6) was recently shown to have high mobility up to 0.1 $cm^2/(V\cdot s)$ with I_{on}/I_{off} ratios up to 10^5 when deposited on SiO_2 at $T_{dep} = 110$ °C.[160] These films display a terraced morphology with step heights equal to the length of the molecule. Most notably, devices made with this oligomer do not show any change in mobility, I_{on}/I_{off} ratio, or threshold voltage when stored in ambient conditions for more than a year. There is evidence that the instability of organic semiconductors is due to the susceptibility to p-type doping by interaction with ambient oxygen and therefore lowering the HOMO energy levels should lead to a decrease in oxidation.[83,161,162] However, in this case the compound with the highest HOMO energy level was found to be more stable than shorter oligomers with lower HOMO levels. Absorption of moisture leading to a change in morphology has also been implicated in device instability[163,164] and may play a role in this case if the longer oligomer is more effective at repelling moisture.

2.3.3. Thiophene–Fluorene Oligomers

Co-oligomers of fluorene and thiophene have been found to be stable in air, ambient light, and UV light exposure. Molecules containing one to four central thiophene units end-capped with fluorene units were explored.[83] OTFTs with a field-effect mobility up to 0.1 $cm^2/(V\cdot s)$ and I_{on}/I_{off} ratio up to 10^5 were achieved with the dihexyl-substituted derivative **34a** (Chart 7) containing a bithiophene core.[83,165] Locklin et al. investigated the same fluorene−bithiophene−fluorene oligomer in which the alkyl end caps were replaced with cyclohexyl rings (**34b**). Mobilities as high as 0.17 $cm^2/(V\cdot s)$ could be achieved when the oligomer was deposited at a substrate temperature of 130 °C.[79] At this temperature, the grain size was found to be larger than 10 μm, which could be contributing to the high charge mobility.

Chart 7. Thiophene−Fluorene Oligomer Structures

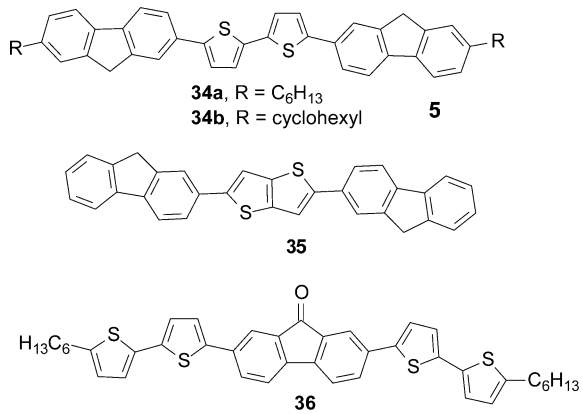

Chart 8. Thiophene−Acene Oligomer Structures

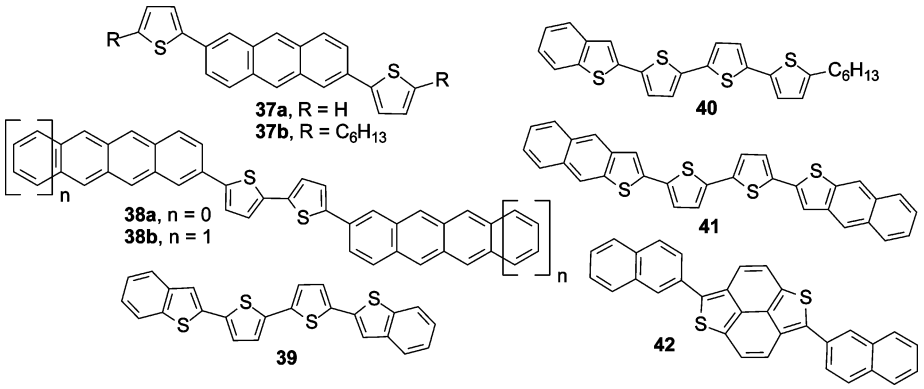

A similar oligomer containing a fused bithiophene core (**35**, Chart 7) has also been synthesized and tested. The fused core was used to lower the HOMO level due to the shorter effective conjugation length. This fused ring derivative gave a slightly lower mobility (0.06 $cm^2/(V\cdot s)$) than the bithiophene derivative but had similar environmental stability.[159] Further studies on this derivative showed that UV irradiation in air led to the formation of keto defects in the fluorene moiety.[166] These defects increased the threshold voltage and decreased mobility and drain current due to the formation of trap states within the material.

Three oligomers containing fluorenone and thiophene units have been synthesized and characterized by Porzio and co-workers.[167] The rationale for using the fluorenone moiety was based on its increased air stability as compared with fluorene and the ability of the carbonyl oxygen to hydrogen bond. Each of the molecules investigated was found to pack closely (3.2 Å) in a herringbone motif. However, only the derivative **36** (Chart 7) showed appreciable charge mobility (0.002 $cm^2/(V\cdot s)$ with an I_{on}/I_{off} ratio up to 10^6). In comparison to the other derivatives, oligomer **36** exhibited a more vertical orientation relative to the substrate and was more oxidatively stable due to the presence of the terminal alkyl chains.

2.3.4. Thiophene–Acene Oligomers

Papers published simultaneously by Ando et al.[168] and Meng et al.[169] utilize a molecule containing a central anthracene unit functionalized in the 2,7-positions with thiophene (**37a**, Chart 8). Meng et al. report higher mobilities of 0.02−0.06 $cm^2/(V\cdot s)$ and found that $T_{dep} = 80$ °C is the optimal deposition temperature.[169] Meng and co-workers also investigated the dihexyl derivative (**37b**) and found that it exhibited much higher mobilities ranging between 0.1 and 0.5 $cm^2/(V\cdot s)$. While films made from a single evaporation cycle performed well, they found that double evaporation (first at $T_{dep} = 120$ °C followed by a second evaporation at $T_{dep} = 80$ °C) produced the best films with high hole mobilities of 0.5 $cm^2/(V\cdot s)$ with I_{on}/I_{off} ratios of 10^7.[169] The first evaporation at high substrate temperatures was found to produce large grains covering the majority of the surface. The second deposition at lower temperatures filled in any cracks and voids resulting in continuous, highly conductive films. The mobility and I_{on}/I_{off} ratio of these devices remained stable over a year. This technique of double evaporation shows great potential for improving the film morphology and charge mobility of all materials deposited by thermal evaporation.

Merlo and co-workers have used anthracene as well as tetracene in co-oligomers with thiophene.[86] Here the thiophene moieties are placed at the center rather than at the ends of the molecules. Both the anthracene (**38a**) and tetracene (**38b**) derivatives (Chart 8) show similar solid-state and thin film structures, where they pack in triclinic unit cells and stand with their long axes nearly perpendicular to the substrate. FET measurements reveal that **38a** and **38b** have hole mobilities in the linear regime as high as 0.1 and 0.5 $cm^2/(V\cdot s)$, respectively.[86] The oligomers were also found to be more stable under ambient conditions than pentacene.

Deman and co-workers have investigated the structure−property relationships among a series of quarterthiophene oligomers with symmetric and asymmetric end functionalization.[128] The addition of alkyl chains was compared with incorporation of a benzo[*b*]thiophene end group. They found that alkyl chains led to a larger increase in mobility than adding a fused benzo[*b*]thienyl end group, as in the symmetric oligomer **39** (Chart 8). However, the asymmetric oligomer **40** (Chart 8) exhibited almost identical electrical characteristics as **39**, giving hole mobilities of 0.01 $cm^2/(V\cdot s)$ with an I_{on}/I_{off} ratio of 10^2.

A thiophene−acene derivative containing fused naphthalene end groups (**41**, Chart 8) was synthesized by Nicolas et al.[170] To synthesize the molecule, they utilize a strategy of introducing trimethylsilyl groups into the β-positions of the central thiophene rings, which cause the molecule to distort from planarity. This distortion prevents π-stacking, and therefore the molecules are soluble and easy to purify. A subsequent elimination of the trimethylsilyl groups restores the planarity of the molecule. Vacuum-evaporated films of this compound had lower charge mobilities than the nonfused acene derivatives discussed above, but that may be due to the use of PMMA/Ta_2O_5 as the dielectric. The reported mobility was 0.01 $cm^2/(V\cdot s)$ with an I_{on}/I_{off} ratio of only 29.[170]

Takimiya et al. synthesized a series of fused naphthodithiophene derivatives with different aryl ring substituents. Depending on the aryl groups used, the hole mobility varied from 10^{-4} to 10^{-1} $cm^2/(V\cdot s)$.[171] The use of naphthyl substituents (**42**, Chart 8) produced the best results, giving high a mobility of 0.11 $cm^2/(V\cdot s)$ with I_{on}/I_{off} ratios of 10^5 when deposited at $T_{dep} = 100-140$ °C.[171] At this temperature, large grains were produced, and the molecules were found to orient nearly vertically from the substrate. The authors attribute the lower mobilities in the other derivatives to the fact that the molecules exhibit a large tilt angle with respect to the substrate, resulting in poor intermolecular π-orbital overlap.

2.4. Selenophene Oligomers

Selenophene oligomers have been synthesized for comparison with thiophene oligomers by Kunugi et al.[172] In a

side-by-side comparison, it was found that an oligomer containing four selenophene units (**43**, Chart 9) could achieve a mobility of 3.6×10^{-3} cm^2/(V·s), while α-T4 had a mobility of $(5-8) \times 10^{-3}$ cm^2/(V·s) when deposited under the same conditions.

Chart 9. Selenophene Oligomer Structures

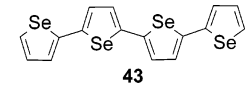

43

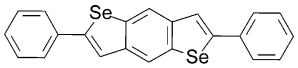

44

Since selenophene oligomers showed promise as semiconductors, the same authors further explored the use of other heavy chalcogen atoms in an attempt to increase the transfer integral between neighboring molecules and thus increase the field-effect mobility.[173] The semiconducting behavior of benzodichalcogenophenes containing thiophene, selenophene, and tellurophene analogues was explored.[174] Takimiya et al. found that the selenophene derivative **44** (Chart 9) performed twice as well as the thiophene analog, and an order of magnitude better than the tellurophene analog, giving field-effect mobilities of 0.17 cm^2/(V·s) with I_{on}/I_{off} ratios of 10^5.[174] The low performance of the tellurophene was attributed to the low aromaticity of the molecule.

2.5. N-Heterocyclic Oligomers

Copper phthalocyanine (**45**, Chart 10) is a commercially available molecule that has demonstrated p-type behavior in OTFT devices. When this molecule is deposited at substrate temperatures of 125 °C, highly crystalline films are formed that can achieve mobilities of 0.02 cm^2/(V·s) with I_{on}/I_{off} ratios of 10^5.[175] Thin films formed via Langmuir−Blodgett techniques also achieved similar mobilities.[176]

Epitaxially grown films of octaethyl platinum porphyrin (**46**, Chart 10) have been investigated by Noh and co-workers. By varying the T_{dep}, they were able to align the molecules either vertically (T_{dep} = room temperature) or horizontally (T_{dep} = 50 °C) with respect to the surface.[75] Films grown vertically had mobilities of 10^{-4} cm^2/(V·s), which was 2 orders of magnitude higher than those grown horizontally (10^{-6} cm^2/(V·s)).

Indolo[3,2-*b*]carbazoles have also demonstrated utility in OTFT devices. Wu and co-workers found that N-alkylation with long alkyl chains can induce self-assembly and dramatically increase the crystallinity and electrical performance of vacuum-sublimed films.[177] The octylphenyl derivative **47** (Chart 10) gave measured mobilities up to 0.12 cm^2/(V·s) and I_{on}/I_{off} ratios of 10^7, as well as good environmental stability under prolonged exposure to amber light. The enhanced environmental stability of this class of organic semiconductors has been attributed to low HOMO levels and large band gaps inherent to the materials. Further investigation into peripheral substitution of the indolo[3,2-*b*]carbazole core with halogen atoms found that bromine derivatives were thermally unstable, but chlorines placed in the 2 and 8 positions (**48**, Chart 10) increased the mobility 2 orders of magnitude as compared with the parent compound.[178] The increase in performance has been attributed to enhanced crystallinity and the ability to use higher substrate deposition temperatures due to the higher melting point of the halogenated derivative.

Amorphous polymeric triarylamines (TAAs) have been used for many years in OLED devices and are known to produce stable FET devices with hole mobilities on the order of 10^{-3} cm^2/(V·s).[179] Recently, Cravino et al. have demonstrated that high hole mobilities can be obtained with an amorphous oligomer that contains a TAA core with hexyl-terminated terthiophene arms (**49**, Chart 10). Hole mobilities up to 0.01 cm^2/(V·s) were measured, but with a fairly low I_{on}/I_{off} ratio of 10^2.[180] The authors present data for a thermally evaporated device, but performance in a solution-processed device as compared with the other TAA analogs presented in section 5.3 has yet to be reported. Furthermore, an in-depth comparison of the charge mobility in a series of commonly used TAA oligomers and their spiro-linked analogs has been done by Saragi and co-workers.[181] All compounds were found to exhibit hole mobilities in the range of $(1-8) \times 10^{-5}$ cm^2/(V·s) with an I_{on}/I_{off} ratio of 10^5 when operated in air. Notably, the parent TAA compounds were found to have slightly higher mobility but degraded rapidly in air, where the spiro-linked TAA analogs demonstrated very good stability over many months.

Extended aniline oligomers have also shown fairly good semiconducting properties when vacuum-deposited onto bare SiO_2. A hole mobility of up to 0.034 cm^2/(V·s) with an I_{on}/I_{off} ratio of 10^4 was measured with an oligomer containing 16 repeat units (**50**, Chart 10).[182]

The use of aryl−acetylene oligomers in FETs has been explored by Roy and co-workers. Surprisingly high mobilities were obtained with the dimethylamine-substituted molecule **51** (Chart 10), where a mobility of 0.3 cm^2/(V·s) with an I_{on}/I_{off} ratio of 10^5 was measured.[183]

Chart 10. Nitrogen-Containing Oligomer Structures

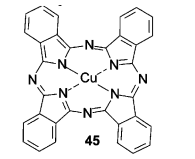

45

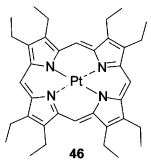

46

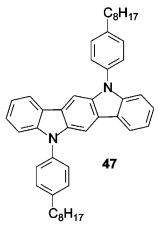

47

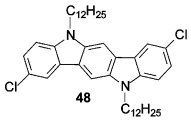

48

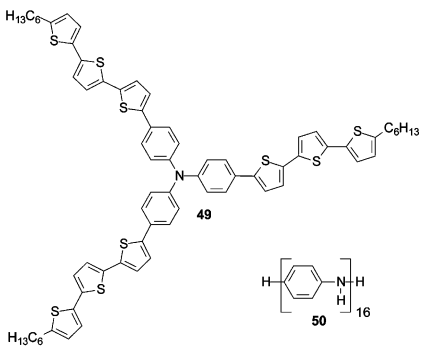

49

50

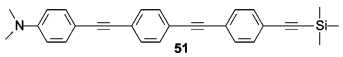

51

2.6. Tetrathiafulvalene Derivatives

To enhance the air stability of tetrathiafulvalene (TTF) by decreasing the electron-donating nature, Naraso and co-workers have synthesized a series of TTF derivatives with extended π-conjugation. The dinaphtho derivative **52** (Chart 11) was found to adopt a herringbone packing motif, and a

hole mobility of up to 0.4 $cm^2/(V\cdot s)$ with an I_{on}/I_{off} ratio of 10^3 could be attained in top contact devices.[184] However, in order to achieve air stability, incorporation of electron-deficient nitrogen heterocycles was needed. The quinoxalino derivative **53** (Chart 11) was found to pack in a face-to-face structure, and mobilities up to 0.2 $cm^2/(V\cdot s)$ with an I_{on}/I_{off} ratio of 10^6 could be measured even when tested under oxygen pressures up to 760 Torr.[184]

Chart 11. Tetrathiafulvalene Structures

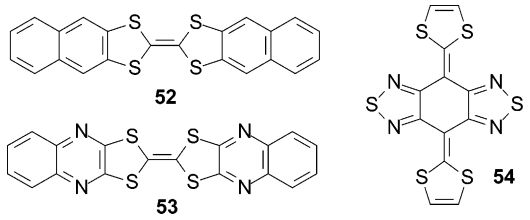

Morioka et al. have synthesized a series of TTF analogs that have a conjugated spacer that extends the π-conjugation. Of the series, only one molecule demonstrated appreciable field-effect mobility. Bis[1,2,5]thiadiazolo-*p*-quinobis(1,3-dithiole) (**54**, Chart 11) exhibited a field-effect mobility of 0.02 $cm^2/(V\cdot s)$ with an I_{on}/I_{off} ratio of 10^7.[185] Other derivatives with strongly electron-donating substituents did not exhibit any semiconducting behavior.

2.7. Summary

Table 1 provides a summary of data for vacuum-deposited p-type oligomers.

3. Vacuum-Deposited N-Type Oligomers

As discussed in section 1.2.3, organic semiconductors are commonly classified as either p-type (hole-conducting) or n-type (electron-conducting) depending on which type of charge carrier is more efficiently transported through the material. Despite inherent instability of organic anions, n-type organic materials are heavily sought for applications such as p−n junction diodes, organic photovoltaic devices,[7] and complementary logic bipolar transistors. The majority of work in this area has been to design molecules with increased electron affinity through substitution with electronegative elements to allow efficient electron injection into the LUMO and to increase hydrophobicity, which can decrease the environmental sensitivity of these materials by repelling moisture.[3,25] Recently a paper by Chua et al. demonstrated that the use of non-hydroxylated dielectric materials dramatically increases the electron mobility by reducing electron trapping at the interface between the semiconductor and the dielectric. Electron field-effect mobilities for organic semiconductors such as polyfluorene and polythiophene-based polymers, previously thought to only exhibit p-type behavior, were found to be in the range of 10^{-3} to 10^{-4} $cm^2/(V\cdot s)$, respectively, when a benzocyclobutene derivative was used as the dielectric.[32] This result has the potential to open the door to a broad range of materials that have not been previously considered for n-type conduction. However, the goal of this review is to highlight the use of synthetic chemistry to control the properties of the organic semiconductors, so further discussion on the effect of the dielectric will not be included here. For recent advances in organic dielectric materials, see reviews by Veres et al.[179] and Facchetti et al.[43] and the references contained within.

3.1. Quinoid Oligomers

One of the first organic oligomers used as an n-type organic semiconductor was tetracyanoquinodimethane (TCNQ) (**55**, Chart 12). Electron charge mobilities were measured from 10^{-10} to 10^{-5} $cm^2/(V\cdot s)$, depending on the amount of tetrathiofulvalene (TTF) dopant added.[57] Unlike p-type semiconductors that become doped upon exposure to air, the on/off ratio in TCNQ devices increased over time in the air from <10 to 450. The naphthalene derivative, 11,11,12,12-tetracyanonaphtho-2,6-quinodimethane (TCNNQ) (**56**, Chart 12), has also been shown to exhibit n-type semiconducting behavior without the need for TTF doping.[187]

Chart 12. Quinoid Oligomers

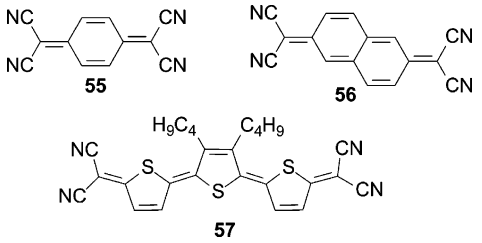

A terthiophene-based quinodimethane stabilized by dicyanomethylene groups at each end (**57**, Chart 12) was found to pack in a dimerized face-to-face π-stack, forming polycrystalline films with the long axes of the molecules approximately perpendicular to the substrate.[188,189] Optimized OTFT measurements gave field-effect mobilities as high as 0.2 $cm^2/(V\cdot s)$ with I_{on}/I_{off} ratios of 10^5 when measured under vacuum.[188] When deposited at $T_{dep} > 135$ °C, this oligomer also exhibited ambipolar behavior giving hole mobilities of 10^{-4} $cm^2/(V\cdot s)$ but a decreased electron mobility of $<10^{-4}$.[188] While the charge mobilities are low, this was one of the first demonstrations of ambipolar behavior from a single molecule.

3.2. Fullerene

The use of C_{60} (**58**, Chart 13) in OTFTs was first explored by Kastner et al.,[190] but Haddon and co-workers were the first to demonstrate efficient n-type semiconducting behavior. However, these materials are typically much less stable in the environment, and most devices must be operated in ultrahigh vacuum (UHV). A method of fabricating and testing devices under UHV was developed, and electron mobilities of 0.08 $cm^2/(V\cdot s)$ were measured. Surface modification of SiO_2 with tetrakis(dimethylamino)ethylene prior to C_{60} deposition was found to increase the mobility to 0.3 $cm^2/(V\cdot s)$.[58] C_{60} has also been used in conjunction with sexithiophene oligomers to form ambipolar field-effect transistors.[191,192]

Chart 13. Fullerene Structure

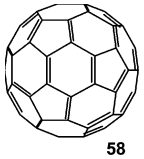

3.3. Tetracarboxylic Diimides and N-Heterocyclic Derivatives

Among the first n-type oligomers reported were naphthalene and perylenetetracarboxylic diimides. Horowitz first

Table 1. Summary of Processing and Device Data for Vacuum-Deposited P-Type Oligomers

oligomer	μ_h ($cm^2/(V\cdot s)$)	I_{on}/I_{off} ratio	T_{dep} (°C)	device structure[a]	physical properties	ref
1	>5.0	10^6	RT	TC gold on Si with poly(α-methyl styrene) dielectric		98
2	0.12	10^7	15	TC gold on Si/SiO_2 treated with OTS		82
3b	0.15	NR	85	TC gold on Si/SiO_2		104
4	0.18	10^4	175	TC gold on Si/SiO_2	λ_{em} = 454 nm	105
5	0.26	10^5	105	TC gold on Si/SiO_2 treated with HMDS		106
6	0.006	10^3	17	TC gold on Si/SiO_2; stable to testing in air		107
7	0.05	10^4	100	TC gold on Si/SiO_2 treated with OTS	λ_{abs}(solid) = 680 nm	108
8	0.45	NR	RT	TC gold on Si/SiO_2	$\pi-\pi$ spacing = 3.28 Å	109
9a	0.006	10^4	NR	BC gold on Si/SiO_2		117
9b	0.08	10^2	90	BC gold on Si/SiO_2		122
9c	0.02	10^4	NR	TC gold on Si/SiO_2 or glass with Al gate and PMMA dielectric		125
9c	0.075	10^4	N/A	TC gold on glass with Al gate and PMMA dielectric		119
9d	0.33	NR	>120	TC gold on Si/SiO_2		74
10a	0.03	10^5	NR	TC gold on Si/SiO_2 or glass with Al gate and PMMA dielectric		125
10a	0.23	NR	80	TC gold on Si/SiO_2	single-crystalline film	126
11a	0.2	10^5	25	BC gold on Si with PHS dielectric	HOMO = −5.41 eV	135
10b	0.1	NR	155	TC gold on Si/SiO_2	single-crystalline film	127
11b	0.5	10^5	25	BC gold on Si with PHS dielectric	HOMO = −5.39 eV	135
10c	0.13	10^4	NR	TC or BC with a metal gate and parylene C dielectric; molecular beam deposition		132
11c	0.5	10^5	RT	BC gold on Si with PHS dielectric; tested in air		134
10d	0.02	10^2	RT	TC gold on glass with Al gate and PMMA dielectric		113
12	3×10^{-4}	10^3	70	BC gold on Si/SiO_2	$\lambda_{abs}(CHCl_3)$ = 420 nm	137
13	0.009	10^3	90	BC gold on Si/SiO_2		122
14	8×10^{-4}	10	140	BC gold on Si/SiO_2		122
15	0.02	NR	80	TC gold on Si/SiO_2	$\pi-\pi$ spacing = 2.59 Å; $\lambda_{abs}(CHCl_3)$ = 388 nm	139
16	0.06	10^3	70	TC gold on Si/SiO_2 treated with HMDS	λ_{abs}(THF) = 429 nm; λ_{em}(THF) = 508 nm; HOMO = −5.78 eV; LUMO = −3.03 eV	140
17	6×10^{-4}	NR	80	TC gold on Si/SiO_2	λ_{abs} = 452 nm; λ_{em} = 503, 537 nm; HOMO = −4.45 eV; LUMO = −1.75 eV	141
18	0.055	NR	60	TC gold on glass with Al gate and PMMA dielectric	λ_{abs} = 487 nm; E_g = 2.55 eV	143
19	0.04	10^3-10^5	100	BC gold on Si/SiO_2		144
20	0.15	10^6	100	TC gold on Si/SiO_2 treated with HMDS		145
21	0.05	10^8	BC = 100 TC = 25	BC gold on Si/SiO_2; TC gold on glass with Al gate and PMMA dielectric	E_g = 2.3 eV; $\pi-\pi$ spacing = 3.5 Å	63, 146
22	0.02	10^6	30	TC gold on Si/SiO_2	λ_{abs} = 438 nm; HOMO = −5.23 eV; LUMO = −2.53 eV	147
23	0.045	10^3	80	TC gold on Si/SiO_2; tested in air	λ_{abs} = 342 nm; E_g(opt) = 3.20 eV; HOMO = −5.33 eV; LUMO = −2.04 eV	149
25	0.01	10^4	55	TC gold on Si/SiO_2; tested in air	λ_{abs} = 455 nm	127
26	0.02	10^4	50	TC gold on Si/SiO_2	$\lambda_{abs}(CHCl_3)$ = 445 nm; $\lambda_{em}(CHCl_3)$ = 502 nm; $\pi-\pi$ spacing = 3.6 Å	151
27a	0.02	10^3	RT	carbon paste TC on Si/SiO_2	HOMO = −4.90 eV; LUMO = −1.77 eV	153
27b	0.3	10^5	RT	BC gold on Si with PHS dielectric	HOMO = −5.55 eV	135
30b	0.07−0.09	10^3-10^5	RT or 50	TC gold on Si/SiO_2 or SiO_2 treated with HMDS	λ_{abs}(THF) = 432 nm; λ_{em}(THF) = 498 nm; E_g = 2.62 eV	157
31	0.03	10^6-10^9	RT	TC gold on Si/SiO_2; tested in vacuum		158
32	0.09	10^4	150	TC gold on Si/SiO_2	HOMO = −5.5 eV; E_g(opt) = 2.67 eV	159
33	0.1	10^5	110	TC gold on Si/SiO_2; tested in air	λ_{abs} = 455 nm; λ_{em} = 524 nm	160

Table 1 (Continued)

oligomer	μ_h ($cm^2/(V\cdot s)$)	I_{on}/I_{off} ratio	T_{dep} (°C)	device structure[a]	physical properties	ref
34a	0.11	10^5	140	TC gold on Si/SiO_2	λ_{abs}(solid) = 350 nm; HOMO = −5.36 eV; LUMO = −2.53 eV; E_g(opt) = 2.65 eV	83, 165
34b	0.17	10^5	130	TC gold on Si/SiO_2		79
35	0.06	10^4	150	TC gold on Si/SiO_2		159
36	0.002	10^6	130	BC Pt on Si/SiO_2; tested in vacuum	E_g(Echem) = 2.1 eV; E_g(opt) = 2.3 eV; IP = 5.38 eV	167, 186
37a	0.06	10^5	80	TC gold on Si/SiO_2	E_g = 2.8 eV	168, 169
37b	0.5	10^7	120/80	TC gold on Si/SiO_2	E_g = 2.8 eV	169
38a	0.12	10^8	100−125	BC gold on Si/SiO_2 bare or coated with poly(α-methyl styrene)		86
38b	0.5	10^8	175−215	BC gold on Si/SiO_2 coated with poly(α-methyl styrene)		86
39	0.01	10^2	70	TC gold on Si with PMMA/Ta_2O_5 dielectric; tested in air		128
41	0.01	10^1	70	TC gold on Si with PMMA/Ta_2O_5 dielectric; tested in air	λ_{abs}(DCB) = 428 nm	170
42	0.1	10^5	100−140	TC gold on Si/SiO_2; tested in vacuum	λ_{abs}(THF) = 501 nm; λ_{em}(THF) = 552 nm	171
43	0.0036	NR	60	BC gold on Si/SiO_2		172
44	0.17	10^5	60	TC gold on Si/SiO_2		174
45	0.02	10^5	125	BC gold on Si/SiO_2		175
46	10^{-4}	10^5	RT	TC gold on Si/SiO_2		75
47	0.12	10^7	50	TC gold on Si/SiO_2	λ_{abs} = 340 nm; HOMO = −5.12 eV; E_g = 2.8 eV	177
48	0.085	10^7	50	TC gold on Si/SiO_2 treated with OTS	HOMO = 5.26 eV; $\pi-\pi$ spacing = 3.5 Å	178
49	0.01	10^2	NR	TC gold on Si/SiO_2	λ_{abs} = 429 nm; λ_{em} = 500 nm	180
50	0.034	10^4	50	BC gold on Si/SiO_2	λ_{abs} = 306 nm; λ_{em} = 606 nm	182
51	0.3	10^5	NR	BC gold on Si/SiO_2		183
52	0.4	10^3	25	TC gold on Si/SiO_2 treated with OTS	E_g = 2.47 eV	184
53	0.2	10^6	80	TC gold on Al/Al_2O_3; operate under oxygen pressure	E_g = 2.11 eV; $\pi-\pi$ spacing = 3.41 Å	184
54	0.02	10^7	NR	BC gold on Si/SiO_2		185

[a] BC = bottom contact; TC = top contact; HMDS = hexamethyldisilazane; OTS = octadecyltrichlorosilane; PMMA = poly(methyl methacrylate); PHS = poly(hydroxystyrene).

demonstrated electron mobilities of 10^{-5} $cm^2/(V\cdot s)$ with *N*,*N*′-diphenyl-3,4,9,10-perylenetetracarboxylic diimide (**59a**, Chart 14).[193] Shortly after, 1,4,5,8-naphthalene tetracarboxylic dianhydride (NTCDA) (**60a**, Chart 14) was shown to have an electron mobility up to 0.003 $cm^2/(V\cdot s)$.[187] As discussed more thoroughly in section 6.1, Katz and co-workers could obtain high electron mobility with a difluoroalkyl-substituted naphthalenetetracarboxylic diimide (**60b**, Chart 14) that was also stable in ambient environments.[194]

Malenfant and co-workers reported that by optimizing deposition conditions, *N*,*N*′-dioctyl-3,4,9,10-perylenetetracarboxylic diimide (**59b**) had measured electron mobilities up to 0.6 $cm^2/(V\cdot s)$ when tested under vacuum but required gate voltages in excess of +75 V.[195] Chesterfield et al. have recently demonstrated that this same molecule can achieve a maximum mobility of 1.7 $cm^2/(V\cdot s)$ with an I_{on}/I_{off} ratio of 10^7 with passivation of the SiO_2 surface with poly(α-methylstyrene).[196]

Jones and co-workers investigated the core substitution of perylenetetracarboxylic diimides with cyano groups and found that it effectively lowered the LUMO energy and increased the solubility of these materials.[197] Cyclohexyl (**59c**) vs fluoroalkyl (**59d**) end substitution was also compared. Both oligomers exhibited low threshold voltages and good air stability. The fluoroalkyl derivative **59d** gave the highest electron mobility values of 0.64 $cm^2/(V\cdot s)$ with an I_{on}/I_{off} ratio of 10^4.

A tetrachloro derivative of didodecyl-perylenetetracarboxylic diimide has also been reported to have electron mobilities up to 0.1 $cm^2/(V\cdot s)$, as measured by pulse radiolysis time-resolved microwave conductivity (PR-TRMC).[198]

Bao and co-workers have demonstrated that commercially available metallophthalocyanines have fairly high electron mobilities and are air stable. In particular, copper hexadecafluorophthalocyanine (F_{16}CuPc) (**61**, Chart 14) could attain a mobility of 0.03 $cm^2/(V\cdot s)$ when deposited at T_{dep} = 125 °C.[199] The F_{16}CuPc molecules were found to stand essentially perpendicular to the SiO_2 surface, providing efficient charge transfer in the π-overlap direction. The air stability of the films was attributed to the low HOMO and LUMO levels of F_{16}CuPc, which make it less susceptible to oxidation. Recently, F_{16}CuPc was used in conjunction with CuPc to form ambipolar FET devices with hole and electron mobilities of 10^{-4} $cm^2/(V\cdot s)$.[200]

Dicyanopyrazinoquinoxaline derivatives have been developed by Nishida and co-workers for use as n-type transistor materials. The cited advantages of these materials are that

Chart 14. Tetracarboxylic Diimides and N-Heterocyclic Derivatives

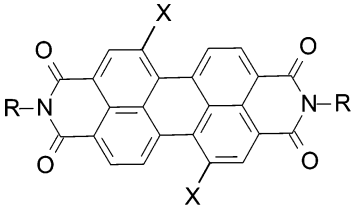

59a, R = phenyl, X= H
59b, R = C_8H_{17}, X= H
59c, R = cyclohexyl, X = CN
59d, R = $CH_2C_3F_7$, X = CN

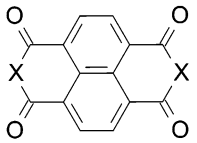

60a, X = O
60b, X = N-$CH_2C_7F_{15}$

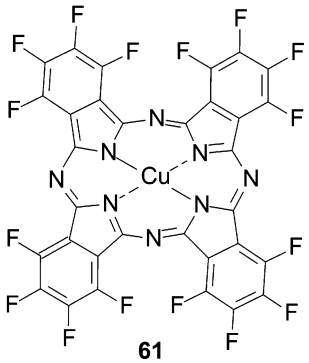

61

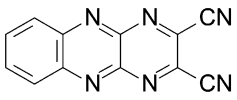

62

they have strong electron-accepting properties and substituents can be easily introduced to control the HOMO−LUMO energy gap and the molecular packing. However, to date, these materials have shown relatively low electron mobilities, the highest being 10^{-8}−10^{-6} cm^2/(V·s) with I_{on}/I_{off} ratios of 10^2−10^3 for molecule **62** (Chart 14).[201]

3.4. Substituted Oligothiophenes

Oligothiophenes are commonly p-type materials, but Demanze and co-workers were among the first to demonstrate that functionalization of these oligomers with electron-withdrawing groups can change them from p-type to n-type materials.[202] Electron injection was found to occur in a series of cyano-functionalized oligothiophenes with three to six thiophene rings (**63**, Chart 15).[203,204] However, no semiconducting behavior was seen in OTFT devices, because these cyano-substituted oligomers orient parallel to the substrate instead of perpendicular, resulting in poor charge transport in the direction measured in field-effect transistors.[204]

Chart 15. Substituted Oligothiophene Structures

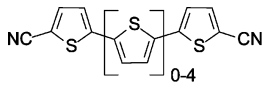

63

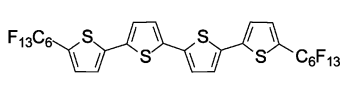

64

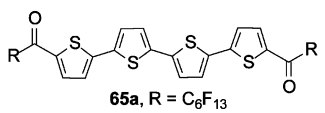

65a, R = C_6F_{13}
65b, R = C_6H_{13}

Facchetti and co-workers were the first to demonstrate that n-type behavior could be obtained in oligothiophenes through functionalization with perfluoroalkyl chains.[205] A series of oligomers was synthesized containing two to six thiophene rings functionalized in the α- or β-positions with perfluorohexyl chains.[140,206,207] The introduction of perfluoroalkyl chains on the oligomer cores was found to increase the ionization potential and electron affinity but minimally affected the ground- and excited-state energies of the molecules. OTFT devices measured under N_2 only displayed semiconducting behavior with positive gate voltages, indicating that these materials are exclusively electron conductors. Although the oligomers containing four to six thiophene rings performed similarly in optimized devices, the quarterthiophene derivative **64** (Chart 15) was found to have the highest electron mobility, up to 0.2 cm^2/(V·s), with an I_{on}/I_{off} ratio of 10^6 when deposited at T_{dep} = 100 °C.[140] All oligomers still exhibited semiconducting behavior when tested in the air, but mobilities were 2 orders of magnitude lower.[206]

In order to increase the air stability of oligomers functionalized with fluoroalkyl chains, Yoon and co-workers have synthesized quarterthiophenes with a ketone linkage between the oligomer and the alkyl chain. A ketone linkage was chosen due to ease of synthesis, added electron-withdrawing properties, and the prevention of fluoride elimination in the fluoroalkyl chain. The highest electron mobility of 0.6 cm^2/(V·s) with an I_{on}/I_{off} ratio $>10^7$ was obtained in vacuum with oligomer **65a** (Chart 15).[208] This oligomer also exhibited mobilities up to 0.02 cm^2/(V·s) when tested in the air. Interestingly, the non-fluorinated analog of this molecule (**65b**) exhibited fairly efficient ambipolar transport where an electron mobility of 0.1 cm^2/(V·s) and a hole mobility of 0.01 cm^2/(V·s) were measured for the same device.

3.5. Co-Oligomers

3.5.1. Thiophene−Phenylene Oligomers

Facchetti et al. have also investigated a series of perfluoroalkylated thiophene−phenylene oligomers, since co-oligomers of thiophene and phenylene have typically shown high p-type charge mobility and solution processiblity.[209] Similar to the all-thiophene derivatives discussed above, the addition of a perfluoroalkyl chains switches the semiconductor from p-type to n-type. Also analogous to the previous study, the phenyl−bithiophene−phenyl oligomer **66** (Chart 16), with the same conjugation length as **64** (Chart 15), was the best performing semiconductor in the series. The highest mobility obtained with **66** was 0.074 cm^2/(V·s) with an I_{on}/I_{off} ratio of 10^6 when deposited at T_{dep} = 110 °C. While these values are lower than the all-thiophene derivative, this oligomer shows promise as a stable memory device.[209]

Chart 16. Thiophene−Phenylene Oligomer Structures

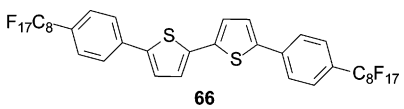

66

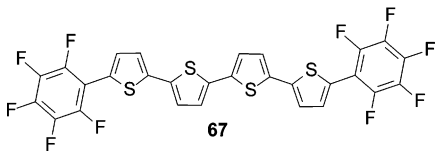

67

Co-oligomers of thiophene and perfluoroarenes were also found to exhibit n-type semiconducting behavior. A series of oligomers was synthesized that varied the placement of the perfluoroarene rings from the periphery to the core of the molecule[210] and the number of thiophene rings.[66] Non-

fluorinated phenyl−thiophene oligomers were also synthesized for comparison. The addition of perfluoroarene rings was found to lower the LUMO energies, thus facilitating electron injection. In addition, the incorporation of electron-rich and electron-deficient aryl rings was found to favor cofacial π-stacking instead of the typical herringbone structural motif exhibited by most oligothiophene derivatives.[66] This unique crystal structure is shown in section 1.3 (Figure 4c), for a quarterthiophene end-functionalized with perfluoroarene rings (**67**, Chart 16). This oligomer was the best performing molecule in the series, and mobilities as high as 0.5 $cm^2/(V\cdot s)$ with I_{on}/I_{off} ratios $>10^8$ have been measured. This oligomer outperforms the others in the series due to the planarity of the molecule, the closely π-stacked crystal structure, and the favorable crystalline film morphology. Ambipolar behavior was not observed in any of the oligomers in this series.

3.5.2. Trifluoromethylphenyl End-Capped Oligomers

Ando and co-workers have investigated anthracene derivatives end-capped with thiophene or a 4-trifluoromethylphenyl ring.[168] As discussed in section 2, the thiophene-capped anthracene **37a** (Chart 8) acts as a p-type semiconductor, while the trifluoromethylphenyl capped oligomer **68** (Chart 17) displays n-type behavior. This inversion in charge carrier

Chart 17. Trifluoromethylphenyl End-Capped Oligomer Structures

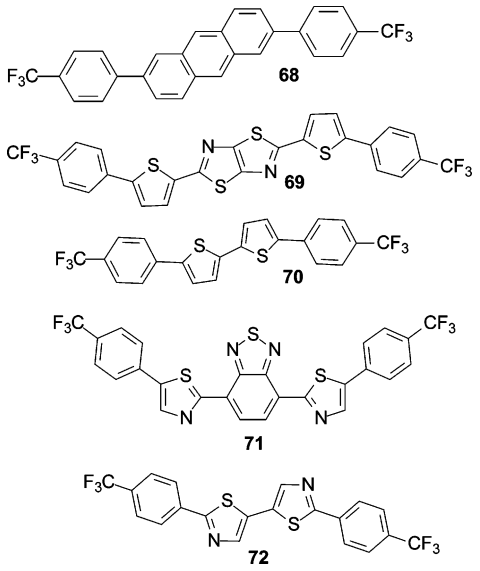

sign once again demonstrates the large effect of the end-group functionality. Electron mobility values of up to 0.0034 $cm^2/(V\cdot s)$ with I_{on}/I_{off} ratios of 10^4 could be obtained with **68**, but only when protected from air exposure. Devices made with this oligomer also required very high gate voltages to turn on (+75 V).[168]

Ando and co-workers have also used trifluoromethylphenyl end groups in conjunction with thiazolothiazole oligomers, which have a higher electron affinity. Electron mobilities for the oligomer **69** (Chart 17) were found to be as high as 0.30 $cm^2/(V\cdot s)$ with I_{on}/I_{off} ratios of 10^5, but similar to the anthracene derivatives, they needed a high gate voltage of +60 V to turn on the devices.[211] A bithiophene derivative with trifluoromethylphenyl end groups (**70**, Chart 17) was also found to give high electron mobilities of 0.18 $cm^2/(V\cdot s)$ but had an even higher threshold voltage of +76 V.[211] Both oligomers were found to have a nearly planar geometry, but the thiazolothiazole derivative (**69**) π-stacks in a face-to-face structure, whereas the bithiophene derivative (**70**) exhibits a herringbone packing motif. This difference in solid-state structure could account for the increased mobility of **69** as compared with **70**.

Oligomers derived from dithiazolylbenzothiadiazole have been synthesized by Akhtaruzzaman et al.[212] Only derivative **71** (Chart 17), with trifluoromethylphenyl end groups, showed appreciable semiconducting behavior, because it was the only oligomer that formed crystalline films as analyzed with XRD. Fairly high electron mobilities, up to 0.068 $cm^2/(V\cdot s)$, with I_{on}/I_{off} ratios of 10^4 were measured in top contact devices when the oligomer was deposited at $T_{dep} = 50$ °C.[212]

Recently, Ando and co-workers have synthesized a series of co-oligomers containing regioselectively linked thiazole and thiophene rings with trifluoromethylphenyl end groups.[67] When thermally evaporated onto bare SiO_2 at $T_{dep} = 25$ °C, all of the oligomers had fairly high electron mobilities ranging from 0.002 to 0.21 $cm^2/(V\cdot s)$ but also had very high threshold voltages from 55 to 78 V. Molecule **72** (Chart 17) exhibited the highest mobility and was also found to have a completely planar geometry with a unique two-dimensional columnar structure. With this molecule, a very substantial increase in charge mobility from 0.21 to 1.83 $cm^2/(V\cdot s)$ was seen when the bare SiO_2 substrates were treated with octadecyltrichlorosilane (OTS).[67] This mobility is among the highest electron mobilities reported to date for an organic semiconductor.

3.6. Perfluorinated Oligomers

As an alternative to adding fluorinated substituents to semiconducting oligomers, Sakamoto and co-workers have directly fluorinated the conjugated core of oligothiophenes,[213,214] pentacene, and tetracene.[215−217] The perfluorinated oligothiophenes (**73**, Chart 18) have positively shifted

Chart 18. Perfluorinated Oligomers

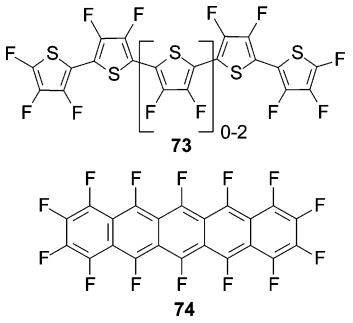

redox potentials relative to the non-fluorinated derivatives and were found to adopt a face-to-face π-stacked structure, which has the potential to give rise to efficient charge mobility.[213,214] However, transistor measurements have not been reported to date. Perfluoropentacene (**74**) also has positively shifted redox potentials and lower HOMO−LUMO levels.[216,217] However, in contrast to perfluorosexithiophene (**73**), perfluoropentacene (**74**, Chart 18) adopts the same herringbone structure as pentacene.[216,217] OTFTs fabricated with **74** gave high electron mobilities of 0.11−0.22 $cm^2/(V\cdot s)$ with I_{on}/I_{off} ratios of 10^5.[215−217] Bipolar OTFTs could also be made by depositing perfluoropentacene (**74**) and pentacene (**1**, Chart 1) layers on the same device. The best performance was attained when pentacene was deposited

Table 2. Summary of Processing and Device Data for Vacuum-Deposited N-Type Oligomers

oligomer	μ_e ($cm^2/(V\cdot s)$)	I_{on}/I_{off} ratio	T_{dep} (°C)	V_{th} (V)	device structure[a]	physical properties	ref
55	10^{-5}	10^3	RT	−15	BC gold on Si/SiO_2 (200 nm)		57
57	$\mu_e = 0.2$ $\mu_h = 10^{-4}$	10^6	130	11	BC gold on Si/SiO_2 (300 nm)	$E_g = 1.85$ eV; $E_{red} = -0.15$ V	188, 189
58	0.3	10^6	NR	−2.7	BC gold on Si/SiO_2 (300 nm) treated with TDAE; tested in UHV		58
59a	10^{-5}	NR	NR	NR	BC gold on glass with Al gate with PMMA dielectric		193
59b	1.7	10^6	75	15	BC gold on Si/SiO_2 (300 nm) coated with poly(α-methyl styrene); tested in 10^{-4} Torr of H_2		196
59c	0.1	10^5	90	15	TC gold on Si/SiO_2 (300 nm) treated with HMDS; tested in air	λ_{abs}(THF) = 530 nm; λ_{em}(THF) = 547 nm; $E_{red} = -0.07, -0.40$ V	197
59d	0.64	10^4	110	−20	TC gold on Si/SiO_2 (300 nm) treated with HMDS; tested in air	λ_{abs}(THF) = 530 nm; λ_{em}(THF) = 545 nm; $E_{red} = +0.04, -0.31$ V	197
60a	0.003	NR	50	NR	BC gold on Si/SiO_2 (500 nm); tested in vacuum		187
60b	0.1	10^5	70	NR	TC gold on Si/SiO_2 (300 nm); tested in air		194
61	0.03	10^4	125	NR	TC gold on Si/SiO_2 (300 nm)		199
62	10^{-6}	10^3	RT	NR	BC gold on Si/SiO_2	λ_{abs} = 398 nm; $E_{red} = -0.03, -0.87$ V	201
64	0.22	10^6	100	20−30	TC gold on Si/SiO_2 (300 nm) treated with HMDS	λ_{abs}(THF) = 398 nm; λ_{em}(THF) = 458, 489 nm; $E_{red} = -1.53, -1.75$ V	140, 206
65a	0.6	10^7	20−90	5−30	TC gold on Si/SiO_2 (300 nm) treated with HMDS	λ_{abs}(THF) = 465 nm; λ_{em}(THF) = 550 nm; $E_{red} = -0.88, -1.01$ V; HOMO = −6.36 eV; LUMO = −3.96 eV	208
65b	$\mu_e = 0.1$ $\mu_h = 0.01$	10^7	70−90	5−30	TC gold on Si/SiO_2 (300 nm) treated with HMDS	λ_{abs}(THF) = 430 nm; λ_{em}(THF) = 530 nm; $E_{red} = -1.06, -1.47$ V; HOMO = −6.38 eV; LUMO = −3.78 eV	208
66	0.074	10^6	110	55	TC gold on Si/SiO_2 treated with HMDS	λ_{abs}(THF)= 386 nm; λ_{em}(THF)= 439 nm; E_g(opt) = 2.9 eV	209
67	0.43	10^8	90	20	TC gold on Si/SiO_2 (300 nm) treated with HMDS	λ_{abs}(THF) = 415 nm; λ_{em}(THF) = 509, 540 nm; $E_{red} = -1.51, -1.65$ V; E_g = 2.63 eV	210
68	0.0034	10^4	20	75	TC gold on Si/SiO_2 (200 nm); no air exposure	$\lambda_{abs}(CHCl_3)$ = 379 nm; $\lambda_{em}(CHCl_3)$ = 439 nm; λ_{em}(solid) = 517 nm; E_g(opt) = 2.85 eV; $E_{red} = -1.68$ V	168
69	0.3	10^6	50	60	TC gold on Si/SiO_2 (200 nm); tested in vacuum	E_g(opt) = 2.48 eV; $E_{red} = -1.48, -1.68$ V	211
70	0.18	10^5	50	76	TC gold on Si/SiO_2 (200 nm); tested in vacuum	E_g(opt) = 2.77 eV; $E_{red} = -1.81, -1.93$ V	211
71	0.068	10^4	50	15	TC gold on Si/SiO_2 (600 nm); tested in vacuum	$\lambda_{abs}(CH_2Cl_2)$ = 465 nm; $\lambda_{em}(CH_2Cl_2)$ = 554 nm; λ_{em}(solid) = 607 nm; $E_{red} = -0.77, -1.3$ V	212
72	1.83	10^4	25	78	TC gold on Si/SiO_2 (200 nm) treated with OTS; tested in vacuum	$\lambda_{abs}(CHCl_3)$ = 363 nm; $\lambda_{em}(CHCl_3)$ = 442 nm; $E_{red} = -1.63$ V; E_g = 2.90 eV	67
74	0.22	10^5	50	50	TC gold on Si/SiO_2 (200 nm) treated with OTS; tested in vacuum	E_g = 1.92 eV; $E_{red} = -1.13$ V	215−217

[a] BC = bottom contact; TC = top contact; HMDS = hexamethyldisilazane; OTS = octadecyltrichlorosilane; PMMA = poly(methylmethacrylate).

first, followed by perfluoropentacene. In these devices, applying a positive and negative gate bias gave rise to μ_e = 0.022 $cm^2/(V\cdot s)$ and μ_h = 0.52 $cm^2/(V\cdot s)$, respectively.[216,217]

3.7. Summary

Table 2 provides a summary of data for vacuum-deposited n-type oligomers.

4. Single-Crystal Organic Semiconductors

As discussed in section 1, organic semiconductors form polycrystalline films, which makes it difficult to measure their intrinsic charge mobility. Therefore, single crystals of organic semiconductors are sought to study conduction that is not limited by grain boundaries and where the trap concentration is minimized.[41] There are many difficulties associated with single-crystalline materials. For example, the growth of large single crystals of organic materials is challenging, time-consuming, and not always possible. The resulting crystals are generally very brittle, and it is difficult to form electrical contact with the crystal without damaging it or introducing charge traps at interfacial sites. Therefore, it is likely that these materials will find use as models to study charge transport through organic materials, rather than being used for industrial purposes.

Despite these problems, new device fabrication methods are being developed to take advantage of the high charge mobilities found in single-crystalline materials. Some preliminary work is also being made on utilizing single-crystalline materials in industrially feasible processes by cocrystallization with a vitrifying agent[218] or using micropatterned self-assembled monolayers that direct the growth and orientation of large crystals in specific locations.[219]

4.1. Rubrene

As far back as 1971, a single-crystalline rubrene (**75**, Chart 19) was reported to have a TOF mobility of 2 $cm^2/(V\cdot s)$,[220] but it was not until 2003 that Podzorov and co-workers first demonstrated high performance organic tranistors with single crystals of rubrene.[221] Optimized fabrication techniques using a parylene dielectric gave a hole mobility of up to 8 $cm^2/(V\cdot s)$ with an on/off ratio of 10^5,[222,223] and mobilities up to 20 $cm^2/(V\cdot s)$ were later attained using air as the insulator.[224] Ambipolar behavior could also be observed in devices using PMMA as the dielectric and silver paste as the source and drain, where $\mu_h = 1.8$ $cm^2/(V\cdot s)$ and $\mu_e = 0.011$ $cm^2/(V\cdot s)$.[225]

Sundar et al. reported that mobilities of up to 15 $cm^2/(V\cdot s)$ could be achieved by constructing the source, drain, and gate electrodes, as well as the gate dielectric, on a flexible elastomeric substrate.[226] Using this method, electrical contact could be applied multiple times without damaging the fragile crystal, and this method was also used to measure the anisotropic charge transport through different crystallographic directions. The highest mobility was found to occur when measured along the *b*-axis, which coincides with the axis of the strongest π-orbital overlap as determined by the crystal structure (Figure 6).[226]

Chart 19. Single-Crystal Chemical Structures

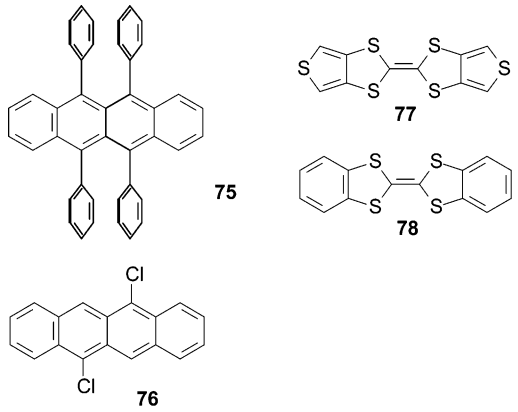

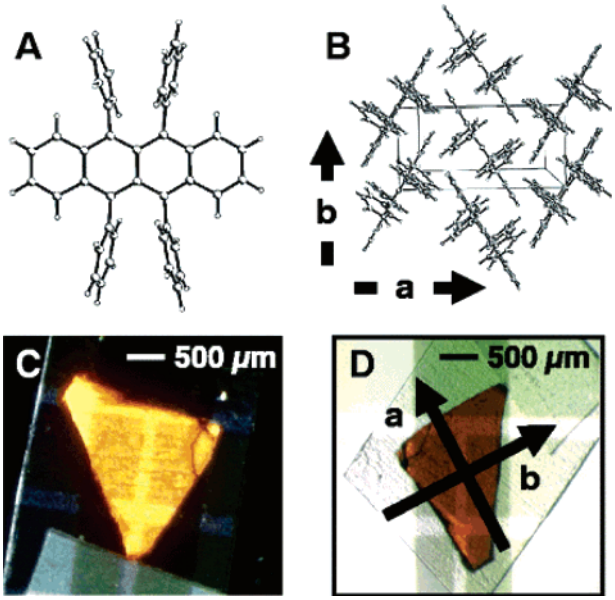

Figure 6. (a) Molecular structure of rubrene, (b) orthorhombic crystallographic structure of a single crystal of rubrene showing the enhanced $\pi-\pi$ overlap along the *b* direction and reduced overlap along the *a* direction, (c) optical micrograph of a sample viewed through crossed polarizers, and (d) natural facets on the crystal surface, which correspond well to the crystallographic data and enable easy identification of the *a* and *b* axes confirmed by Laue diffraction.[226] Reprinted with permission from *Science* (http://www.sciencemag.org), ref 226. Copyright 2006 American Association for the Advancement of Science.

Further studies have revealed that increasing the dielectric constant of the gate dielectric results in a decrease in mobility in rubrene single-crystal FETs.[227] The authors surmise that the dielectric becomes locally polarized due to the high concentration of charge carriers at the semiconductor/dielectric interface, which causes free carriers in the semiconductor to become self-trapped.[227] Therefore, even in single-crystal devices, mobility is dependent on the organic/dielectric interface.

While the electrical properties obtained with single crystals of rubrene are very important for determining intrinsic conductivity and the mobility limits for organic semiconductors, the type of device described above is not amenable to large-scale manufacturing processes. Therefore, Stingelin-Stutzmann and co-workers have devised a method where they cast a solution of rubrene containing 45 wt % 5,12-diphenylanthracene, which prevents the crystallization of rubrene.[218] After heating above the crystallization temperature of 240 °C and cooling, the mixture undergoes solid−solid demixing forming polycrystalline films where the rubrene is oriented parallel to the substrate surface. These films can be tested in air and give hole mobilities up to 0.7 $cm^2/(V\cdot s)$ with an I_{on}/I_{off} ratio of 10^8.[218] This is the first demonstration of an industrially feasible method for fabrication of rubrene transistors.

4.2. Linear Acenes

Field-effect transistors using tetracene (**2**, Chart 1) single crystals have been fabricated by a variety of methods giving mobilities ranging from 0.1 to 0.4 $cm^2/(V\cdot s)$.[228−230] The highest reported mobility of 1.3 $cm^2/(V\cdot s)$ by Goldmann et al. was obtained by first treating the gold contacts with trifluoromethylbenzenethiol and the SiO_2 with octadecyltrichlorosilane (OTS).[231] Devices fabricated this way with

Table 3. Summary of Processing and Device Data for Organic Single Crystals

oligomer	μ_h ($cm^2/(V\cdot s)$)	I_{on}/I_{off} ratio	processing conditions[a]	device structure[b]	ref
75	$\mu_h = 1.8$ $\mu_e = 0.011$	10^5	crystals grown from vapor in a stream of argon	TC silver paste on Si with PMMA dielectric	225
75	15	10^6	crystals grown from vapor in a stream of H_2	BC gold on PDMS with gold gate	226
75	0.7	10^8	mixture of 5% UHMW-PS, 45% 5,12-diphenyl anthracene, and 55% rubrene cast from toluene then crystallized at 240 °C	BC gold on Si with PHS dielectric	218
2	1.3	10^5	crystals grown from vapor in a stream of argon	BC gold treated with trifluoromethylbenzene thiol on Si/SiO_2 treated with OTS	231
1	1.4	10^5	crystals grown from vapor in a stream of argon	BC gold treated with trifluoromethylbenzene thiol on Si/SiO_2 treated with OTS	231
76	1.3	10^5	crystals grown from vapor	TC/TG graphite ink with parylene dielectric	232
77	1.4	10^5	crystals grown by slow evaporation from CB	BC gold on Si/SiO_2	234

[a] UHMW-PS = ultrahigh molecular weight polystyrene; CB = chlorobenzene. [b] BC = bottom contact; TC = top contact; TG = top gate; PMMA = poly(methyl methacrylate); PHS = poly(hydroxystyrene); OTS = octadecyltrichlorosilane.

single crystals of pentacene (**1**, Chart 1) also had a measured hole mobility of 1.4 $cm^2/(V\cdot s)$.[231]

Moon and co-workers have synthesized halogen-substituted tetracene derivatives and investigated the charge mobility in single crystals of these oligomers.[232] Monosubstitution of tetracene gave rise to herringbone molecular packing and lower mobilities ranging from 10^{-4} to 0.3 $cm^2/(V\cdot s)$. However, 5,11-dichlorotetracene (**76**, Chart 19) was found to have a slipped π-stacked structure and gave rise to hole mobilities up to 1.6 $cm^2/(V\cdot s)$ in FET devices.

4.3. Tetrathiafulvalene Derivatives

Tetrathiafulvalene (TTF) and its derivatives and their use as organic conductors and superconductors has been extensively reviewed by Bendikov et al.,[233] but a few examples of their use in field-effect transistors will be highlighted here.

A simple method for the growth of single crystals of dithiophene−tetrathiafulvalene (**77**, Chart 19)[234,235] and dibenzo-tetrathiafulvalene (**78**, Chart 19)[236] from a drop-cast solution has been demonstrated by Mas-Torrent and co-workers. These single-crystalline devices show field-effect mobilities as high as 1.4 $cm^2/(V\cdot s)$ with I_{on}/I_{off} ratios of 10^5, and polycrystalline OTFTs of **77** have mobilities in the range 0.01−0.1 $cm^2/(V\cdot s)$.[235] Further studies of the effect of the crystal structure on the electrical properties of TTF derivatives revealed that compounds that crystallize into herringbone molecular stacks of molecules with face-to-face π-orbital overlap have the highest hole field-effect mobilities.[234] Table 3 provides a summary of data for organic single crystals.

5. Solution-Processed P-Type Oligomers

As discussed in the previous sections, great strides are being made in producing organic semiconductors with properties that rival amorphous silicon. However, the majority of these materials are insoluble requiring the use of thermal evaporation to obtain thin films. Organic semiconductors have been touted as a "low cost" alternative to silicon, but for these devices to be cost-effective manufacturers must be able to use large-area, continuous, reel-to-reel methods for production, which would likely involve solution-based methods of semiconductor deposition. Solution-based methods also have the advantage of being conducted at ambient temperatures, expanding the repertoire of tolerant substrates to include flexible plastics or fabrics. Advances in deposition methods for organic semiconductors have been reviewed extensively and will not be discussed in detail here.[2,3,237,238]

Upon examination of the results in the following section on solution-processed oligomers, it becomes very evident that soluble, solution-processed organic semiconductors offer lower performance than their insoluble, vacuum-deposited counterparts. This fact can be attributed to a number of reasons. Chemical functionalization required to impart solubility acts to interrupt the natural π-stacking tendency of the molecules, which can inhibit charge mobility that relies heavily on π-orbital overlap. Also, typical solubilizing groups consist of insulating hydrocarbons, which can lower the overall conductivity of the materials. There are also many more variables to optimize in a solution-based deposition process as compared with thermal evaporation,[2] which complicates matters yet offers a greater parameter space within which to work. A few of the necessary considerations include (1) solubility of the oligomer (i.e., solvent, concentration, temperature), (2) solvent impurities, (3) deposition method (i.e., spin-casting, drop-casting, printing, stamping), (4) surface treatments, (5) solvent evaporation rate, (6) ability of the semiconductor to crystallize or self-assemble during or after solvent evaporation, etc. Many of these variables have been studied in depth for polymeric materials, but unfortunately most studies on oligomeric organic semiconductors focus on optimizing thermally evaporated films, and data for an unoptimized solution-processed device is presented as a side note. A recent emphasis on the synthesis and testing of soluble oligomers has produced promising results, but there is still very little information at present in the literature about the effect of the variables outlined above, and even fewer studies have been made to investigate the chemical structure−property relationships of solution-processed oligomers. Lessons learned from the polymeric systems are useful starting points for optimizing oligomeric

solution-processed films but do not necessarily apply because polymers have substantially different film-forming properties and surface-wetting characteristics than oligomeric systems.

5.1. Substituted Acenes

Pentacene has consistently shown the highest charge mobility of any of the organic semiconductors when deposited by vacuum evaporation, and thus many research groups have set out to synthesize processible versions of the small molecule. The first method for solubilizing pentacene was demonstrated by Herwig and Müllen.[239] A Diels−Alder reaction on the central ring of pentacene, producing oligomer **79** (Chart 20), was used to disrupt the planarity of the molecule, thus rendering it soluble. A similar, but more synthetically accessible route to the pentacene precursor **80** (Chart 20) was later demonstrated by Afzali et al.[240] In both cases, these precursors were spun-cast into films then heated to initiate a retro Diels−Alder reaction to convert the precursor to pentacene. The performance of OTFTs using this precursor route are competitive with vacuum-deposited pentacene devices, where solution-processed mobilities have been reported to be as high as 1.5 $cm^2/(V\cdot s)$ with an I_{on}/I_{off} ratio above 10^7 when films are annealed at 200 °C.[240] Tulevski et al. have further demonstrated that covalent attachment of a complementary monolayer onto the source and drain electrodes improves the electrical device characteristics of this solution-processed pentacene derivative.[241]

Afzali and co-workers have also demonstrated that conversion of pentacene precursors to pentacene can be photopatterned using UV light.[242] The most successful case was demonstrated by Weidkamp et al. where pentacene was derivatized with an acid-sensitive *N*-sulfinyl-*tert*-butyl carbamate. Co-deposition of this precursor with a photoacid generator gave efficient conversion to pentacene under UV light.[243] The ability to affect this conversion using light instead of heat is of great interest to further enhance substrate compatibility of these materials.

Chart 20. Structures of Substituted Acenes

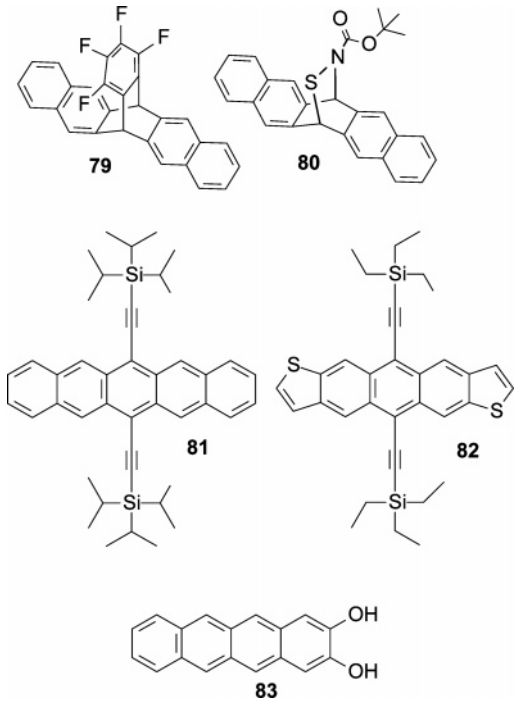

More recently, the Anthony group has developed elegant methods for solubilizing pentacene through the use of strategically placed substituents. They found that placement of bulky silyl groups separated from the acene by an alkyne spacer at the peri positions of pentacene not only gives rise to good solubility but also disrupts edge-to-face interactions and causes the molecules to adopt either 1-D "slipped-stack" or 2-D "bricklayer" face-to-face conformations rather than the usual herringbone pattern (see Figure 4b).[65] Face-to-face arrangement of the molecules significantly increases the π-orbital overlap of the pentacene rings in adjacent molecules and decreases the interplanar spacing of the aromatic rings.[244] This solubilizing method has also been demonstrated with other acene derivatives such as pentacene ethers,[245] acene-dithiophenes,[246] and longer hexa- and heptacenes.[247]

It was found that the only derivatives to give good OTFT performance were those that adopted a 2-D π-stacked arrangement. Solution-deposited films of these functionalized acenes gave rise to OTFT device hole mobilities up to 1.5 $cm^2/(V\cdot s)$ for pentacene derivatives such as **81** (Chart 20)[248] and mobilities as high as 1.0 $cm^2/(V\cdot s)$ for the anthradithiophene derivatives such as **82** (Chart 20).[249] These values were comparable to thermally evaporated devices made from the same materials,[250] suggesting that the molecules can assemble just as well in the solution as in the vapor phase. Notably, all the measurements reported were performed in air at room temperature suggesting that the introduction of these substituents improves the stability of the acenes.

Laquindanum and co-workers investigated solution-processed films of anthradithiophenes alkylated at the α-positions (**3b,c**, Chart 1).[104,251] They found that these materials had greater solubility and oxidative stability than pentacene while maintaining comparable charge mobility. Alkylated derivatives were sparingly soluble but could be cast from dilute solutions of hot chlorobenzene, followed by solvent evaporation in a vacuum oven at relatively high temperatures. Field-effect mobilities up to 0.02 $cm^2/(V\cdot s)$ were obtained with **3b**, but these had an order of magnitude lower mobility as compared with vacuum-evaporated films of the same material.[104]

Finally, Tulevski and co-workers demonstrated the first monolayer solution deposition of an acene derivative.[252] A tetracene derivatized at one end with ortho-hydroxyl functionalities (**83**, Chart 20) organizes into upright monolayers on the surface of aluminum oxide. Assembling these molecules into nanoscale transistor channels produced gate-voltage-dependent devices but only when the source−drain distance was less than 60 nm. While this idea of attaching the semiconductor to the gate dielectric could have wide reaching applications, it still remains to be seen whether it is a viable approach to transistor fabrication.

5.2. Substituted Oligothiophenes

By far the most commonly investigated candidates for solution-processed organic semiconductors are oligothiophenes.[59,253] Like most highly conjugated molecules, unsubstituted oligothiophenes have very poor solubility as a consequence of $\pi-\pi$ stacking. However, thiophenes offer many possibilities for functionalization in both the α- and β-positions and are compatible with a wide range of chemical transformations.[59,254]

One of the first solution-processed oligothiophenes was reported by Dimitrakopoulos and co-workers. They synthesized an oligothiophene containing internal vinyl linkages

(**83a**, Chart 21) that was soluble in hot *N*-methylpyrrolidinone (NMP). Spun-cast top contact devices gave mobilities up to 0.001 $cm^2/(V\cdot s)$ with I_{on}/I_{off} ratios of 10^2.[255] These values are much lower than that obtained with films deposited by molecular beam deposition ($\mu = 0.012$ $cm^2/(V\cdot s)$, $I_{on}/I_{off} = 10^3$), but the authors state that no effort was made to optimize the films.[255]

Chart 21. Substituted Oligothiophenes

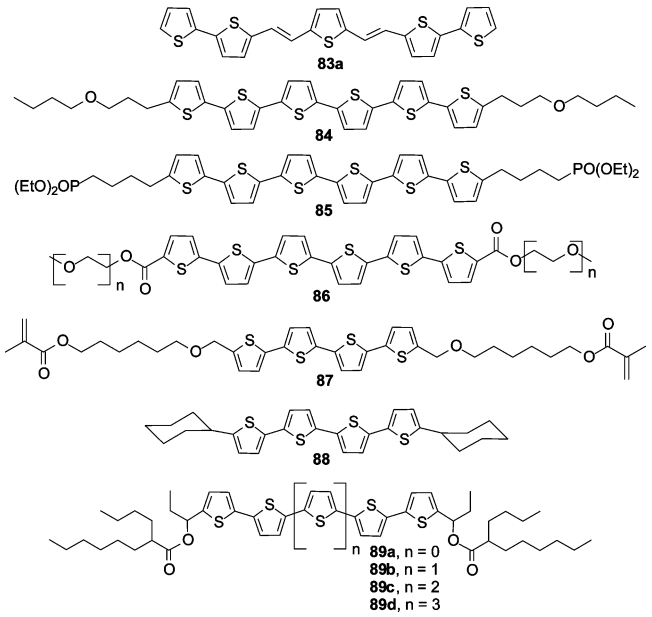

The majority of the early efforts to solubilize oligothiophenes used linear alkyl chains at the α- and ω-positions. Dihexyl-substituted quarter-,[125,126] penta-,[251] and sexithiophenes[251,256] were all sufficiently soluble to fabricate transistors from solution, giving decent mobilities ranging from 0.01 to 0.05 $cm^2/(V\cdot s)$. However, these materials were only sparingly soluble and required the use of either hot chlorinated deposition solvents or pre-heated substrates, which limits the feasibility of a large-scale manufacturing process. Katz et al. found that incorporating an oxygen into the alkyl chains (**84**, Chart 21) effectively doubled the solubility without decreasing the electrical properties,[256] but the solubility was still low in these materials.

To further increase the room temperature solubility, Afzali et al. developed a method to incorporate α,ω-dibutylphosphonate end groups into sexithiophene oligomers (**85**, Chart 21).[257] The incorporation of this polar moiety renders the material highly soluble and greatly simplifies the purification. These oligomers can be spun-cast from a variety of solvents and exhibit charge mobilities up to 0.002 $cm^2/(V\cdot s)$ after annealing at 80 °C. While the charge mobility is fairly low, the materials do exhibit high I_{on}/I_{off} ratios of 10^6, indicating that this synthetic method produces very pure materials.

Sandberg et al. have synthesized sexithiophene oligomers end-functionalized with poly(ethylene oxide) (PEO) (**86**, Chart 21).[258] The materials were found to have very interesting self-assembly behavior[259] and form alternating thiophene and PEO lamella in thin films. However, PEO tends to sequester ions so it was found that extensive washing was necessary to remove impurities and ions from the films. The charge mobilities of washed films were on the order of 10^{-4} $cm^2/(V\cdot s)$ with I_{on}/I_{off} ratios up to 10^3.[258]

McCulloch and co-workers[260] followed by Huisman and co-workers[261] both published oligomers utilizing bisacrylate end groups on a oligothiophene core (**87**, Chart 21) to allow crosslinking of the films after processing. Introduction of these end groups gave the oligomers enhanced solubility and film-forming properties. McCulloch et al. also demonstrated that the liquid crystalline nature of these materials could be exploited to enhance order and packing.[260] In both cases, however, the charge mobilities decreased by an order of magnitude after polymerization of the end groups, suggesting that polymerization induces a morphology change that decreases the degree of π-orbital overlap between the aromatic cores. While there is much room for improvement in the charge transport of cross-linking oligomers, these approaches demonstrate an interesting way to align and pattern organic semiconductors.

A quarterthiophene oligomer with cyclohexyl end groups (**88**, Chart 21) was reported by Locklin et al. Cyclohexyl substitution gave the material high solubility in warm chlorinated solvents, and devices fabricated by drop-casting a solution of the oligomer in a closed, static atmosphere of solvent vapor gave mobilities as high as 0.06 $cm^2/(V\cdot s)$ with I_{on}/I_{off} ratios of 10^5.[79]

Murphy, Chang, and co-workers have developed a general synthetic method for incorporating thermally removable solubilizing groups into a series of oligothiophenes containing four to seven thiophene rings (**89**, Chart 21).[90,262] Branched secondary esters were introduced at the α- and ω-positions of the oligomers, rendering up to seven linear thiophene rings soluble in common organic solvents at room temperature.[90] After spin-casting films from chloroform onto SiO_2, the solubilizing groups can be removed via an ester thermolysis reaction by heating to 200 °C. It was found that the quarterthiophene derivative performed poorly due to incomplete surface coverage after thermolysis. However, very reproducible, highly ordered films of the penta-, sexi-, and heptathiophene derivatives were formed using this method. No odd/even effects were observed, and charge mobility was found to slightly increase with conjugation length. Measured mobilities ranged from 0.02 to 0.06 $cm^2/(V\cdot s)$ for the series, with I_{on}/I_{off} ratios greater than 10^5.[78,89,90,262] It was found that surface treatments that rendered the substrate hydrophobic resulted in poor quality films and low charge mobility. Further increases in mobility and I_{on}/I_{off} ratio, as well as a decrease in hysteresis in devices can be obtained by depositing ultrathin films from an inkjet printer.[263] Notably, high mobilities were measured even in single monolayer films, indicating that efficient charge transport can be attained in monolayer films, contrary to previous thought.[48,49]

5.3. Star-Shaped Oligomers

Instead of adding substituents to the sides or ends of linear oligomers, altering the architecture to a branched or star shape has also been demonstrated as a viable method for increasing the solubility. One of the first examples of radial-substituted molecules was given by the Müllen group, where the hexabenzocoronene derivative **90** (Chart 22) was found to have TOF mobilities up to 1.0 $cm^2/(V\cdot s)$.[264] This group recently demonstrated that FET mobilities up to 0.01 $cm^2/(V\cdot s)$ with I_{on}/I_{off} ratios of 10^4 could be attained through a specialized zone casting technique from THF.[265]

Since then a variety of cores including hexaethynylbenzene,[266] trithienobenzene,[267,268] benzene,[269,270] and truxene[271] have been radially substituted with oligothiophenes. In general, the star-shaped oligothiophenes have good solubility and film-forming properties but show decreased mobilities

Chart 22. Star-Shaped Oligomers

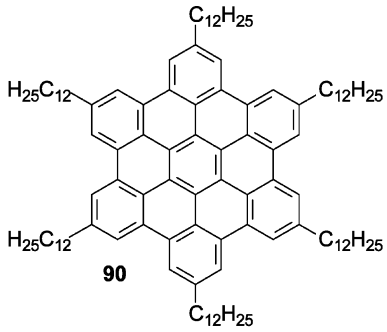

90

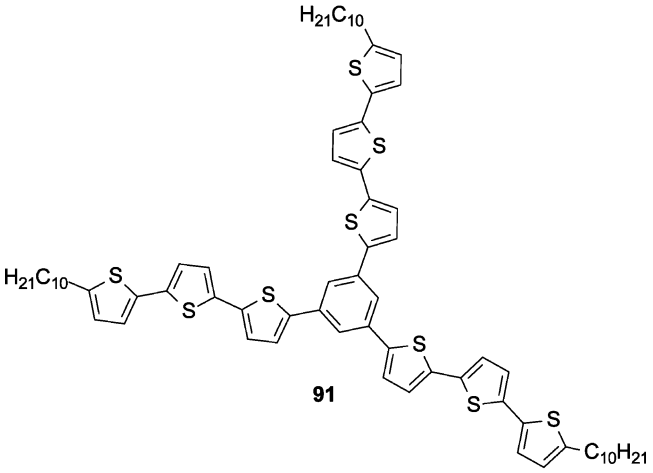

91

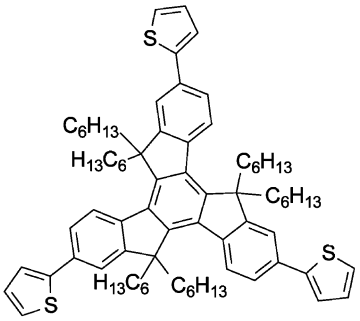

92

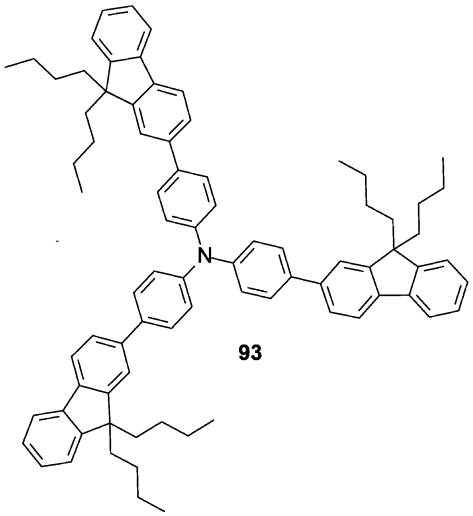

93

as compared with the linear thiophene analogs. The highest charge mobility reported in an OTFT device for these materials is 10^{-3} cm^2/(V·s) with I_{on}/I_{off} ratios of 10^3 for molecule **92** (Chart 22) containing a truxene core.[271] The higher mobility of this material could be due to the extended π-delocalization through this core as compared with the other cores mentioned. It is interesting to note, however, that increasing the length of the thiophene arms on the truxene core was found to decrease the crystallinity of the stars and thus resulted in lower hole mobilities.[271]

Another class of star-shaped semiconducting oligomers is the triarylamines (TAAs). TAA oligomers and polymers are commonly used as the hole transport material in OLEDs but have also been used to some extent in OTFTs. (For further discussion on the TOF mobility of molecular glasses, see the references contained in the review by Strohriegl and Grazulevicius.[272]) Sonntag et al. have reported star-shaped molecules incorporating a TAA core with carbazole or fluorene (**93**, Chart 22) side arms.[273] Charge mobilities of these materials were all similar at $\sim 10^{-4}$ cm^2/(V·s), which is comparable to that of the star-shaped oligothiophenes discussed above. However, the TAA stars had much higher I_{on}/I_{off} ratios of 10^5, low threshold voltages, and high stability under ambient conditions.

5.4. N-Heterocyclic Oligomers

Locklin et al. reported ambipolar behavior in layer-by-layer deposited phthalocyanines with alternating cationic and anionic functional groups (**94**, Chart 23).[274] The ambipolar transport was attributed to an ion-modulated electrical conduction mechanism, which stabilizes the oxidized or reduced species in the channel region. Measured mobilities were on the order of 10^{-5} to 10^{-4} cm^2/(V·s).[274]

A tetrabenzoporphyrin derivative (**95**, Chart 23), solubilized in a similar fashion to the pentacene precursor reported

Chart 23. N-Heterocyclic Oligomers

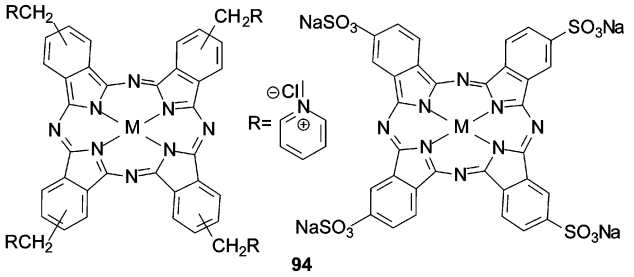

94

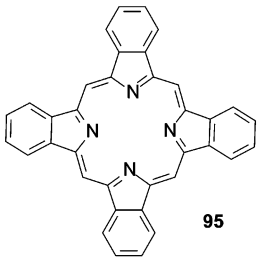

95

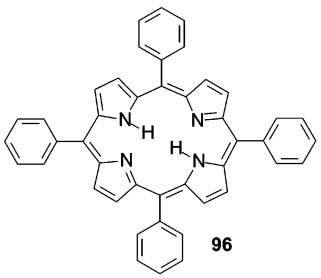

96

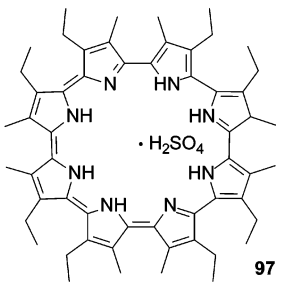

97

Chart 24. Oligofluorene Structure

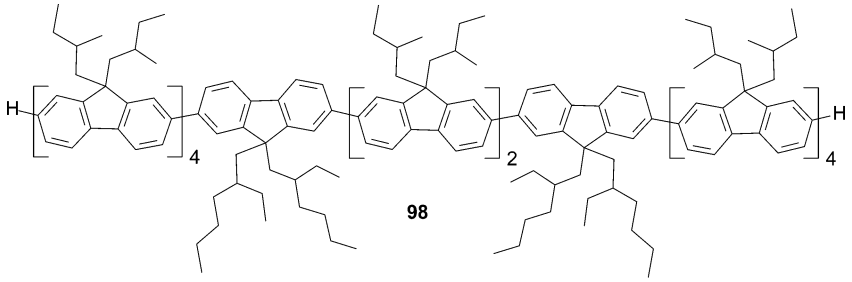

98

by Herwig and Müllen,[239] was synthesized by Ito and co-workers.[275] Spun-cast films of the precursor were heated at 210 °C for 5 min to initiate a retro-Diels−Alder reaction that gives the pure benzoporphyrin. Reported mobilities range up to $\sim 10^{-2}$ cm^2/(V·s) with I_{on}/I_{off} ratios of 10^5.[275,276]

Checcoli et al. reported the use of 5,10,15,20-tetraphenylporphyrin (**96**, Chart 23) as a p-type organic semiconductor for OTFT devices.[277] The porphyrin was deposited by spray coating from a chloroform solution, and mobilities from 0.007 to 0.012 cm^2/(V·s) were measured. One drawback to the use of porphyrins in OTFTs is the sensitivity to oxygen, which requires operation of these devices under vacuum.

The use of the Langmuir−Blodgett solution deposition technique to make oriented multilayer films of cyclo[8]-pyrrole (**97**, Chart 23) on silicon has been reported by Xu and co-workers.[278] Based on the area per molecule calculated from the isotherm curves, the molecules orient perpendicularly on the water surface, tilted at about 65° in a face-to-face conformation. The field-effect mobility of films consisting of 30 layers varied between 0.09 and 0.68 cm^2/(V·s) with I_{on}/I_{off} ratios above 10^4.[278] While these materials look promising, the current−voltage curves given are not ideal and could be affected by oxygen or acid doping.

Indolo[3,2-*b*]carbazoles have been synthesized and tested by Wu and co-workers and have been found to give good OTFT performance as well as good environmental stability under prolonged exposure to amber light. As is common with most organic semiconductors, films deposited by vacuum sublimation give much higher performance ($\mu = 0.12$ cm^2/(V·s), I_{on}/I_{off} ratio $= 10^7$), but the 5,11-bis(4-octylphenyl)-indolo[3,2-*b*]carbazole derivative **47** (Chart 10) also gave decent mobilities of 10^{-3} cm^2/(V·s) with I_{on}/I_{off} ratios 10^5 when spun-cast from chlorobenzene.[177] The enhanced environmental stability of this class of organic semiconductors has been attributed to low HOMO levels and large band gaps inherent to the materials.

5.5. Co-Oligomers

Several co-oligomers based on fluorene and thiophene have been reported by Meng and co-workers. The best performing material was the dihexyl-substituted fluorene−bithiophene−fluorene oligomer **34a** (Chart 7), which was soluble enough to be cast from hot chlorinated solvents. The measured charge carrier mobility of solution-cast films was on the order of 10^{-3} cm^2/(V·s).[83,165] Devices made from vacuum-evaporated films of the same oligomer could achieve field-effect mobilities of 0.1 cm^2/(V·s),[165] indicating that the materials are much less ordered when deposited from solution. More notably, these semiconductors do not exhibit any decrease in the I_{on}/I_{off} ratios after more than 2 months exposure to air and ambient light.

Hong and co-workers have synthesized a series of phenylene−thiophene oligomers, and thoroughly examined several parameters for solution processing of the dihexyl-substituted bithiophene−phenylene−bithiophene derivative **27a** (Chart 6).[153] Films were cast from xylene, toluene, 1,2-dichloroethane, and chlorobenzene onto bare silicon, PMMA, or glass resin coated substrates heated to 80−110 °C. Mobilities obtained were in the range of 0.005−0.02 cm^2/(V·s) with I_{on}/I_{off} ratios ranging from 10^2−10^4.[153] These values are similar to those obtained with sublimed films of this oligomer.

Mushrush and co-workers have also published a similar series of mixed phenylene−thiophene oligomers that have good solubility and performance.[157] Here, the most notable compound in the series is a dihexyl-substituted phenyl−bithiophene−phenyl oligomer (**30a**, Chart 6) that displays solution-cast mobilities up to 0.02 cm^2/(V·s) and vacuum-evaporated mobilities up to 0.09 cm^2/(V·s), both with I_{on}/I_{off} ratios of 10^4.[157] In order to obtain high performance from the solution-processed films, the authors found that casting from a xylene solution onto substrates heated to $\sim$110−120 °C patterned with a fluorocarbon electronic coating gave the best results.[157]

Yasuda et al. have reported OTFT measurements on a monodisperse dodecafluorene substituted with ethylhexyl solubilizing groups (**98**, Chart 24).[69] Spun-cast films deposited on rubbed polyamide, heated to 140 °C then quenched to room temperature exhibit a monodomain glassy-nematic structure. In these films, a hole mobility of 0.012 cm^2/(V·s) with an I_{on}/I_{off} ratio of 10^4 was measured, which is twice as high as polyfluorene.[69] The measured field-effect mobilities were also found to be anisotropic, where charge transport parallel to the backbone is greater than that perpendicular.

5.6. Summary

Table 4 provides a summary of data for solution-processed p-type oligomers.

6. Solution-Processed N-Type Oligomers

6.1. Naphthalenetetracarboxy Diimide Derivatives

Katz and co-workers reported one of the first air-stable n-type oligomers based on a naphthalenetetracarboxylic diimide framework incorporating fluorinated alkyl chains (**60b**, Chart 14). Films were drop cast from a heated solution of the oligomers in α,α,α-trifluorotoluene. This method produced devices with mobilities up to 0.01 cm^2/(V·s), which is an order of magnitude lower than mobilities obtained in vacuum-deposited films.[194] It was also noted that

Table 4. Summary of Processing and Device Data for Solution-Processed P-Type Oligomers

oligomer	μ_h ($cm^2/(V\cdot s)$)	I_{on}/I_{off} ratio	processing technique[a]	device structure[b]	physical properties	ref
80	0.9	10^7	SC 1−2 wt % $CHCl_3$; heat at 200 °C for 1.5 min	BC gold on Si/SiO_2 treated with HMDS	λ_{abs} = 254 nm	240
81	1.5	10^5	spread 1−2 wt % in toluene; heated in air at 90 °C for 2 min	BC gold on Si/SiO_2 treated with pentafluorobenzene thiol; measured in air	λ_{abs} = 307 nm	248
82	1.0	10^7	spread 1−2 wt % in toluene; heated in air at 90 °C for 2 min	BC gold on Si/SiO_2 treated with pentafluorobenzene thiol; measured in air	λ_{abs}= 555 nm; λ_{em} = 561 nm	249
3b	0.01−0.02	$<10^3$	DC 0.2−1 wt % hot CB; evaporate solvent at 100 °C	BC gold on Si/SiO_2		104, 251
83	0.0014	10^2	SC from NMP heated to 80 °C	TC gold on Si/SiO_2	λ_{abs}(solid) = 545, 411, 370 nm	255
10a	0.0015−0.07	NR	DC 0.1 wt % CB onto substrates heated to 100 °C	BC gold on Si/SiO_2	λ_{abs} = 391 nm[279]	126
10a	0.012	10^4	SC 6 × 10^{-2} M $CHCl_3$ onto substrates heated to 110 °C	TC gold on Si/SiO_2 treated with octylsilane		125
10b	0.04	$< 10^3$	DC 0.1 wt % in hot CB; anneal at 50 °C	TC gold on Si/SiO_2		251
10c	0.015−0.05	$>10^4$	DC 0.1 wt % CB or TCB; anneal at 70 °C	BC gold on Si/SiO_2		251, 256
84	0.006−0.01	NR	DC 0.1 wt % CB or TCB; anneal at 70−100 °C	BC gold on Si/SiO_2		256
85	0.0005−0.004	10^3−10^4	SC from $CHCl_3$; anneal at 80 °C	BC gold on Si/SiO_2		257
86	0.0001−0.001	$<10^3$	SC 2−4 mg/mL $CHCl_3$; vacuum anneal at 100 °C; soak in water 2 h; anneal in 100 °C toluene vapor	BC gold on Si/SiO_2 treated with HMDS		258
88	0.06	10^5	DC 7 × 10^{-2} M bromobenzene at 40 °C in a closed atmosphere of solvent vapor	BC gold on Si/SiO_2		79
89a,b	0.01−0.06	10^5	SC 3 mg/mL $CHCl_3$; anneal at 200 °C in N_2 20 min	TC gold on Si/SiO_2	λ_{abs}($CHCl_3$): 4 = 400 nm 5 = 424 nm	78, 90, 262
89c	0.08	10^8	inkjet printed 2 mg/mL anisole; anneal at 200 °C in N_2 for 20 min	BC gold on Si/SiO_2	λ_{abs}($CHCl_3$) = 440 nm	263
89d	0.12	10^8	inkjet printed 2 mg/mL anisole; anneal at 200 °C in N_2 for 20 min	BC gold on Si/SiO_2	λ_{abs}($CHCl_3$) = 455 nm	280
90	0.01	10^4	zone cast from 0.25 mg/mL THF at 51 °C onto substrate at 46 °C	TC gold on Si/SiO_2		265
91	0.0002	10^2	spun-cast from $CHCl_3$	BC gold on Si/SiO_2	λ_{abs} = 405 nm; λ_{em} = 464, 489 nm	270
92	10^{-3}	10^3	SC from $CHCl_3$	TC gold on Si/SiO_2; tested in air	λ_{abs}(solid) = 343 nm; λ_{em}(solid) = 381 nm	271
93	10^{-4}	10^5	DC from toluene or $CHCl_3$	BC gold on Si/SiO_2	λ_{abs} = 365 nm; λ_{em} = 408 nm; HOMO = −5.2 eV; LUMO = −2.1 eV	273
95	10^{-2}	10^5	SC 0.7 wt % $CHCl_3$ at 55 °C; annealed at 210 °C for 5 min in N_2	BC gold on Si/SiO_2		281
96	7 × 10^{-3}	NR	spray coated from $CHCl_3$	BC Al/Cr coplanar grid source and drain on Si/SiO_2; tested in vacuum		277
97	0.09−0.68	10^4	30 layers deposited from a Langmuir−Blodgett trough	TC gold on Si/SiO_2	E_g = 0.63 eV	278
47	7 × 10^{-3}	10^5	SC 1.0 wt % CB; dry in vacuum oven	TC gold on Si/SiO_2 treated with OTS	HOMO = −5.12 eV; E_g(opt) = 2.8 eV	177
34a	0.002	NR	DC 2 mg/mL hot CB	NR	HOMO = −5.36 eV; LUMO = −2.53 eV	83, 165
27a	0.005−0.02	10^3−10^4	cast 200 ppm CB on substrates heated to 80−110 °C	carbon paste TC with PMMA dielectric	HOMO = −4.90 eV; LUMO = −1.77 eV	153
30a	0.001−0.02	10^4	cast 200−400 ppm xylenes onto fluorocarbon patterned substrates heated to 110 °C	TC gold on Si/SiO_2 treated with HMDS or ITO/glass	λ_{abs} = 373 nm; λ_{em} = 436, 460 nm; E_g(opt) = 2.97 eV	157
98	0.01	10^4	SC 0.5 wt % $CHCl_3$; anneal under N_2 at 140 °C	BC gold on rubbed polyimide substrate with gold top gate		69

[a] SC = spun-cast; DC = drop-cast; CB = chlorobenzene. [b] TC = top contact; BC = bottom contact.

this method of solution deposition produced uneven films that resulted in a range of mobilities across the substrate. Although the stability of the solution-processed films was not reported, the authors point out that substitution with fluorinated alkyl chains renders the thermally evaporated films air stable, allowing devices to be cycled many times over in the air.

Though this review aims to highlight synthetic efforts toward small molecule organic semiconductors, it is worth noting that Babel and Jenekhe have synthesized and tested a ladder polymer, namely, poly(benzobisimidazobenzophenanthroline) (BBL) (**99**, Chart 25),[282] that is also based on a naphthalenetetracarboxylic diimide derivative. These ladder polymers can be spun-cast from methanesulfonic acid and exhibit electron field-effect mobilities up to 0.1 $cm^2/(V\cdot s)$ in ambient conditions. When compared with a similar polymer with identical optical and redox properties, it was found that film morphology was the major determinate in obtaining high charge mobility.[282]

Chart 25. Chemical Structures of Solution-Processed N-Type Oligomers

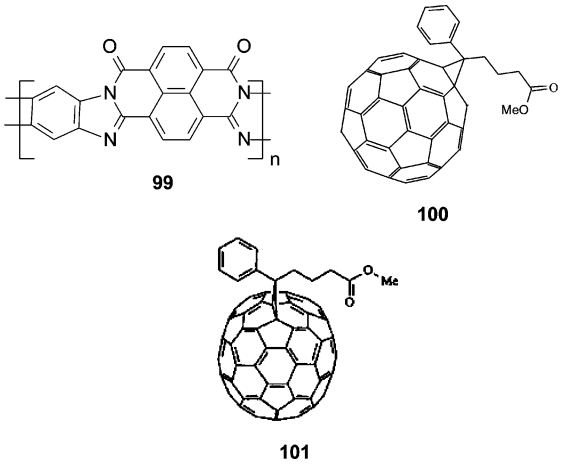

6.2. Fullerene Derivatives

Fullerene-based materials have demonstrated promise for n-type conduction in organic materials. Therefore, efforts to solublize this small molecule have been made through a variety of methods. The most successful of these has been [6,6]-phenyl C_{61}-butyric acid methyl ester (**100**, Chart 25), commonly referred to as PCBM, which was originally developed for use in heterojunction photovoltaics.[283−285] The charge transport in PCBM has been investigated in depth[286] and has been found to be dependent on the choice of electrodes[287,288] and the gate dielectric used.[289] The highest electron mobilities reported are 0.2 $cm^2/(V\cdot s)$, obtained when a PVA dielectric layer is used with top contact LiF/Al electrodes.[289] However, a large hysteresis was seen and attributed to charge trapping at the dielectric−semiconductor interface. Lee and co-workers also demonstrated that devices fabricated from solution-processed dielectric and semiconductor layers, as well as a soluble silver precursor for the electrodes, were able to obtain mobilities up to 0.003 $cm^2/(V\cdot s)$.[287]

Ambipolar transistors were first demonstrated by Dodabalapur and co-workers using thermally evaporated oligomers (discussed in section 3).[191,192] Meijer and co-workers were the first to demonstrate a solution-processed ambipolar field-effect transistor, using a blend of PCBM and poly[2-methoxy-5-(3′,7′-dimethyloctyloxy)]-*p*-phenylene vinylene (MDMO-PPV).[290] The blend device gave hole and electron mobilities in the range of 10^{-4} and 10^{-5} $cm^2/(V\cdot s)$, respectively. These hole mobilities are comparable to transistors utilizing only the PPV derivative, but the electron mobility was 2 orders of magnitude lower than that in a pure PCBM transistor. Anthopoulos and co-workers later demonstrated that devices consisting of PCBM alone could exhibit ambipolar transport, giving hole and electron mobilities in the range of 10^{-3} and 10^{-2} $cm^2/(V\cdot s)$, respectively.[291] However, this material is unstable in ambient conditions and must be tested under high vacuum. Recently, Anthopoulos and co-workers have also tested the soluble C_{70} equivalent ([70]PCBM) (**101**, Chart 25) and found similar, albeit lower,

Table 5. Summary of Processing and Device Data for Solution-Processed N-Type Oligomers

oligomer	μ_e ($cm^2/(V\cdot s)$)	I_{on}/I_{off} ratio	processing technique[a]	device structure[b]	physical properties	ref
60b	0.01	NR	DC from 200−400 ppm trifluorotoluene heated to 100 °C	TC gold on Si/SiO_2		194
99	0.1	10^3-10^5	SC 0.1 wt % solution in MSA; washed with water and dried under vacuum at 70 °C; anneal at 100−125 °C for 10−30 min	BC gold on Si/SiO_2 treated with HMDS	E_g(opt) = 1.8 eV	282
57	0.002	NR	cast from CB; annealed in a stream of H_2 at 60 °C for 1 h	TC silver on Si/SiO_2		189
100	0.01 (μ_h = 0.008)	10^6	SC 1 mg/mL CB; vacuum annealed	BC gold on Si/SiO_2 treated with HMDS; test under high vacuum	HOMO = −6.1 eV; LUMO = −3.7 eV; E_g = 2.4 eV	291
100	0.2	10^5	SC 3 wt % CB	TC LiF/Al or Cr on ITO/glass with a PVA dielectric; test under argon		289
101	0.001	10^4	DC 10 mg/mL CB onto substrate heated to 60 °C; annealed in vacuum at 115 °C for several hours	BC gold on Si/SiO_2 treated with HMDS; test under high vacuum at 40 °C		292

[a] SC = spun-cast; DC = drop-cast; CB = chlorobenzene; MSA = methanesulfonic acid. [b] TC = top contact; BC = bottom contact; HMDS = hexamethyldisilazane; PVA = poly(vinyl alcohol).

mobilities to PCBM. However, devices made with [70]PCBM are much more stable and reproducible, and the necessary annealing time to produce high-quality transistors is also reduced.[292]

6.3. Other Oligomers

Pappenfus et al. gave an account of the electron charge mobility of the terthiophene-based quinodimethane **57** (Chart 12). Films cast from chlorobenzene had electron mobilities up to 0.002 $cm^2/(V \cdot s)$, which is comparable to values obtained with the thermally evaporated devices.[189]

6.4. Summary

Table 5 provides a summary of data for solution-processed n-type oligomers.

7. Conclusions and Outlook

When one surveys the vast amount of literature on organic semiconductors that has emerged in the last 10 years, it becomes apparent that great strides are being made to develop materials that have properties that equal or surpass those of the standard inorganic semiconductors. Yet, there is still much to be learned, because we still do not have a complete understanding of the fundamental limits of charge mobility through organic materials and the true effect that oxygen, moisture, and light has on device performance. It has been shown that through chemical modification of the core oligomer or the addition of peripheral functional groups, the dominant charge carrier sign and the three-dimensional molecular structure can be tuned. However, it is still difficult to ascertain absolute structure−property relationships due to the large variation of processing conditions, device structure, and testing method used by each individual research group. A standardized method for evaluating new organic semiconductors could allow for comparison between materials and help predict chemical structures that would give superior properties.

Also, reproducibility and the standard deviation in performance of devices made with organic semiconductors have largely been ignored in the literature. This information is crucial for determining the true efficacy of a material, and reporting this information should become routine. In order to correlate device performance with film morphology and molecular structure, the electrical properties across the entire substrate must be taken into account. Reporting only the best mobility is misleading because it is likely that the one working device has a different morphology or molecular structure than the bulk of the film.

Therefore, when designing the next generation of organic semiconducting materials one must strive to (1) balance processibility with electrical performance, (2) control the molecular structure and morphology when the material is processed into thin films, (3) balance the molecular energy levels to achieve efficient charge injection and mobility while maintaining stability to the ambient environment, and (4) tailor the semiconductor/dielectric and the semiconductor/electrode interfaces to minimize charge trapping and contact resistance. Accomplishing these goals is no small feat and will require effort from many different scientific disciplines to successfully synthesize new materials, understand the fundamental processes governing ordering and charge transport, and manufacture devices at a low cost.

8. Glossary

AFM	atomic force microscopy
BC	bottom contact
CB	chlorobenzene
DC	drop-cast
DMF	*N*,*N*-dimethylformamide
DMSO	dimethylsulfoxide
E_g	HOMO−LUMO gap
GIXD	grazing incidence X-ray diffraction
IP	ionization potential
HMDS	hexamethyldisilazane
HOMO	highest occupied molecular orbital
ITO	indium tin oxide
LUMO	lowest unoccupied molecular orbital
NEXAFS	near-edge X-ray absorption fine structure
n-type	negative-type (electron-conducting)
OFET	organic field-effect transistor
OLED	organic light-emitting diode
OTFT	organic thin film transistor
OTS	octadecyltrichlorosilane
p-type	positive-type (hole-conducting)
PCBM	phenyl C_{61}-butryic acid methyl ester
PDMS	poly(dimethyl siloxane)
PHS	poly(hydroxystyrene)
PMMA	poly(methyl methacrylate)
PVA	poly(vinyl alcohol)
RF-ID	radio frequency identification tag
SC	spun-cast
SCLC	space charge limited current
SEM	scanning electron microscopy
T_{dep}	substrate deposition temperature
TAA	triarylamine
TEM	transmission electron microscopy
TC	top contact
THF	tetrahydrofuran
TOF	time-of-flight
TTF	tetrathiafulvalene
XRD	X-ray diffraction

9. Acknowledgments

This work was supported by the Director, Office of Science, Office of Basic Energy Sciences, and the Division of Materials Sciences and Engineering of the U.S. Department of Energy under Contract No. DE-AC03-76SF00098.

10. References

(1) Horowitz, G. *Adv. Mater.* **1998**, *10*, 365.
(2) Bao, Z.; Rogers, J. A.; Katz, H. E. *J. Mater. Chem.* **1999**, *9*, 1895.
(3) Dimitrakopoulos, C. D.; Malenfant, P. R. L. *Adv. Mater.* **2002**, *14*, 99.
(4) Dimitrakopoulos, C. D. *Thin-Film Transistors* **2003**, 333.
(5) Burroughes, J. H.; Bradley, D. D. C.; Brown, A. R.; Marks, R. N.; Mackay, K.; Friend, R. H.; Burns, P. L.; Holmes, A. B. *Nature* **1990**, *347*, 539.
(6) Kovac, J.; Peternai, L.; Lengyel, O. *Thin Solid Films* **2003**, *433*, 22.
(7) Brabec, C. J.; Sariciftci, N. S.; Hummelen, J. C. *Adv. Funct. Mater.* **2001**, *11*, 15.
(8) Coakley, K. M.; McGehee, M. D. *Chem. Mater.* **2004**, *16*, 4533.
(9) Crone, B.; Dodabalapur, A.; Gelperin, A.; Torsi, L.; Katz, H. E.; Lovinger, A. J.; Bao, Z. *Appl. Phys. Lett.* **2001**, *78*, 2229.
(10) Someya, T.; Katz, H. E.; Gelperin, A.; Lovinger, A. J.; Dodabalapur, A. *Appl. Phys. Lett.* **2002**, *81*, 3079.
(11) Brown, A. R.; Pomp, A.; Hart, C. M.; Deleeuw, D. M. *Science* **1995**, *270*, 972.
(12) Crone, B.; Dodabalapur, A.; Lin, Y. Y.; Filas, R. W.; Bao, Z.; LaDuca, A.; Sarpeshkar, R.; Katz, H. E.; Li, W. *Nature* **2000**, *403*, 521.
(13) Drury, C. J.; Mutsaers, C. M. J.; Hart, C. M.; Matters, M.; de Leeuw, D. M. *Appl. Phys. Lett.* **1998**, *73*, 108.
(14) Forrest, S. R. *Nature* **2004**, *428*, 911.

(15) Garnier, F.; Hajlaoui, R.; Yassar, A.; Srivastava, P. *Science* **1994**, *265*, 1684.
(16) Sirringhaus, H.; Tessler, N.; Friend, R. H. *Science* **1998**, *280*, 1741.
(17) Rogers, J. A.; Bao, Z.; Meier, M.; Dodabalapur, A.; Schueller, O. J. A.; Whitesides, G. M. *Synth. Met.* **2000**, *115*, 5.
(18) Rogers, J. A.; Bao, Z.; Baldwin, K.; Dodabalapur, A.; Crone, B.; Raju, V. R.; Kuck, V.; Katz, H.; Amundson, K.; Ewing, J.; Drzaic, P. *Proc. Natl. Acad. Sci. U.S.A.* **2001**, *98*, 4835.
(19) Sirringhaus, H.; Kawase, T.; Friend, R. H.; Shimoda, T.; Inbasekaran, M.; Wu, W.; Woo, E. P. *Science* **2000**, *290*, 2123.
(20) Speakman, S. P.; Rozenburg, G. G.; Clay, K. J.; Milne, W. I.; Ille, A.; Gardner, I. A.; Bresler, E.; Steinke, J. H. G. *Org. Electron.* **2001**, *2*, 65.
(21) Bao, Z. N.; Dodabalapur, A.; Lovinger, A. J. *Appl. Phys. Lett.* **1996**, *69*, 4108.
(22) Heeney, M.; Bailey, C.; Genevicius, K.; Shkunov, M.; Sparrowe, D.; Tierney, S.; McCulloch, I. *J. Am. Chem. Soc.* **2005**, *127*, 1078.
(23) Ong, B. S.; Wu, Y. L.; Liu, P.; Gardner, S. *J. Am. Chem. Soc.* **2004**, *126*, 3378.
(24) Sirringhaus, H.; Tessler, N.; Friend, R. H. *Science* **1998**, *280*, 1741.
(25) Newman, C. R.; Frisbie, C. D.; Silva Filho, D. A.; Bredas, J. L.; Ewbank, P. C.; Mann, K. R. *Chem. Mater.* **2004**, *16*, 4436.
(26) Sirringhaus, H. *Adv. Mater.* **2005**, *17*, 2411.
(27) Horowitz, G.; Hajlaoui, R.; Fichou, D.; El Kassmi, A. *J. Appl. Phys.* **1999**, *85*, 3202.
(28) Horowitz, G.; Hajlaoui, M. E. *Adv. Mater.* **2000**, *12*, 1046.
(29) Horowitz, G.; Hajlaoui, M. E.; Hajlaoui, R. *J. Appl. Phys.* **2000**, *87*, 4456.
(30) Jain, S. *IEEE Proc. Solid-State Electron Devices* **1988**, *135*, 162.
(31) Katz, H. E.; Bao, Z. *J. Phys. Chem. B* **2000**, *104*, 671.
(32) Chua, L. L.; Zaumseil, J.; Chang, J. F.; Ou, E. C. W.; Ho, P. K. H.; Sirringhaus, H.; Friend, R. H. *Nature* **2005**, *434*, 194.
(33) Farchioni, R.; Grosso, G. *Organic Electronic Materials*; Springer-Verlag: Berlin, 2001.
(34) Pope, M.; Swenberg, C. E. *Electronic Processes in Organic Crystals and Polymers*, 2nd ed.; Oxford University Press: Oxford, U.K., 1999.
(35) Shen, Y.; Hosseini, A. R.; Wong, M. H.; Malliaras, G. G. *Chem. Phys. Chem.* **2004**, *5*, 16.
(36) Podzorov, V.; Menard, E.; Rogers, J. A.; Gershenson, M. E. *Phys. Rev. Lett.* **2005**, *95*, 226601/1.
(37) Takeya, J.; Tsukagoshi, K.; Aoyagi, Y.; Takenobu, T.; Iwasa, Y. *Jpn. J. Appl. Phys. Part 2* **2005**, *44*, L1393.
(38) Fichou, D. *J. Mater. Chem.* **2000**, *10*, 571.
(39) Nelson, S. F.; Lin, Y. Y.; Gundlach, D. J.; Jackson, T. N. *Appl. Phys. Lett.* **1998**, *72*, 1854.
(40) de Boer, R. W. I.; Gershenson, M. E.; Morpurgo, A. F.; Podzorov, V. *Phys. Status Solidi A* **2004**, *201*, 1302.
(41) Karl, N. *Synth. Met.* **2003**, *133*, 649.
(42) Dimitrakopoulos, C. D.; Purushothaman, S.; Kymissis, J.; Callegari, A.; Shaw, J. M. *Science* **1999**, *283*, 822.
(43) Facchetti, A.; Yoon, M. H.; Marks, T. J. *Adv. Mater.* **2005**, *17*, 1705.
(44) Huang, D.; Liao, F.; Molesa, S.; Redinger, D.; Subramanian, V. *J. Electrochem. Soc.* **2003**, *150*, G412.
(45) Loo, Y. L.; Someya, T.; Baldwin, K. W.; Bao, Z. N.; Ho, P.; Dodabalapur, A.; Katz, H. E.; Rogers, J. A. *Proc. Natl. Acad. Sci. U.S.A.* **2002**, *99*, 10252.
(46) Dimitrakopoulos, C. D.; Malenfant, P. R. L. *Adv. Mater.* **2002**, *14*, 99.
(47) Halik, M.; Klauk, H.; Zschieschang, U.; Schmid, G.; Ponomarenko, S.; Kirchmeyer, S.; Weber, W. *Adv. Mater.* **2003**, *15*, 917.
(48) Dinelli, F.; Murgia, M.; Levy, P.; Cavallini, M.; Biscarini, F.; De Leeuw, D. M. *Phys. Rev. Lett.* **2004**, *92*, 116802.
(49) Dodabalapur, A.; Torsi, L.; Katz, H. E. *Science* **1995**, *268*, 270.
(50) Peisert, H.; Knupfer, M.; Fink, J. *Recent Res. Dev. Appl. Phys.* **2002**, *5*, 129.
(51) Bredas, J. L.; Calbert, J. P.; da Silva, D. A.; Cornil, J. *Proc. Natl. Acad. Sci. U.S.A.* **2002**, *99*, 5804.
(52) Horowitz, G.; Hajlaoui, R.; Bourguiga, R.; Haijlaoui, M. *Synth. Met.* **1999**, *101*, 401.
(53) Horowitz, G.; Hajlaoui, R.; Delannoy, P. *J. Phys. III* **1995**, *5*, 355.
(54) Katz, H. E.; Bao, Z. *J. Phys. Chem. B* **2000**, *104*, 671.
(55) Hutchison, G. R.; Ratner, M. A.; Marks, T. J. *J. Am. Chem. Soc.* **2005**, *127*, 16866.
(56) De Leeuw, D. M.; Simenon, M. M. J.; Brown, A. R.; Einerhand, R. E. F. *Synth. Met.* **1997**, *87*, 53.
(57) Brown, A. R.; De Leeuw, D. M.; Lous, E. J.; Havinga, E. E. *Synth. Met.* **1994**, *66*, 257.
(58) Haddon, R. C.; Perel, A. S.; Morris, R. C.; Palstra, T. T. M.; Hebard, A. F.; Fleming, R. M. *Appl. Phys. Lett.* **1995**, *67*, 121.
(59) Fichou, D. *Handbook of Oligo- and Polythiophenes*; Wiley-VCH, New York, 1998.
(60) Horowitz, G.; Bachet, B.; Yassar, A.; Lang, P.; Demanze, F.; Fave, J. L.; Garnier, F. *Chem. Mater.* **1995**, *7*, 1337.
(61) Lovinger, A. J.; Katz, H. E.; Dodabalapur, A. *Chem. Mater.* **1998**, *10*, 3275.
(62) Curtis, M. D.; Cao, J.; Kampf, J. W. *J. Am. Chem. Soc.* **2004**, *126*, 4318.
(63) Li, X. C.; Sirringhaus, H.; Garnier, F.; Holmes, A. B.; Moratti, S. C.; Feeder, N.; Clegg, W.; Teat, S. J.; Friend, R. H. *J. Am. Chem. Soc.* **1998**, *120*, 2206.
(64) Zhang, X.; Cote, A. P.; Matzger, A. J. *J. Am. Chem. Soc.* **2005**, *127*, 10502.
(65) Anthony, J. E.; Brooks, J. S.; Eaton, D. L.; Parkin, S. R. *J. Am. Chem. Soc.* **2001**, *123*, 9482.
(66) Yoon, M. H.; Facchetti, A.; Stern, C. E.; Marks, T. J. *J. Am. Chem. Soc.* **2006**, *128*, 5792.
(67) Ando, S.; Murakami, R.; Nishida, J.; Tada, H.; Inoue, Y.; Tokito, S.; Yamashita, Y. *J. Am. Chem. Soc.* **2005**, *127*, 14996.
(68) Chen, X. L.; Lovinger, A. J.; Bao, Z.; Sapjeta, J. *Chem. Mater.* **2001**, *13*, 1341.
(69) Yasuda, T.; Fujita, K.; Tsutsui, T.; Geng, Y. H.; Culligan, S. W.; Chen, S. H. *Chem. Mater.* **2005**, *17*, 264.
(70) Cicoira, F.; Santato, C.; Dinelli, F.; Murgia, M.; Loi, M. A.; Biscarini, F.; Zamboni, R.; Heremans, P.; Muccini, M. *Adv. Funct. Mater.* **2005**, *15*, 375.
(71) Kim, D. H.; Park, Y. D.; Jang, Y. S.; Yang, H. C.; Kim, Y. H.; Han, J. I.; Moon, D. G.; Park, S. J.; Chang, T. Y.; Chang, C. W.; Joo, M. K.; Ryu, C. Y.; Cho, K. W. *Adv. Funct. Mater.* **2005**, *15*, 77.
(72) Verlaak, S.; Steudel, S.; Heremans, P.; Janssen, D.; Deleuze, M. S. *Phys. Rev. B* **2003**, *68*, 195409.
(73) Dinelli, F.; Murgia, M.; Biscarini, F.; De Leeuw, D. M. *Synth. Met.* **2004**, *146*, 373.
(74) Hajlaoui, M. E.; Garnier, F.; Hassine, L.; Kouki, F.; Bouchriha, H. *Synth. Met.* **2002**, *129*, 215.
(75) Noh, Y. Y.; Kim, J. J.; Yoshida, Y.; Yase, K. *Adv. Mater.* **2003**, *15*, 699.
(76) Sarkar, U. K.; Chakrabarti, S.; Misra, T. N.; Pal, A. J. *Chem. Phys. Lett.* **1992**, *200*, 55.
(77) Stabel, A.; Rabe, J. P. *Synth. Met.* **1994**, *67*, 47.
(78) Chang, P. C.; Lee, J.; Huang, D.; Subramanian, V.; Murphy, A. R.; Frechet, J. M. J. *Chem. Mater.* **2004**, *16*, 4783.
(79) Locklin, J.; Li, D.; Mannsfeld, S. C. B.; Borkent, E. J.; Meng, H.; Advincula, R.; Bao, Z. *Chem. Mater.* **2005**, *17*, 3366.
(80) Azumi, R.; Goto, M.; Honda, K.; Matsumoto, M. *Bull. Chem. Soc. Jpn.* **2003**, *76*, 1561.
(81) Garnier, F.; Yassar, A.; Hajlaoui, R.; Horowitz, G.; Deloffre, F.; Servet, B.; Ries, S.; Alnot, P. *J. Am. Chem. Soc.* **1993**, *115*, 8716.
(82) Gundlach, D. J.; Nichols, J. A.; Zhou, L.; Jackson, T. N. *Appl. Phys. Lett.* **2002**, *80*, 2925.
(83) Meng, H.; Zheng, J.; Lovinger, A. J.; Wang, B. C.; Van Patten, P. G.; Bao, Z. *Chem. Mater.* **2003**, *15*, 1778.
(84) Moret, M.; Campione, M.; Borghesi, A.; Miozzo, L.; Sassella, A.; Trabattoni, S.; Lotz, B.; Thierry, A. *J. Mater. Chem.* **2005**, *15*, 2444.
(85) Fritz, S. E.; Martin, S. M.; Frisbie, C. D.; Ward, M. D.; Toney, M. F. *J. Am. Chem. Soc.* **2004**, *126*, 4084.
(86) Merlo, J. A.; Newman, C. R.; Gerlach, C. P.; Kelley, T. W.; Muyres, D. V.; Fritz, S. E.; Toney, M. F.; Frisbie, C. D. *J. Am. Chem. Soc.* **2005**, *127*, 3997.
(87) Moulin, J. F.; Dinelli, F.; Massi, M.; Albonetti, C.; Kshirsagar, R.; Biscarini, F. *Nucl. Instrum. Methods Phys. Res., Sect. B* **2006**, *246*, 122.
(88) Yang, H.; Shin, T. J.; Ling, M. m.; Cho, K.; Ryu, C. Y.; Bao, Z. *J. Am. Chem. Soc.* **2005**, *127*, 11542.
(89) DeLongchamp, D. M.; Sambasivan, S.; Fischer, D. A.; Lin, E. K.; Chang, P.; Murphy, A. R.; Frechet, J. M. J.; Subramanian, V. *Adv. Mater.* **2005**, *17*, 2340.
(90) Murphy, A. R.; Chang, P. C.; VanDyke, P.; Liu, J.; Frechet, J. M. J.; Subramanian, V.; DeLongchamp, D. M.; Sambasivan, S.; Fischer, D. A.; Lin, E. K. *Chem. Mater.* **2005**, *17*, 6033.
(91) Pattison, L. R.; Hexemer, A.; Kramer, E. J.; Krishnan, S.; Petroff, P. M.; Fischer, D. A. *Macromolecules* **2006**, *39*, 2225.
(92) DeLongchamp, D. M.; Vogel, B. M.; Jung, Y.; Gurau, M. C.; Richter, C. A.; Kirillov, O. A.; Obrzut, J.; Fischer, D. A.; Sambasivan, S.; Richter, L. J.; Lin, E. K. *Chem. Mater.* **2005**, *17*, 5610.
(93) Gundlach, D. J.; Lin, Y. Y.; Jackson, T. N.; Nelson, S. F.; Schlom, D. G. *IEEE Electron Device Lett.* **1997**, *18*, 87.
(94) Klauk, H.; Halik, M.; Zschieschang, U.; Schmid, G.; Radlik, W.; Weber, W. *J. Appl. Phys.* **2002**, *92*, 5259.
(95) Klauk, H.; Halik, M.; Zschieschang, U.; Eder, F.; Schmid, G.; Dehm, C. *Appl. Phys. Lett.* **2003**, *82*, 4175.
(96) Volkel, A. R.; Street, R. A.; Knipp, D. *Phys. Rev. B* **2002**, *66*, 195336/1.
(97) Baude, P. F.; Ender, D. A.; Haase, M. A.; Kelley, T. W.; Muyres, D. V.; Theiss, S. D. *Appl. Phys. Lett.* **2003**, *82*, 3964.
(98) Kelley, T. W.; Muyres, D. V.; Baude, P. F.; Smith, T. P.; Jones, T. D. *Mater. Res. Soc. Symp. Proc.* **2003**, *771*, 169.

(99) Heringdorf, F. J. M. Z.; Reuter, M. C.; Tromp, R. M. *Nature* **2001**, *412*, 517.
(100) Moriguchi, N.; Nishikawa, T.; Anezaki, T.; Unno, A.; Tachibana, M.; Kojima, K. *Physica B* **2006**, *376*−*377*, 276.
(101) Choi, J. M.; Lee, J.; Hwang, D. K.; Kim, J. H.; Im, S.; Kim, E. *Appl. Phys. Lett.* **2006**, *88*, 043508/1.
(102) Reynaert, J.; Cheyns, D.; Janssen, D.; Muller, R.; Arkhipov, V. I.; Genoe, J.; Borghs, G.; Heremans, P. *J. Appl. Phys.* **2005**, *97*, 114501/1.
(103) Santato, C.; Manunza, I.; Bonfiglio, A.; Cicoira, F.; Cosseddu, P.; Zamboni, R.; Muccini, M. *Appl. Phys. Lett.* **2005**, *86*, 141106/1.
(104) Laquindanum, J. G.; Katz, H. E.; Lovinger, A. J. *J. Am. Chem. Soc.* **1998**, *120*, 664.
(105) Ito, K.; Suzuki, T.; Sakamoto, Y.; Kubota, D.; Inoue, Y.; Sato, F.; Tokito, S. *Angew. Chem., Int. Ed.* **2003**, *42*, 1159.
(106) Meng, H.; Bendikov, M.; Mitchell, G.; Helgeson, R.; Wudl, F.; Bao, Z.; Siegrist, T.; Kloc, C.; Chen, C. H. *Adv. Mater.* **2003**, *15*, 1090.
(107) Miao, Q.; Nguyen, T. Q.; Someya, T.; Blanchet, G. B.; Nuckolls, C. *J. Am. Chem. Soc.* **2003**, *125*, 10284.
(108) Miao, Q.; Lefenfeld, M.; Nguyen, T. Q.; Siegrist, T.; Kloc, C.; Nuckolls, C. *Adv. Mater.* **2005**, *17*, 407.
(109) Swartz, C. R.; Parkin, S. R.; Bullock, J. E.; Anthony, J. E.; Mayer, A. C.; Malliaras, G. G. *Org. Lett.* **2005**, *7*, 3163.
(110) Fichou, D.; Horowitz, G.; Garnier, F. *Mol. Cryst. Liq. Cryst. Sci. Technol., Sect. A* **1992**, *217*, 193.
(111) Garnier, F.; Horowitz, G.; Fichou, D.; Yassar, A. *Synth. Met.* **1996**, *81*, 163.
(112) Hajlaoui, R.; Horowitz, G.; Garnier, F.; Arce-Brouchet, A.; Laigre, L.; El, Kassmi, A.; Demanze, F.; Kouki, F. *Adv. Mater.* **1997**, *9*, 389.
(113) Hajlaoui, R.; Fichou, D.; Horowitz, G.; Nessakh, B.; Constant, M.; Garnier, F. *Adv. Mater.* **1997**, *9*, 557.
(114) Lovinger, A. J.; Davis, D. D.; Dodabalapur, A.; Katz, H. E.; Torsi, L. *Macromolecules* **1996**, *29*, 4952.
(115) Lovinger, A. J.; Davis, D. D.; Dodabalapur, A.; Katz, H. E. *Chem. Mater.* **1996**, *8*, 2836.
(116) Fichou, D.; Teulade-Fichou, M. P.; Horowitz, G.; Demanze, F. *Adv. Mater.* **1997**, *9*, 75.
(117) Katz, H. E.; Torsi, L.; Dodabalapur, A. *Chem. Mater.* **1995**, *7*, 2235.
(118) Katz, H. E.; Bao, Z.; Gilat, S. L. *Acc. Chem. Res.* **2001**, *34*, 359.
(119) Horowitz, G.; Garnier, F.; Yassar, A.; Hajlaoui, R.; Kouki, F. *Adv. Mater.* **1996**, *8*, 52.
(120) Horowitz, G.; Peng, X. Z.; Fichou, D.; Garnier, F. *J. Mol. Electron.* **1991**, *7*, 85.
(121) Nagamatsu, S.; Kaneto, K.; Azumi, R.; Matsumoto, M.; Yoshida, Y.; Yase, K. *J. Phys. Chem. B* **2005**, *109*, 9374.
(122) Ostoja, P.; Maccagnani, P.; Gazzano, M.; Cavallini, M.; Kengne, J. C.; Kshirsagar, R.; Biscarini, F.; Melucci, M.; Zambianchi, M.; Barbarella, G. *Synth. Met.* **2004**, *146*, 243.
(123) Waragai, K.; Akimichi, H.; Hotta, S.; Kano, H.; Sakaki, H. *Synth. Met.* **1993**, *57*, 4053.
(124) Waragai, K.; Akimichi, H.; Hotta, S.; Kano, H.; Sakaki, H. *Phys. Rev. B* **1995**, *52*, 1786.
(125) Garnier, F.; Hajlaoui, R.; El Kassmi, A.; Horowitz, G.; Laigre, L.; Porzio, W.; Armanini, M.; Provasoli, F. *Chem. Mater.* **1998**, *10*, 3334.
(126) Katz, H. E.; Lovinger, A. J.; Laquindanum, J. G. *Chem. Mater.* **1998**, *10*, 457.
(127) Li, W.; Katz, H. E.; Lovinger, A. J.; Laquindanum, J. G. *Chem. Mater.* **1999**, *11*, 458.
(128) Deman, A. L.; Tardy, J.; Nicolas, Y.; Blanchard, P.; Roncali, J. *Synth. Met.* **2004**, *146*, 365.
(129) Garnier, F.; Hajlaoui, R.; Yassar, A.; Srivastava, P. *Science* **1994**, *265*, 1684.
(130) Horowitz, G.; Deloffre, F.; Garnier, F.; Hajlaoui, R.; Hmyene, M.; Yassar, A. *Synth. Met.* **1993**, *54*, 435.
(131) Katz, H. E.; Dodabalapur, A.; Torsi, L.; Elder, D. *Chem. Mater.* **1995**, *7*, 2238.
(132) Dimitrakopoulos, C. D.; Furman, B. K.; Graham, T.; Hegde, S.; Purushothaman, S. *Synth. Met.* **1998**, *92*, 47.
(133) Ponomarenko, S.; Kirchmeyer, S. *J. Mater. Chem.* **2003**, *13*, 197.
(134) Halik, M.; Klauk, H.; Zschieschang, U.; Schmid, G.; Radlik, W.; Ponomarenko, S.; Kirchmeyer, S.; Weber, W. *J. Appl. Phys.* **2003**, *93*, 2977.
(135) Ponomarenko, S. A.; Kirchmeyer, S.; Halik, M.; Klauk, H.; Zschieschang, U.; Schmid, G.; Karbach, A.; Drechsler, D.; Alpatova, N. M. *Synth. Met.* **2005**, *149*, 231.
(136) Halik, M.; Klauk, H.; Zschieschang, U.; Schmid, G.; Ponomarenko, S.; Kirchmeyer, S.; Weber, W. *Adv. Mater.* **2003**, *15*, 917.
(137) Barbarella, G.; Ostoja, P.; Maccagnani, P.; Pudova, O.; Antolini, L.; Casarini, D.; Bongini, A. *Chem. Mater.* **1998**, *10*, 3683.
(138) Rittner, M.; Baeuerle, P.; Goetz, G.; Schweizer, H.; Calleja, F. J. B.; Pilkuhn, M. H. *Synth. Met.* **2006**, *156*, 21.
(139) Barbarella, G.; Zambianchi, M.; Antolini, L.; Ostoja, P.; Maccagnani, P.; Bongini, A.; Marseglia, E. A.; Tedesco, E.; Gigli, G.; Cingolani, R. *J. Am. Chem. Soc.* **1999**, *121*, 8920.
(140) Facchetti, A.; Mushrush, M.; Yoon, M. H.; Hutchison, G. R.; Ratner, M. A.; Marks, T. J. *J. Am. Chem. Soc.* **2004**, *126*, 13859.
(141) Turbiez, M.; Frere, P.; Allain, M.; Videlot, C.; Ackermann, J.; Roncali, J. *Chem.*−*Eur. J.* **2005**, *11*, 3742.
(142) Frere, P.; Raimundo, J. M.; Blanchard, P.; Delaunay, J.; Richomme, P.; Sauvajol, J. L.; Orduna, J.; Garin, J.; Roncali, J. *J. Org. Chem.* **2003**, *68*, 7254.
(143) Videlot, C.; Ackermann, J.; Blanchard, P.; Raimundo, J. M.; Frere, P.; Allain, M.; de Bettignies, R.; Levillain, E.; Roncali, J. *Adv. Mater.* **2003**, *15*, 306.
(144) Laquindanum, J. G.; Katz, H. E.; Lovinger, A. J.; Dodabalapur, A. *Adv. Mater.* **1997**, *9*, 36.
(145) Sirringhaus, H.; Friend, R. H.; Wang, C.; Leuninger, J.; Mullen, K. *J. Mater. Chem.* **1999**, *9*, 2095.
(146) Sirringhaus, H.; Friend, R. H.; Li, X. C.; Moratti, S. C.; Holmes, A. B.; Feeder, N. *Appl. Phys. Lett.* **1997**, *71*, 3871.
(147) Iosip, M. D.; Destri, S.; Pasini, M.; Porzio, W.; Pernstich, K. P.; Batlogg, B. *Synth. Met.* **2004**, *146*, 251.
(148) Zhang, X.; Matzger, A. J. *J. Org. Chem.* **2003**, *68*, 9813.
(149) Xiao, K.; Liu, Y.; Qi, T.; Zhang, W.; Wang, F.; Gao, J.; Qiu, W.; Ma, Y.; Cui, G.; Chen, S.; Zhan, X.; Yu, G.; Qin, J.; Hu, W.; Zhu, D. *J. Am. Chem. Soc.* **2005**, *127*, 13281.
(150) Nenajdenko, V. G.; Sumerin, V. V.; Chernichenko, K. Y.; Balenkova, E. S. *Org. Lett.* **2004**, *6*, 3437.
(151) Ando, S.; Nishida, J. I.; Inoue, Y.; Tokito, S.; Yamashita, Y. *J. Mater. Chem.* **2004**, *14*, 1787.
(152) Ando, S.; Nishida, J.; Fujiwara, E.; Tada, H.; Inoue, Y.; Tokito, S.; Yamashita, Y. *Chem. Lett.* **2004**, *33*, 1170.
(153) Hong, X. M.; Katz, H. E.; Lovinger, A. J.; Wang, B. C.; Raghavachari, K. *Chem. Mater.* **2001**, *13*, 4686.
(154) Chwang, A. B.; Frisbie, C. D. *J. Appl. Phys.* **2001**, *90*, 1342.
(155) Chwang, A. B.; Frisbie, C. D. *J. Phys. Chem. B* **2000**, *104*, 12202.
(156) Ponomarenko, S. A.; Kirchmeyer, S.; Elschner, A.; Alpatova, N. M.; Halik, M.; Klauk, H.; Zschieschang, U.; Schmid, G. *Chem. Mater.* **2006**, *18*, 579.
(157) Mushrush, M.; Facchetti, A.; Lefenfeld, M.; Katz, H. E.; Marks, T. J. *J. Am. Chem. Soc.* **2003**, *125*, 9414.
(158) Mohapatra, S.; Holmes, B. T.; Newman, C. R.; Prendergast, C. F.; Frisbie, C. D.; Ward, M. D. *Adv. Funct. Mater.* **2004**, *14*, 605.
(159) Noh, Y. Y.; Azumi, R.; Goto, M.; Jung, B. J.; Lim, E.; Shim, H. K.; Yoshida, Y.; Yase, K.; Kim, D. Y. *Chem. Mater.* **2005**, *17*, 3861.
(160) Videlot-Ackermann, C.; Ackermann, J.; Brisset, H.; Kawamura, K.; Yoshimoto, N.; Raynal, P.; El Kassmi, A.; Fages, F. *J. Am. Chem. Soc.* **2005**, *127*, 16346.
(161) McCulloch, L.; Bailey, C.; Giles, M.; Heeney, M.; Love, I.; Shkunov, M.; Sparrowe, D.; Tierney, S. *Chem. Mater.* **2005**, *17*, 1381.
(162) Murphy, A. R.; Liu, J. S.; Luscombe, C.; Kavulak, D.; Frechet, J. M. J.; Kline, R. J.; McGehee, M. D. *Chem. Mater.* **2005**, *17*, 4892.
(163) Hoshino, S.; Yoshida, M.; Uemura, S.; Kodzasa, T.; Takada, N.; Kamata, T.; Yase, K. *J. Appl. Phys.* **2004**, *95*, 5088.
(164) Meijer, E. J.; Detcheverry, C.; Baesjou, P. J.; van Veenendaal, E.; De Leeuw, D. M.; Klapwijk, T. M. *J. Appl. Phys.* **2003**, *93*, 4831.
(165) Meng, H.; Bao, Z.; Lovinger, A. J.; Wang, B. C.; Mujsce, A. M. *J. Am. Chem. Soc.* **2001**, *123*, 9214.
(166) Noh, Y. Y.; Kim, D. Y.; Yoshida, Y.; Yase, K.; Jung, B. J.; Lim, E.; Shim, H. K.; Azumi, R. *J. Appl. Phys.* **2005**, *97*, 104504/1.
(167) Porzio, W.; Destri, S.; Giovanella, U.; Pasini, M.; Motta, T.; Natali, D.; Sampietro, M.; Campione, M. *Thin Solid Films* **2005**, *492*, 212.
(168) Ando, S.; Nishida, J. I.; Fujiwara, E.; Tada, H.; Inoue, Y.; Tokito, S.; Yamashita, Y. *Chem. Mater.* **2005**, *17*, 1261.
(169) Meng, H.; Sun, F.; Goldfinger, M. B.; Jaycox, G. D.; Li, Z.; Marshall, W. J.; Blackman, G. S. *J. Am. Chem. Soc.* **2005**, *127*, 2406.
(170) Nicolas, Y.; Blanchard, P.; Roncali, J.; Allain, M.; Mercier, N.; Deman, A. L.; Tardy, J. *Org. Lett.* **2005**, *7*, 3513.
(171) Takimiya, K.; Kunugi, Y.; Toyoshima, Y.; Otsubo, T. *J. Am. Chem. Soc.* **2005**, *127*, 3605.
(172) Kunugi, Y.; Takimiya, K.; Yamane, K.; Yamashita, K.; Aso, Y.; Otsubo, T. *Chem. Mater.* **2003**, *15*, 6.
(173) Takimiya, K.; Otsubo, T. *Phosphorus, Sulfur Silicon Relat. Elem.* **2005**, *180*, 873.
(174) Takimiya, K.; Kunugi, Y.; Konda, Y.; Niihara, N.; Otsubo, T. *J. Am. Chem. Soc.* **2004**, *126*, 5084.
(175) Bao, Z.; Lovinger, A. J.; Dodabalapur, A. *Appl. Phys. Lett.* **1996**, *69*, 3066.
(176) Cherian, S.; Donley, C.; Mathine, D.; LaRussa, L.; Xia, W.; Armstrong, N. *J. Appl. Phys.* **2004**, *96*, 5638.
(177) Wu, Y.; Li, Y.; Gardner, S.; Ong, B. S. *J. Am. Chem. Soc.* **2005**, *127*, 614.
(178) Li, Y.; Wu, Y.; Gardner, S.; Ong, B. S. *Adv. Mater.* **2005**, *17*, 849.

(179) Veres, J.; Ogier, S.; Lloyd, G.; deLeeuw, D. *Chem. Mater.* **2004**, *16*, 4543.
(180) Cravino, A.; Roquet, S.; Aleveque, O.; Leriche, P.; Frere, P.; Roncali, J. *Chem. Mater.* **2006**, *18*, 2584.
(181) Saragi, T. P. I.; Fuhrmann-Lieker, T.; Salbeck, J. *Adv. Funct. Mater.* **2006**, *16*, 966.
(182) Kuo, C. T.; Weng, S. Z. *Polym. Adv. Technol.* **2000**, *11*, 716.
(183) Roy, V. A. L.; Zhi, Y. G.; Xu, Z. X.; Yu, S. C.; Chan, P. W. H.; Che, C. M. *Adv. Mater.* **2005**, *17*, 1258.
(184) Naraso Nishida, J.; Ando, S.; Yamaguchi, J.; Itaka, K.; Koinuma, H.; Tada, H.; Tokito, S.; Yamashita, Y. *J. Am. Chem. Soc.* **2005**, *127*, 10142.
(185) Morioka, Y.; Nishida, J. I.; Fujiwara, E.; Tada, H.; Yamashita, Y. *Chem. Lett.* **2004**, *33*, 1632.
(186) Porzio, W.; Destri, S.; Pasini, A.; Giovanella, U.; Motta, T.; Iosip, M. D.; Natali, D.; Sampietro, M.; Franco, L.; Campione, M. *Synth. Met.* **2004**, *146*, 259.
(187) Laquindanum, J. G.; Katz, H. E.; Dodabalapur, A.; Lovinger, A. J. *J. Am. Chem. Soc.* **1996**, *118*, 11331.
(188) Chesterfield, R. J.; Newman, C. R.; Pappenfus, T. M.; Ewbank, P. C.; Haukaas, M. H.; Mann, K. R.; Miller, L. L.; Frisbie, C. D. *Adv. Mater.* **2003**, *15*, 1278.
(189) Pappenfus, T. M.; Chesterfield, R. J.; Frisbie, C. D.; Mann, K. R.; Casado, J.; Raff, J. D.; Miller, L. L. *J. Am. Chem. Soc.* **2002**, *124*, 4184.
(190) Kastner, J.; Paloheimo, J.; Kuzmany, H. *Springer Ser. Solid-State Sci.* **1993**, 512−515.
(191) Dodabalapur, A.; Katz, H. E.; Torsi, L.; Haddon, R. C. *Science* **1995**, *269*, 1560.
(192) Dodabalapur, A.; Katz, H. E.; Torsi, L.; Haddon, R. C. *Appl. Phys. Lett.* **1996**, *68*, 1108.
(193) Horowitz, G.; Kouki, F.; Spearman, P.; Fichou, D.; Nogues, C.; Pan, X.; Garnier, F. *Adv. Mater.* **1996**, *8*, 242.
(194) Katz, H. E.; Lovinger, A. J.; Johnson, J.; Kloc, C.; Slegrist, T.; Li, W.; Lin, Y. Y.; Dodabalapur, A. *Nature* **2000**, *404*, 478.
(195) Malenfant, P. R. L.; Dimitrakopoulos, C. D.; Gelorme, J. D.; Kosbar, L. L.; Graham, T. O.; Curioni, A.; Andreoni, W. *Appl. Phys. Lett.* **2002**, *80*, 2517.
(196) Chesterfield, R. J.; McKeen, J. C.; Newman, C. R.; Ewbank, P. C.; daSilvaFilho, D. A.; Bredas, J. L.; Miller, L. L.; Mann, K. R.; Frisbie, C. D. *J. Phys. Chem. B* **2004**, *108*, 19281.
(197) Jones, B. A.; Ahrens, M. J.; Yoon, M. H.; Facchetti, A.; Marks, T. J.; Wasielewski, M. R. *Angew. Chem., Int. Ed.* **2004**, *43*, 6363.
(198) Chen, Z.; Debije, M. G.; Debaerdemaeker, T.; Osswald, P.; Wuerthner, F. *Chem. Phys. Chem.* **2004**, *5*, 137.
(199) Bao, Z.; Lovinger, A. J.; Brown, J. *J. Am. Chem. Soc.* **1998**, *120*, 207.
(200) Wang, J.; Wang, H.; Yan, X.; Huang, H.; Jin, D.; Shi, J.; Tang, Y.; Yan, D. *Adv. Funct. Mater.* **2006**, *16*, 824.
(201) Nishida, J.; Naraso Murai, S.; Fujiwara, E.; Tada, H.; Tomura, M.; Yamashita, Y. *Org. Lett.* **2004**, *6*, 2007.
(202) Demanze, F.; Yassar, A.; Fichou, D. *Synth. Met.* **1999**, *101*, 620.
(203) Hapiot, P.; Demanze, F.; Yassar, A.; Garnier, F. *J. Phys. Chem.* **1996**, *100*, 8397.
(204) Yassar, A.; Demanze, F.; Jaafari, A.; El Idrissi, M.; Coupry, C. *Adv. Funct. Mater.* **2002**, *12*, 699.
(205) Facchetti, A.; Deng, Y.; Wang, A.; Koide, Y.; Sirringhaus, H.; Marks, T. J.; Friend, R. H. *Angew. Chem.* **2000**, *39*, 4547.
(206) Facchetti, A.; Mushrush, M.; Katz, H. E.; Marks, T. J. *Adv. Mater.* **2003**, *15*, 33.
(207) Facchetti, A.; Yoon, M. H.; Stern, C. L.; Hutchison, G. R.; Ratner, M. A.; Marks, T. J. *J. Am. Chem. Soc.* **2004**, *126*, 13480.
(208) Yoon, M. H.; DiBenedetto, S. A.; Facchetti, A.; Marks, T. J. *J. Am. Chem. Soc.* **2005**, *127*, 1348.
(209) Facchetti, A.; Letizia, J.; Yoon, M. H.; Mushrush, M.; Katz, H. E.; Marks, T. J. *Chem. Mater.* **2004**, *16*, 4715.
(210) Facchetti, A.; Yoon, M. H.; Stern, C. L.; Katz, H. E.; Marks, T. J. *Angew. Chem., Int. Ed.* **2003**, *42*, 3900.
(211) Ando, S.; Nishida, J. I.; Tada, H.; Inoue, Y.; Tokito, S.; Yamashita, Y. *J. Am. Chem. Soc.* **2005**, *127*, 5336.
(212) Akhtaruzzaman, M.; Kamata, N.; Nishida, J. I.; Ando, S.; Tada, H.; Tomura, M.; Yamashita, Y. *Chem. Commun.* **2005**, *25*, 3183.
(213) Sakamoto, Y.; Komatsu, S.; Suzuki, T. *J. Am. Chem. Soc.* **2001**, *123*, 4643.
(214) Osuna, R. M.; Ortiz, R. P.; Delgado, M. C. R.; Sakamoto, Y.; Suzuki, T.; Hernandez, V.; Navarrete, J. T. L. *J. Phys. Chem. B* **2005**, *109*, 20737.
(215) Inoue, Y.; Sakamoto, Y.; Suzuki, T.; Kobayashi, M.; Gao, Y.; Tokito, S. *Jpn. J. Appl. Phys. Part 1* **2005**, *44*, 3663.
(216) Sakamoto, Y.; Suzuki, T.; Kobayashi, M.; Gao, Y.; Fukai, Y.; Inoue, Y.; Sato, F.; Tokito, S. *J. Am. Chem. Soc.* **2004**, *126*, 8138.
(217) Sakamoto, Y.; Suzuki, T.; Kobayashi, M.; Gao, Y.; Inoue, Y.; Tokito, S. *Mol. Cryst. Liq. Cryst.* **2006**, *444*, 225.
(218) Stingelin-Stutzmann, N.; Smits, E.; Wondergem, H.; Tanase, C.; Blom, P.; Smith, P.; de Leeuw, D. *Nat. Mater.* **2005**, *4*, 601.
(219) Briseno, A. L.; Aizenberg, J.; Han, Y. J.; Penkala, R. A.; Moon, H.; Lovinger, A. J.; Kloc, C.; Bao, Z. *J. Am. Chem. Soc.* **2005**, *127*, 12164.
(220) Williams, W. G. *Discuss. Faraday Soc.* **1971**, *51*, 61.
(221) Podzorov, V.; Pudalov, V. M.; Gershenson, M. E. *Appl. Phys. Lett.* **2003**, *82*, 1739.
(222) Podzorov, V.; Sysoev, S. E.; Loginova, E.; Pudalov, V. M.; Gershenson, M. E. *Appl. Phys. Lett.* **2003**, *83*, 3504.
(223) Zeis, R.; Besnard, C.; Siegrist, T.; Schlockermann, C.; Chi, X.; Kloc, C. *Chem. Mater.* **2006**, *18*, 244.
(224) Menard, E.; Podzorov, V.; Hur, S. H.; Gaur, A.; Gershenson, M. E.; Rogers, J. A. *Adv. Mater.* **2004**, *16*, 2097.
(225) Takahashi, T.; Takenobu, T.; Takeya, J.; Iwasa, Y. *Appl. Phys. Lett.* **2006**, *88*, 033505/1.
(226) Sundar, V. C.; Zaumseil, J.; Podzorov, V.; Menard, E.; Willett, R. L.; Someya, T.; Gershenson, M. E.; Rogers, J. A. *Science* **2004**, *303*, 1644.
(227) Stassen, A. F.; de Boer, R. W. I.; Iosad, N. N.; Morpurgo, A. F. *Appl. Phys. Lett.* **2004**, *85*, 3899.
(228) de Boer, R. W. I.; Klapwijk, T. M.; Morpurgo, A. F. *Appl. Phys. Lett.* **2003**, *83*, 4345.
(229) Butko, V. Y.; Chi, X.; Ramirez, A. P. *Solid State Commun.* **2003**, *128*, 431.
(230) Newman, C. R.; Chesterfield, R. J.; Merlo, J. A.; Frisbie, C. D. *Appl. Phys. Lett.* **2004**, *85*, 422.
(231) Goldmann, C.; Haas, S.; Krellner, C.; Pernstich, K. P.; Gundlach, D. J.; Batlogg, B. *J. Appl. Phys.* **2004**, *96*, 2080.
(232) Moon, H.; Zeis, R.; Borkent, E. J.; Besnard, C.; Lovinger, A. J.; Siegrist, T.; Kloc, C.; Bao, Z. *J. Am. Chem. Soc.* **2004**, *126*, 15322.
(233) Bendikov, M.; Wudl, F.; Perepichka, D. F. *Chem. Rev.* **2004**, *104*, 4891.
(234) Mas-Torrent, M.; Hadley, P.; Bromley, S. T.; Ribas, X.; Tarres, J.; Mas, M.; Molins, E.; Veciana, J.; Rovira, C. *J. Am. Chem. Soc.* **2004**, *126*, 8546.
(235) Mas-Torrent, M.; Durkut, M.; Hadley, P.; Ribas, X.; Rovira, C. *J. Am. Chem. Soc.* **2004**, *126*, 984.
(236) Mas-Torrent, M.; Hadley, P.; Bromley, S. T.; Crivillers, N.; Veciana, J.; Rovira, C. *Appl. Phys. Lett.* **2005**, *86*, 012110.
(237) Katz, H. E. *Chem. Mater.* **2004**, *16*, 4748.
(238) Ling, M.; Bao, Z. *Chem. Mater.* **2004**, *16*, 4824.
(239) Herwig, P. T.; Mullen, K. *Adv. Mater.* **1999**, *11*, 480.
(240) Afzali, A.; Dimitrakopoulos, C. D.; Breen, T. L. *J. Am. Chem. Soc.* **2002**, *124*, 8812.
(241) Tulevski, G. S.; Miao, Q.; Afzali, A.; Graham, T. O.; Kagan, C. R.; Nuckolls, C. *J. Am. Chem. Soc.* **2006**, *128*, 1788.
(242) Afzali, A.; Dimitrakopoulos, C. D.; Graham, T. O. *Adv. Mater.* **2003**, *15*, 2066.
(243) Weidkamp, K. P.; Afzali, A.; Tromp, R. M.; Hamers, R. J. *J. Am. Chem. Soc.* **2004**, *126*, 12740.
(244) Anthony, J. E.; Eaton, D. L.; Parkin, S. R. *Org. Lett.* **2002**, *4*, 15.
(245) Payne, M. M.; Delcamp, J. H.; Parkin, S. R.; Anthony, J. E. *Org. Lett.* **2004**, *6*, 1609.
(246) Payne, M. M.; Odom, S. A.; Parkin, S. R.; Anthony, J. E. *Org. Lett.* **2004**, *6*, 3325.
(247) Payne, M. M.; Parkin, S. R.; Anthony, J. E. *J. Am. Chem. Soc.* **2005**, *127*, 8028.
(248) Park, S. J.; Kuo, C. C.; Anthony, J. E.; Jackson, T. N. *Tech. Dig. − Int. Electron Devices Meet.* **2006**, 113.
(249) Payne, M. M.; Parkin, S. R.; Anthony, J. E.; Kuo, C. C.; Jackson, T. N. *J. Am. Chem. Soc.* **2005**, *127*, 4986.
(250) Sheraw, C. D.; Jackson, T. N.; Eaton, D. L.; Anthony, J. E. *Adv. Mater.* **2003**, *15*, 2009.
(251) Katz, H. E.; Li, W.; Lovinger, A. J.; Laquindanum, J. *Synth. Met.* **1999**, *102*, 897.
(252) Tulevski, G. S.; Miao, Q.; Fukuto, M.; Abram, R.; Ocko, B.; Pindak, R.; Steigerwald, M. L.; Kagan, C. R.; Nuckolls, C. *J. Am. Chem. Soc.* **2004**, *126*, 15048.
(253) Barbarella, G.; Melucci, M.; Sotgiu, G. *Adv. Mater.* **2005**, *17*, 1581.
(254) Lukevics, E.; Arsenyan, P.; Pudova, O. *Heterocycles* **2003**, *60*, 663.
(255) Dimitrakopoulos, C. D.; Afzali-Ardakani, A.; Furman, B.; Kymissis, J.; Purushothaman, S. *Synth. Met.* **1997**, *89*, 193.
(256) Katz, H. E.; Laquindanum, J. G.; Lovinger, A. J. *Chem. Mater.* **1998**, *10*, 633.
(257) Afzali, A.; Breen, T. L.; Kagan, C. R. *Chem. Mater.* **2002**, *14*, 1742.
(258) Sandberg, H.; Henze, O.; Kilbinger, A. F. M.; Sirringhaus, H.; Feast, W. J.; Friend, R. H. *Synth. Met.* **2003**, *137*, 885.
(259) Schenning, A. P. H. J.; Kilbinger, A. F. M.; Biscarini, F.; Cavallini, M.; Cooper, H. J.; Derrick, P. J.; Feast, W. J.; Lazzaroni, R.; Leclere, P.; McDonell, L. A.; Meijer, E. W.; Meskers, S. C. J. *J. Am. Chem. Soc.* **2002**, *124*, 1269.

(260) McCulloch, I.; Zhang, W.; Heeney, M.; Bailey, C.; Giles, M.; Graham, D.; Shkunov, M.; Sparrowe, D.; Tierney, S. *J. Mater. Chem.* **2003**, *13*, 2436.
(261) Huisman, B. H.; Valeton, J. J. P.; Nijssen, W.; Lub, J.; ten Hoeve, W. *Adv. Mater.* **2003**, *15*, 2002.
(262) Murphy, A. R.; Frechet, J. M. J.; Chang, P.; Lee, J.; Subramanian, V. *J. Am. Chem. Soc.* **2004**, *126*, 1596.
(263) Chang, P. C.; Molesa, S. E.; Murphy, A. R.; Frechet, J. M. J.; Subramanian, V. *62nd DRC Conf. Dig.* **2004**, *1*, 183.
(264) van de Craats, A. M.; Warman, J. M.; Fechtenkotter, A.; Brand, J. D.; Harbison, M. A.; Mullen, K. *Adv. Mater.* **1999**, *11*, 1469.
(265) Pisula, W.; Menon, A.; Stepputat, M.; Lieberwirth, I.; Kolb, U.; Tracz, A.; Sirringhaus, H.; Pakula, T.; Mullen, K. *Adv. Mater.* **2005**, *17*, 684.
(266) Pappenfus, T. M.; Mann, K. R. *Org. Lett.* **2002**, *4*, 3043.
(267) de Bettignies, R.; Nicolas, Y.; Blanchard, P.; Levillain, E.; Nunzi, J. m.; Roncali, J. *Adv. Mater.* **2003**, *15*, 1939.
(268) Nicolas, Y.; Blanchard, P.; Levillain, E.; Allain, M.; Mercier, N.; Roncali, J. *Org. Lett.* **2004**, *6*, 273.
(269) Geng, Y. H.; Fechtenkotter, A.; Mullen, K. *J. Mater. Chem.* **2001**, *11*, 1634.
(270) Ponomarenko, S. A.; Kirchmeyer, S.; Elschner, A.; Huisman, B. H.; Karbach, A.; Drechsler, D. *Adv. Funct. Mater.* **2003**, *13*, 591.
(271) Sun, Y.; Xiao, K.; Liu, Y.; Wang, J.; Pei, J.; Yu, G.; Zhu, D. *Adv. Funct. Mater.* **2005**, *15*, 818.
(272) Strohriegl, P.; Grazulevicius, J. V. *Adv. Mater.* **2002**, *14*, 1439.
(273) Sonntag, M.; Kreger, K.; Hanft, D.; Strohriegl, P.; Setayesh, S.; De Leeuw, D. *Chem. Mater.* **2005**, *17*, 3031.
(274) Locklin, J.; Shinbo, K.; Onishi, K.; Kaneko, F.; Bao, Z.; Advincula, R. C. *Chem. Mater.* **2003**, *15*, 1404.
(275) Ito, S.; Murashima, T.; Uno, H.; Ono, N. *Chem. Commun.* **1998**,1661.
(276) Shea, P. B.; Kanicki, J.; Ono, N. *J. Appl. Phys.* **2005**, *98*, 014503/1.
(277) Checcoli, P.; Conte, G.; Salvatori, S.; Paolesse, R.; Bolognesi, A.; Berliocchi, A.; Brunetti, F.; D'Amico, A.; Di Carlo, A.; Lugli, P. *Synth. Met.* **2003**, *138*, 261.
(278) Xu, H.; Yu, G.; Xu, W.; Xu, Y.; Cui, G.; Zhang, D.; Liu, Y.; Zhu, D. *Langmuir* **2005**, *21*, 5391.
(279) Becker, R. S.; Demelo, J. S.; Macanita, A. L.; Elisei, F. *Pure Appl. Chem.* **1995**, *67*, 9.
(280) Chang, P. C.; Murphy, A. R.; Subramanian, V.; Frechet, J. M. J. Unpublished results, 2005.
(281) Aramaki, S.; Sakai, Y.; Ono, N. *Appl. Phys. Lett.* **2004**, *84*, 2085.
(282) Babel, A.; Jenekhe, S. A. *J. Am. Chem. Soc.* **2003**, *125*, 13656.
(283) Gonzalez, R.; Hummelen, J. C.; Wudl, F. *J. Org. Chem.* **1995**, *60*, 2618.
(284) Brabec, C. J.; Shaheen, S. E.; Fromherz, T.; Padinger, F.; Hummelen, J. C.; Dhanabalan, A.; Janssen, R. A. J.; Sariciftci, N. S. *Synth. Met.* **2001**, *121*, 1517.
(285) Sariciftci, N. S.; Smilowitz, L.; Heeger, A. J.; Wudl, F. *Science* **1992**, *258*, 1474.
(286) Mihailetchi, V. D.; van Duren, J. K. J.; Blom, P. W. M.; Hummelen, J. C.; Janssen, R. A. J.; Kroon, J. M.; Rispens, M. T.; Verhees, W. J. H.; Wienk, M. M. *Adv. Funct. Mater.* **2003**, *13*, 43.
(287) Lee, T. W.; Byun, Y.; Koo, B. W.; Kang, I. N.; Lyu, Y. Y.; Lee, C. H.; Pu, L.; Lee, S. Y. *Adv. Mater.* **2005**, *17*, 2180.
(288) Waldauf, C.; Schilinsky, P.; Perisutti, M.; Hauch, J.; Brabec, C. J. *Adv. Mater.* **2003**, *15*, 2084.
(289) Singh, T. B.; Marjanović, N.; Stadler, P.; Auinger, M.; Matt, G. J.; Günes, S.; Sariciftci, N. S.; Schwödiauer, R.; Bauer, S. *J. Appl. Phys.* **2005**, *97*, 083714.
(290) Meijer, E. J.; De Leeuw, D. M.; Setayesh, S.; van Veenendaal, E.; Huisman, B. H.; Blom, P. W. M.; Hummelen, J. C.; Scherf, U.; Klapwijk, T. M. *Nat. Mater.* **2003**, *2*, 678.
(291) Anthopoulos, T. D.; Tanase, C.; Setayesh, S.; Meijer, E. J.; Hummelen, J. C.; Blom, P. W. M.; de Leeuw, D. M. *Adv. Mater.* **2004**, *16*, 2174.
(292) Anthopoulos, T. D.; de Leeuw, D. M.; Cantatore, E.; van't Hof, P.; Alma, J.; Hummelen, J. C. *J. Appl. Phys.* **2005**, *98*, 054503/1.

CR0501386